Charles University

Faculty of Science

Department of Plant Experimental Biology

Study programme: Biology

Branch of study: Experimental Plant Biology

Dynamics and role of the *Arabidopsis thaliana* IAA17/AXR3 protein in regulation of root growth by auxin

Dynamika a role proteinu IAA17/AXR3 v regulaci růstu kořenů *Arabidopsis thaliana* auxinem

Diploma thesis

Bc. Monika Kubalová

Supervisor: Mgr. Matyáš Fendrych, PhD.

Prague, 2020

Prohlašuji, že předkládanou diplomovou práci jsem vypracovala samostatně pod vedením Mgr. Matyáša Fendrycha, PhD. Předkládaný text je výsledkem mé vlastní práce, použité informační zdroje jsou vždy řádně odcitovány. Tato práce ani žádná její část nebyla předložena k získání jiného nebo stejného akademického titulu.

I hereby confirm that my diploma thesis was prepared independently under the guidance of Mgr. Matyáš Fendrych, PhD. This study represents my own work and results, otherwise the source is always properly cited. This work or a substantial part has not been submitted to obtain another or the same academic degree.

Prague, May 31st 2020 Monika Kubalová

Acknowledgements

First of all, I would like to thank my supervisor, Matyáš Fendrych, for his tremendous help, consultation, guidance, and support throughout the completion of this work. I am grateful not only for the valuable advice, but also for the opportunity to work in a great laboratory with friendly and professional atmosphere. Many thanks belongs also to all the lab members, especially I would like to thank our technician Eva Medvecká for the technical help and to Shiv Mani Dubey for the guidance in the molecular cloning and to Nelson Bernard Calixte Serre for the help with statistics analysis. I also thank all my friends and family who supported me throughout my studies.

This work was carried out at Cell Growth Laboratory, Department of Experimental Plant Biology, Charles University, Viničná 5, 128 00, Prague, CZ.

This project has received funding from the European Research Council (ERC) under the European Union's Horizon 2020 research and innovation programme (grant agreement No 803048).

Abstract

Auxin is phytohormone that regulates several developmental processes and environmental responses. One of the most well-described outcome of the auxin signalling pathway is regulation of gene transcription. Aux/IAA proteins play an important role in this process, acting as transcriptional repressors. Recent studies revealed that several root growth responses are too rapid to be explained by changes in the level of transcription. The correlation between the amount of Aux/IAAs and the root growth rate suggests that these proteins might be involved in root growth regulation, especially during rapid growth responses that are not associated with transcriptional reprogramming. This work is focused on one of the 29 *Arabidopsis* Aux/IAA proteins - the IAA17/AXR3 protein.

First, we produced stable transgenic lines of *Arabidopsis thaliana* expressing different combinations of fluorescently labelled AXR3-1 proteins and/or fused to subcellular localization tags under the control of different tissue-specific promoters, in order to characterize the subcellular localization of the studied protein. Subsequent visualization by confocal microscopy methods confirmed information about the role of IAA17/AXR3 protein in root growth responses, its involvement in auxin signalling, and gravitropism.

Next, we showed that the induction of AXR3-1 mutant protein stimulates root growth rate in the initial stages. Moreover, in these mutant lines, an unusual loss of DII-Venus signal in roots indicates either high concentration of auxin or a disruption of its signalling. The dynamics of both IAA17/AXR3 and AXR3-1 protein in Arabidopsis root were studied with unexpected results. Although the AXR3-1 protein was driven by cell specific promoter, the signal was also observed outside the expression domain - in the vascular cylinder, indicating its possible intercellular transport.

This work provides in a basis and a toolset for further research that could help understand the molecular principles of the rapid root growth response and their relationship to auxin signalling.

Key words: IAA17/AXR3 protein, *axr3-1* mutant, auxin, auxin signalling, rapid root growth responses, gravitropism

Abstract in Slovak language

Auxín je rastlinný hormón regulujúci mnoho vývinových procesov a environmentálnych odpovedí. Jedným z najviac opísaných spôsobov auxínovej signálnej dráhy je regulácia génovej transkripcie. Aux/IAA proteíny hrajú v tomto procese dôležitú úlohu - pôsobia ako transkripčné represory. Nedávne štúdie odhalili, že niektoré rastové odpovede koreňov sú príliš rýchle na to, aby ich bolo možné vysvetliť zmenami na úrovni transkripcie. Korelácia medzi množstvom Aux/IAA proteínov a rýchlosťou rastu koreňov naznačuje, že tieto proteíny sa môžu podieľať na regulácii rastu koreňov, najmä počas včasných rýchlych rastových odpovedí, ktoré nie sú spojené s transkripčným preprogramovaním. Táto práca je zameraná na jeden z 29 Aux/IAA proteínov Arabidopsis - IAA17/AXR3 proteín.

Najskôr sme vytvorili stabilné transgénne línie Arabidopsis thaliana exprimujúce rôzne kombinácie fluorescenčne značeného AXR3-1 proteínu a/alebo fúzovaného so subcelulárnymi lokalizačnými značkami pod kontrolou rôznych pletivovo špecifických promótorov, ktoré umožňujú charakterizovať subcelulárnu lokalizáciu tohto proteínu. Následná vizualizácia metódami konfokálnej mikroskopie potvrdila informácie o úlohe IAA17/AXR3 proteínu v rastových odpovediach koreňov, jeho zapojenie do auxínovej signalizácie a gravitropismu.

Ďalej sme ukázali, že indukcia mutantného proteínu AXR3-1 stimuluje rýchly rast koreňov v počiatočných fázach. Okrem toho, v mutantných líniách nezvyčajná strata signálu DII-Venus naznačuje buď vysokú koncentráciu auxínu alebo narušenie jeho signalingu. Štúdium dynamiky IAA17/AXR3 a AXR3-1 proteínov v koreňoch Arabidopsis prinieslo neočakávané výsledky. Aj keď bol AXR3-1 proteín exprimovaný pod kontrolou pletivovo špecifického promotoru, signál bol pozorovaný aj mimo jeho expresnej domény – a to vo vaskulárnom valci, čo naznačuje možný medzibunkový transport AXR3-1 proteínu.

Táto práca poskytuje základ a súbor nástrojov pre ďalší výskum, ktorý by mohol pomôcť pochopiť molekulárne princípy rýchlej reakcie koreňového rastu a ich vzťah k auxínovej signalizácii.

***Kľúčové slová**: IAA17/AXR3, axr3-1mutant, auxín, auxínový signaling, rýchle rastové odpovede koreňa, gravitropizmus*

Contents

Abbreviations

AREs	- Auxin Response Elements
ARF	- auxin response factor
Aux/IAA	- Auxin/Indole-3-Acetic Acid
Aux/IAA17	- Auxin-responsive protein/Indoleacetic acid-induced protein 17
AXR3	- Auxin-responsive protein 3
DEX	- dexamethasone
DMSO	- dimethyl sulfoxide
EAR	- ethylene response factor (ERF)–associated amphiphilic repression motif
FP	- fluorescent proteins
GFP	- green fluorescent protein
GH3	- Gretchen Hagen 3
GR	- glucocorticoid receptor
HS	- heat shock (promoter)
HSP	- heat shock protein
IAA	- indole-3-acetic acid
LB	- Luria-Bertani (medium)
LRC	- lateral root cap
MS	- Murashige Skoog (salt mixture)
NES	- nuclear export signal
NLS	- nuclear localization signal
PB1	- Phox and Bem1p (domain)
PIN	- PIN-FORMED (protein)
PLT	- PLETHORA (protein)
PTRE1	- PROTEASOME REGULATOR1 (protein)
QC	- quiescent centre
SAUR	- small auxin upregulated RNA
SCF	- Skp1Cullin-F-box (complex)
SWI/SNF	- SWITCH/SUCROSE NONFERMENTING (protein)
TIR1/AFB	- TRANSPORT INHIBITOR RESPONSE 1/ AUXIN SIGNALLING F-BOX (receptor)

TMV	- tobacco mosaic virus
TPL	- TOPLESS (corepressor)
TPR	- TPL-related (corepressor)
VGI	- vertical growth index
WT	- wild type

Introduction

Auxin as a phytohormone plays a role in many developmental processes throughout the life cycle of plants. There are several groups of genes that are induced by auxin, many of which play an important role in the development of the root. Regulation of auxin levels plays a key role in determining the identity of the root meristem already in the embryo, and in the QC centre. Moreover, it is associated with the ability of undetermined root growth and regenerative ability. Auxin maxima also play an important role in root patterning, initiation and elongation of root hairs or lateral roots. Auxin also has an important function in gravitropism, which is the bending of the root in the direction of gravity (Overvoorde et al., 2010). The root tip perceives gravity using specialized cells – statocytes, which contain starch-filled plastids (statoliths), the position of which can be perceived by the cell. As a response to the change in the position of the statoliths, columella cells export auxin towards the lower side of the root, where it affects the growth of cells, thus causing root bending (Sato et al., 2015).

This work focuses on the study of components of the auxin signalling pathway in the root. The previously known and described auxin gene expression regulation pathway involves several components: the auxin receptor TIR1/AFB, which is „glued" by auxin to Aux/IAA coreceptors - transcriptional repressors. The interaction leads to Aux/IAA ubiquitination and subsequent degradation. Degradation of transcriptional repressors allows modulation of gene expression by ARFs that are no longer bound in complex with Aux/IAAs (Leyser, 2018).

In addition to this canonical pathway, there appears to be another signalling branch of this pathway, that is not yet fully described. Such claims are supported by different structural variations in Aux/IAAs that preclude their interaction with TIR1/AFB, or the possibility of auxin action on a non-transcriptional level. An important argument was made based on the results of several studies in the root, which point to the relatively rapid growth response of roots to auxin. As it seems, the dynamics of this response cannot be explained by transcriptional regulation. Several models of auxin-regulated inhibition of root growth have been proposed, both TIR-dependent and -independent.

My focus is IAA17/AXR3 protein, its role in regulation of root growth and the possible involvement in the an as yet undescribed auxin-mediated TIR1-dependent signalling

pathway, which, however, differs from the well-known auxin transcriptional signalling. The theoretical part provides an overview of Aux/IAA structure, localization, interactions, regulatory mechanisms and functions. Aux/IAAs are characterized as short-lived nuclear proteins, however some studies suggested localization outside the nucleus. Although the structure of canonical Aux/IAAs is well known, some of the Aux/IAAs differ from this structure, lacking some domains or possessing degenerated NLS signal. Molecular structure determines physical interactions with other components. Many analyses are pointing to a large number of Aux/IAAs interactors which are not only part of transcriptional regulation but also other processes. Regulation of Aux/IAAs has also been demonstrated at various levels - transcriptional, posttranscriptional, but also at the level of epigenetic modification or protein turnover. In terms of their function, not only in *Arabidopsis* have they been shown to play a role in many processes throughout plant life. At the level of root tissues, Aux/IAAs are involved since the establishment of the identity of future root cells, in all processes from initiation through the growth of lateral roots, root hairs and the primary root. They are also important in the gravitropic response (Luo et al., 2018).

The practical part of this thesis focuses on the IAA17/AXR3 protein, the mutant of which was characterized and described in 1996 (Leyser et al., 1996). This protein belongs to the canonical Aux/IAAs and has been characterized as nuclear localized, but some studies have characterized the signal in the cytoplasm. The IAA17/AXR3 protein has been shown to be an interaction partner for many proteins, not just components of the TIR1/AFB auxin perception pathway. Also, many articles point out that IAA17/AXR3 plays an important role in many processes during the plant life cycle. A point mutation in the DII domain causes auxin insensitivity and results in an auxin phenotype. From the point of view of this work, the most interesting is the root phenotype. Two different inducible systems were used to study the role of IAA17/AXR3 protein in the root, in which growth rate, auxin response and plant gravitropic response were analysed. Another goal was to determine the tissue or subcellular localization and dynamics of the IAA17/AXR3 protein. I cloned constructs using fast-maturing fluorescent proteins, which made it possible to trace the natural localization of both the mutant and WT forms of the protein directly in root cells of *Arabidopsis*. By altering the subcellular localization of the AXR3-1 protein, it was also possible to monitor the effect of the localization change on the root phenotype.

Hypotheses and aims

Established hypotheses are:

- "Non-ubiquitinated Aux/IAAs promote root growth."
- "Aux/IAAs change their subcellular localization after auxin perception and this change is part of the signalling pathway."

The aim of my diploma thesis is to test these hypotheses and bring answers to several questions:

- Do non-ubiquitinated Aux/IAAs promote root growth?
- What role does the AXR3-1 protein play in rapid root growth response, auxin signalling, and gravitropism?
- What is the subcellular localization and dynamics of the IAA17/AXR3 and AXR3-1 protein?
- Does altering the localization of the AXR3-1 protein at the subcellular and tissue levels affect gravitropism?

Literature overview

Auxin and its function in the root

Auxins, as the first discovered plant hormones, are a class of small tryptophan-derived compounds with a common morphogenetic characteristic. The most widespread auxin in plants is indole-3-acetic acid (IAA), which was discovered in the 1930s because of its function in plant phototropism. Auxins are essential in many plant developmental processes throughout their life cycle (Luo et al., 2018).

Many studies point to the key role of auxin in the determination of root architecture. From the very beginning of root development, i.e. in the embryo, the management of auxin concentrations is necessary for proper development. Auxin gradients and their conversion into a molecular response coordinate root development. Although auxin has been characterized as being produced in the aboveground part and subsequently transported to the roots, recent studies point to the importance of root-produced auxin. The transport of auxin at the cellular and tissue level can happen by diffusion into the cell or by active transport by membrane transporters in both directions. These processes are precisely regulated. It is thought that auxin itself may regulate distribution of its transporters and thus its own flow. Root IAA homeostasis appears to be maintained through the formation of inactive reversible IAA conjugates (reviewed in Overvoorde et al., 2010). Therefore, the level of auxin in the root cells is the result of the combination of auxin transport, production, degradation, and conjugation in the cells. Important is the capacity of a given cell to generate a molecular, biochemical, or physiological response to the given level of auxin, which is specific for different tissues within the whole plant (Leyser, 2018). For example, the same concentration of auxin acts activating in the aboveground part of plants, but inhibitory in the root. In addition, auxin interacts with other hormones in many root developmental processes. The local control of auxin levels generates regional concentration gradients and local maxima that are crucial for establishing and maintaining a root primordium. Differentiation processes in the root, such as root hair formation, are also strongly dependent on auxin concentration. Auxin maximum is also created in the QC (quiescent centre) that creates an organizing centre of the root. QC organizes the root tip through contact with neighbouring stem cell initials. The maintenance of stems cells underlies the indeterminate growth of the root. Also, auxin appears to be essential for root regeneration. Proper auxin movement is essential for root patterning and its maintaining.

Several transcription factors affecting the auxin level in the root have been described. E.g. PLETHORA (PLT) and its root gradient correlate with auxin concentration, suggesting that this protein directly reflects the underlying auxin gradients. Likewise, each phase of lateral root life: priming, initiation, patterning, and emergence is dependent on a certain concentration of auxin, with the formation of lateral roots appearing to involve both shoot- and root-derived auxin pools (reviewed in Overvoorde et al., 2010).

Auxin and gravitropism

Auxin also plays an important role in different types of tropisms. Tropisms are plant growth responses to various environmental stimuli. This work focuses on studying the role of auxin in the root especially. In roots, one type of tropism is particularly interesting – gravitropism. Gravitropism is a process in which the plant orients its organs accordingly to the gravitational vector. Negatively gravitropic root is composed of several tissue types, which can be seen in Figure 1 (A). Gravitropism, which Darwin already studied in detail in the 19th century (Darwin, 1869), can be divided into several phases: gravitropic perception, signal transduction, and gravitropic response (Sato et al., 2015). Root perceives changes in gravity vector through specialized gravity sensing cells in the columella root cap (Figure 1). Auxin, as the main signal transmitter, is synthesized in the above-ground parts of the plant and transported through the central vascular cylinder of the stem, then through the root into the root cap and into cells called statocytes, in which starch grains called statoliths (Figure 1, C) are found. In 1900, Professor Němec studied these grains and suggested their function in gravitropism (Němec, 1900). The location and movement of statoliths within the cell provides information about the direction of gravity. If the root is in the horizontal position, the PIN-FORMED (PIN) protein family of auxin transporters accumulates on the lower membrane of the statocytes and the auxin flow preferentially flows through the lower side of the root (Figure 1, B). On this side, auxin has an inhibitory effect on root cell elongation, whereas the upper side of the root is less affected by auxin and grows faster, thereby bending the root into an arc in the direction of gravity. In the vertical root position the auxin flows through the vascular cylinder and at the root tip the flow turns upwards (Figure 1, B). After signal transduction, a gravitropic response occurs in the elongation zone of the root. However, the detailed mechanism of this response is still not entirely clear. It is interesting that root tissue can respond to auxin relatively rapidly, leading to the hypothesis that the gravitropic response

of plants consists of two phases: the initiating non-genomic phase, which is followed by the genomic one (Sato et al., 2015). The non-genomic initial phase is associated with changes in Ca^{2+}, pH, ROS, inositol triphosphate, and NO formation, while the genomic phase represents a well-known auxin-regulated transcriptional response. However, this hypothesis does not agree with the results of Fendrych et al. (2018). A more detailed description of possible explanations can be found in the following chapters.

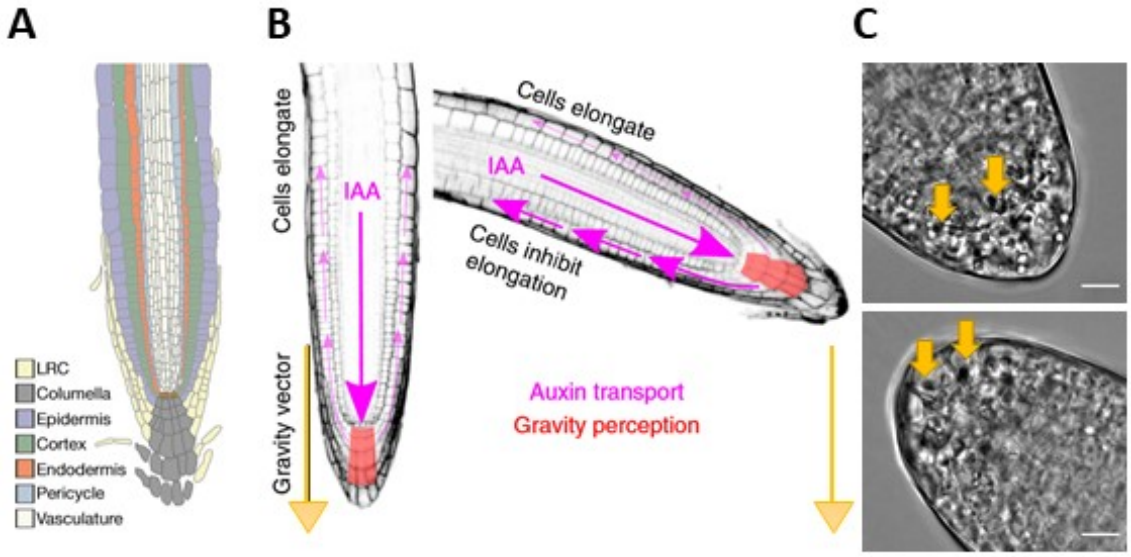

Figure 1) **Root tissues and their response to gravistimulation.** A) Schematic diagram of tissues in *Arabidopsis* root apex with color-coded key (adapted from Swarup et al., 2005). Lateral root cap (LRC), columella, epidermis, cortex, endodermis, pericycle and vasculature can be recognized on the longitudinal section of the root. B) Schematics of auxin fluxes in the root tip during gravitropism (adapted from Fendrych et al., 2018). If the root is parallel to the gravitational vector, the IAA will flow towards the root cap where flow rotates upward. When the root is in an unnatural position, IAA inhibits growth in parts of the root to allow bending. As a result, the root starts to grow in the direction of gravity. C) Detail of root tip with statocytes in root cap. Statocytes are cells where perception of gravity occurs. Arrows indicate a change in the localization of statoliths within these cells after a change in the gravitational vector. Source: Denisa Oulehlová. Scale bars = 10 μm.

Auxin signalling

Hundreds of genes respond to exogenously applied auxin and to changes in its concentration (Overvoorde et al., 2010). Auxin responsive genes comprise of many gene groups, including the Auxin/Indole-3-Acetic Acid (Aux/IAA) family, the auxin response factor (ARF) family, small auxin upregulated RNA (SAUR), and the auxin-responsive Gretchen Hagen3 (GH3) family. In plants, GH3 family is involved in free auxin and amino acid conjugation, thus controlling auxin homeostasis (Feng et al., 2019). SAUR gene family is the largest family of early auxin response genes in higher plants, which

have been implicated in the regulation of multiple biological processes. The products of these genes are involved in many cellular, physiological and developmental processes (Feng et al., 2019). The other two groups of auxin-responsive genes (ARF and Aux/IAA) are, among other things, capable of interacting with each other. ARFs activity during auxin signalling is dependent on Aux/IAAs, which is also reflected in their molecular structure. ARFs contain 3 different sequence parts: a conserved N-terminal DNA-binding domain, a non-conserved middle region that confers either activation or repression domain potential to the ARF, and a conserved C-terminal dimerization domain. C-terminal domain of ARF and C-terminal domains (domains III and IV) of Aux/IAA share a common consensus in a way that they can form heterodimers. Due to the DNA-binding domain, ARFs can bind to the specific Auxin Response Elements (AREs) with the consensus sequence TGTCTC in the promoters of auxin-regulated genes (Abel et al., 1994) and through recruitment of chromatin remodelling enzymes may work as transcriptional activators (Wu et al., 2017).

This work is focused on the last group, the Aux/IAA gene family. Information about this gene family is summarized in the following sections.

Regulation of gene expression

To understand how auxin affects plant responses, it is necessary to know the molecular mechanism of its action. To date, the most known and described pathway of auxin-mediated regulation is the regulation of transcription. Luo et al. (2018) provides a detailed review of this process, which you can find in the following paragraphs and schematically illustrated in the Figure 2.

The process of this regulatory pathway is dependent on the endogenous concentration of auxin. Briefly, at a high concentration, auxin acts as a molecular glue that connects its receptor to transcriptional repressors (co-receptors), leading to their degradation and thereby allowing transcription. Auxin receptor known to date is TRANSPORT INHIBITOR RESPONSE 1/AUXIN SIGNALLING F-BOX (TIR1/AFB) family, which contain Leu-rich repeats including an auxin binding pocket. Aux/IAA genes, which are substrates for degradation by the 26S proteasome, act as transcriptional repressors. The whole ubiquitination process is very specific and consists of 3 processes catalysed by different enzymes (named Ub activation (E1), Ub conjugation (E2) and Ub ligation (E3) enzymes). One of the E3 types of the enzyme is the Skp1Cullin-F-box (SCF) class (Figure

2). TIR1/AFBs are F-box proteins that are responsible for recognition of the substrate to be ubiquitinated. The dimer of the other subunits of this complex – Cullin (Cul1) and RBX1 transfers activated ubiquitin from the E1 enzyme and conjugates it to the target protein - in this case to Aux/IAA proteins. Their degradation leads to the release of ARFs, with which they form dimers at low auxin levels. ARFs that are no longer inhibited by Aux/IAAs can then modulate transcription. Next, free ARF proteins may recruit SWITCH/SUCROSE NONFERMENTING (SWI/SNF) to remodel the chromatin into an active state. At low levels of auxin, Aux/IAA proteins dimerize with ARFs to prevent their physical interactions with transcription initiation complexes. In addition, Aux/IAAs recruit TOPLESS (TPL) and the four TPL-related (TPR) corepressors (TPL/TPR) that interact with histone deacetylases to induce chromatin condensation and thereby stabilizing transcriptional repression.

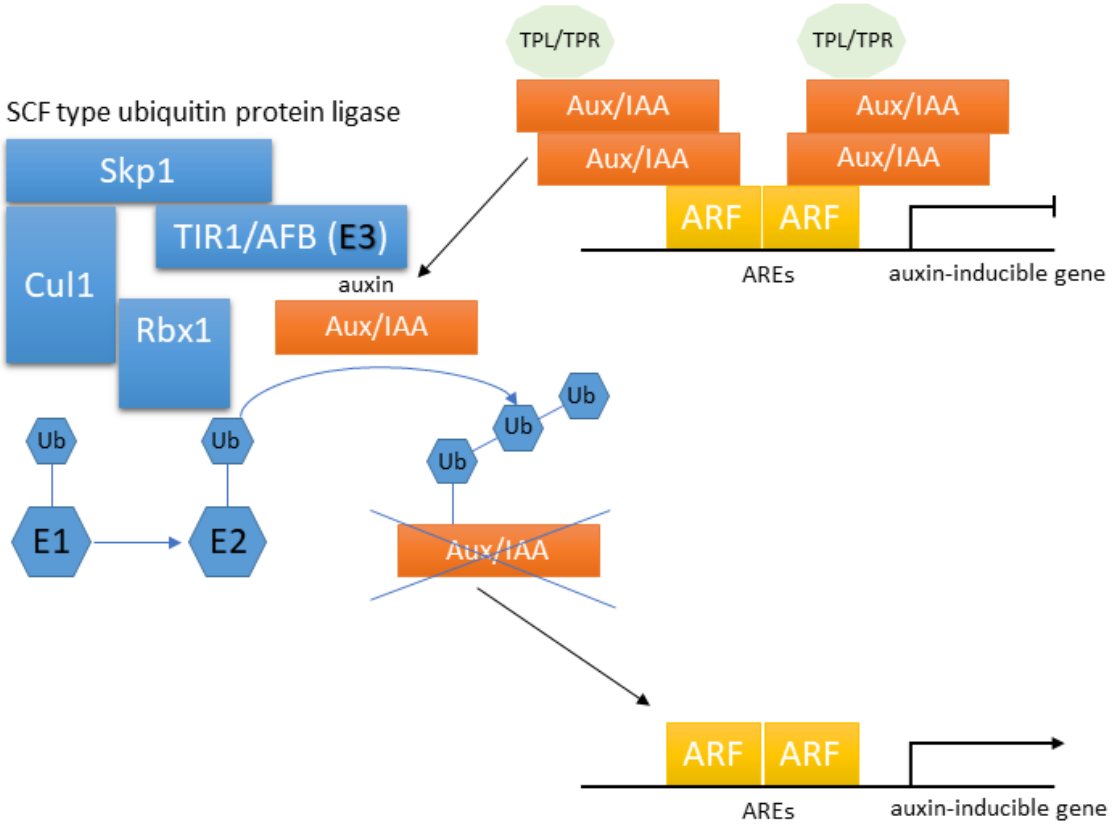

Figure 2) **Skp, Cullin, F-box containing complex (or SCF complex) and auxin regulated transcription.** The SCF complex is composed of several proteins - F-box proteins (in our case TIR1/AFB), Skp1, Cul1 and RBX1. RBX1 contains the domain to which the E2 ubiquitin-conjugation enzyme binds. CUL1 serves as a scaffold to which RBX1 and Skp1 bind. Skp1 is an adapter necessary for the recognition and binding of F-box proteins, which are responsible for the substrate specificity of the whole complex. At low levels of auxin, Aux/IAAs bind to ARFs and transcription is repressed. At higher auxin levels, auxin acts as a molecular glue and binds TIR1/AFB with Aux/IAAs. Ubiquitin is transferred to these transcriptional repressors, leading to their degradation. The ARFs are subsequently free and transcription is active (adapted from Leyser, 2018).

An interesting feature of this system is that auxin plays a role in the degradation of a non-DNA-binding component. Leyser (2018) suggested that, from an evolutionary perspective, it is likely that auxin was only involved secondarily in the process of transcriptional regulation based solely on the activation and repressive role of ARFs competing for the same promoter.

Other (possible) aspects of the auxin signalling pathway

There are several facts suggesting that the pathway described above is probably not the only mechanism by which auxin can regulate plant responses. One of the arguments comes from the very different sensitivity of several auxin responses to various concentrations (Overvoorde et al., 2010). In addition, auxin is known to affect ion pumps on the membrane, and since many membrane transporters are regulated post-transcriptionally, this rises speculations about possible auxin-mediated regulation at a different level (Leyser, 2018). The significance of the TIR1/AFB-Aux/IAA-ARF signalling system is obvious and evidenced by the dramatic phenotype of many mutants of this pathway (Li et al., 2016). However, the results of several studies suggest that other mechanisms are involved in auxin signalling, mainly in the root tissues.

The study of Sato et al. (2015), which is based on the summarized studies, suggested that the gravitropic response of the root has two phases, the first of which is rapid and not associated with transcriptional reprogramming. There are several suggested models theoretically explaining process of rapid root response.

Shih et al. (2015) pointed to very rapid root responses to auxin and the importance of auxin-induced cytosolic Ca^{2+} changes that are required for rapid growth inhibition. They proposed a model according to which an unknown cell surface auxin receptor is proposed to activate the CNGC14 channel to mediate Ca^{2+} influx into the cytosol. The claim that it is a cell surface receptor is based on data according to which auxin-induced cytoplasm Ca^{2+} concentration changes do not appear to require auxin uptake into the cytoplasm. They suggested that Ca^{2+} ions could serve as part of a conserved ion-signalling module to rapidly limit growth, which is also known in other plant tissues. The whole process was evolved to be independent of the TIR1/AFB-Aux/IAA-ARF pathway.

The Ca^{2+}-dependent signalling pathway in the earliest stages of the gravitropic response has been previously described by Monshausen et al. (2011). They also observed temporal and spatial changes in the flux of hydrogen ions that changed during gravistimulation.

This pathway was suggested as a TIR1/AFB-Aux/IAA-ARF independent pathway and it was not clear whether it was related to auxin.

An important argument for the existence of another signal pathway is the result of the study of Fendrych et al. (2018) which showed that the root tissue is able to respond to an auxin level change as early as 30 seconds, this response was reversible and the root has been able to respond in this way for a long time. This time does not seem sufficient to allow transcription and translation to proceed. In addition, even after inhibition of protein synthesis, root tissue did not stop responding. Analysis of mutants unable to transport auxin into the cell suggested that auxin is perceived by an intracellular receptor that mediates the rapid growth inhibition. These results indicate the existence of a rapid reversible growth control mechanism that does not require transcriptional changes. Similar results and rapid growth responses are also reported by Dindas et al. (2018). Fendrych et al. (2018) suggested that canonical signalling pathway regulates root growth via an unknown, non-transcriptional signalling branch of the TIR1/AFB coreceptor. However, this pathway is still dependent on the TIR1/AFB-Aux/IAA-ARF pathway. Based on the correlation between the amount of Aux/IAAs and the growth rate, they suggested that free Aux/IAA proteins promote root growth, ubiquitinated Aux/IAA proteins inhibit it, or there is an unknown interactor or substrate of the TIR1/AFB receptor that might regulate growth. My diploma thesis should bring further information that could help to verify this hypothesis.

Next, Prigge et al. (2020) focused on the TIR1/AFB coreceptor system and its functions in the rapid auxin response in the root. Analysis of different *tir/afb* mutant lines showed the importance of the AFB1 protein in the rapid auxin response, as its mutant was almost completely insensitive to inhibition of root growth by auxin. However, this mutant did not show other auxin-typical phenotypes, suggesting that this protein is involved as a receptor for the rapid non-transcriptional phase of root growth. Interestingly, unlike other AFB and TIR proteins of *Arabidopsis*, AFB1 is highly expressed in the root epidermis and vascular tissues and is not expressed in the embryo. Regarding subcellular localization, the AFB1 protein was localized in the cytoplasm. They also analysed the response of these mutants to gravitropic stimuli. Again, mutant analysis suggests that the AFB1 protein is important for the initiation phase of the gravitropic response, but the *afb1* mutant transitioned to the last phase of the gravitropic response is delayed, suggesting that the role of AFB1 could be broader. It was interesting to compare *tir1* and *afb1* mutants and their combinations. The *tir1/afb1* mutant showed a similar delay in the initial

phase of gravitropism as the *tir1* mutant, but the *afb1* mutant alone did not have such a strong effect on gravitropism.

Fast, slow, transcriptionally or non-transcriptionally regulated root responses to auxin still lack the understanding of the molecular and cellular mechanism, and it is still not entirely clear what signal cascade links stimulus perception to the rapid modulation of growth patterns. Further detailed studies are needed and could provide a deeper understanding of the gravitropic response of plants.

Aux/IAAs

The aim of this thesis is to focus in detail on the role and localization of Aux/IAA transcriptional repressors in the root. Aux/IAAs were first isolated as members of the genes that were rapidly induced in responses to auxin (Abel et al., 1994). These proteins are widespread throughout the plant kingdom, varying in number among species. The origin of Aux/IAA proteins could be traced back to the common ancestor of land plants and green algae (Wu et al., 2017). Individual members of this large gene family are characterized by very short half-lives, and genes encoding Aux/IAA proteins are themselves rapidly up-regulated in response to auxin (Abel & Theologis, 1996). These genes and their products are the main focus of many research papers and have been characterized as (predominantly) nuclear localized and many results point to their involvement in various plant developmental processes.

Molecular structure of Aux/IAAs

As is well known, molecular structure, which is linked to the evolutionary kinship of gene family members, is very important for function specification. The paper of Wu et al. (2017) analysed the evolutionary relationship of Aux/IAAs from various plant species covering all major lineages of plants. In this study, in total 434 Aux/IAA proteins were identified and separated into elevated types according to their motif compositions. The canonical Aux/IAA proteins can be divided into 11 clades based on phylogenetic analysis. In addition, many truncated Aux/IAA proteins were found.

Arabidopsis Aux/IAAs are the most interesting for this work. 29 *Arabidopsis* Aux/IAA proteins have been identified. The canonical structure was well documented and

summarized in a review by Luo et al. (2018). Bioinformatic and molecular studies have relabelled most Aux/IAA proteins to indicate that they generally harbour four conserved characteristic domains: Domain I, II, III, and IV (Figure 3) - each of these domains has a characterized role depending on its sequence characteristics.

Domain I contains an ethylene response factor (ERF)–associated amphiphilic repression (EAR) motif, "LxLxL". EAR motif can recruit a TPL/TPR co-repressor, which is important for transcriptional repression. Domain II is essential for auxin interaction and contains an auxin degron with a conserved "GWPPV" motif that can directly interact with SCF/TIR1 receptor. Moreover, this domain contains a bipartite structural nuclear localization signal (NLS), which probably guide Aux/IAAs to the nucleus. So far, two types of NLS have been characterized in most Aux/IAAs - the bipartite NLS and SV40-like NLS. Bipartite NLS contains the first part between domains I and II and the second part in domain IV. The first part consists of a conservative KR (lysine and arginine) basic doublet located and the second part consists of basic amino acids. The conserved KR motif was identified as a rate motif that aids in tuning the dynamic turnover of Aux/IAA proteins. SV40-like NLS is composed predominantly of basic amino acids and is found in domain IV (Wu et al., 2017). The last two domains (domains III and IV) are collectively called the PB1 (Phox and Bem1p) domain. Domain III and IV were identified as important for the homo and heterodimerization of Aux/IAAs and the study of their exact molecular structure was solved by Han et al. (2015). Type I/II of the PB1 domain contains two types, a basic and an acidic motif. Type I contains several conserved motifs, namely the octicosapeptide (OPCA)-like motif (Dx(D/E)GDx8[E/D], the Phox and Cdc motif, and the atypical protein kinase C interaction domain motif. Domain III contains an amphipathic βαα-fold. Domain IV composes of an acidic region and an SV40 type NLS (PKKKRKV). In addition, a conserved "GDVP" motif between β4 and α2 in Domain IV may contribute to electrostatic protein interactions. Aux/IAA PB1 domain shares homology with the carboxy-terminal dimerization domain in ARF proteins. These protein-protein interactions are important for regulating the activity of ARFs (reviewed in Luo et al., 2018).

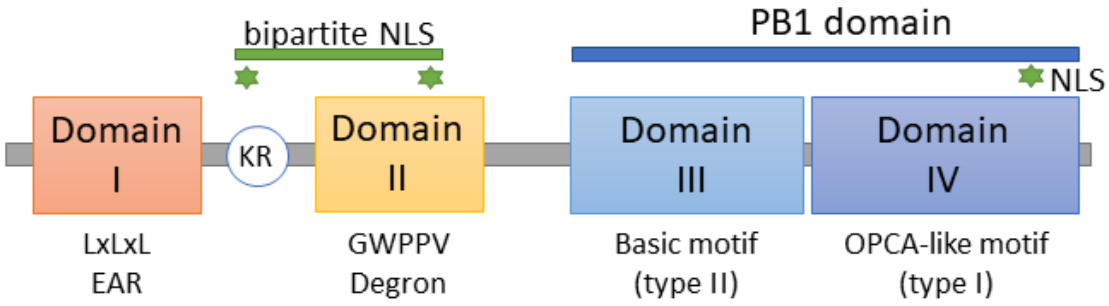

Figure 3) **Structure of canonical Aux/IAAs.** Typical Aux/IAAs are composed of 4 domains (namely, Domain I, II, III and IV). Their function is determined by their sequence. Domain one contains the EAR motif - the LxLxL sequence for TPL/TPR co-repressor binding. Domain II in its molecular structure contains the degron motif GWPPV, which is essential for auxin binding. Domains III and IV are collectively called the PB1 domain and, thanks to their molecular structure containing different β and α folds, allow the formation of homo or heterodimers of Aux/IAAs and ARFs. The NLS signal is found in domain IV, but also in domain II, where it is associated with the sequence between domains I and II (simplified from Luo et al., 2018).

Within different plant species, however, we can also find exceptions to this canonical structure. Although most Aux/IAA proteins harbour the typical four domains, species with altered Aux/IAA structure have been identified, even with complete lack of some domains. Tomato and potato proteins lacking both domain I and domain II, papaya proteins without domains III and IV, and others have been characterized (Liu et al., 2017; Wu et al., 2017). An interesting example is the result of populus genomic analysis, which showed that the IAA7 protein contains tandem duplication of domain II (Kalluri et al., 2007).

Localisation of Aux/IAAs

Localization at the tissue level

According to data obtained from https://bar.utoronto.ca/eplant/, most *Arabidopsis* Aux/IAA genes are expressed in various tissues across the entire plant. Some of them are tissue-specifically expressed, others not. In terms of root expression, various Aux/IAAs are also expressed in the meristematic, elongation, and maturation zones. It is also possible to monitor the expression of these proteins in the epidermis (these Aux/IAA are often specific for either the trichoblast or atrichoblast), the cortex, the endodermis even in the stele. Most Aux/IAAs do not have only one specific expression tissue, but it is possible to see their expression in various tissues within the root.

Subcellular localization

Many Aux/IAAs have been characterized as nuclear localized (Liscum & Reed, 2002). Not only the presence of the NLS signal in the sequence of canonical Aux/IAAs, but also the results of many analysis of Aux/IAA localisation confirm this claim.

However, in recent years, studies have been published where the signal of various Aux/IAAs was also visible outside the nucleus. For the study of localization, mostly microscopic methods were used using various fluorescent proteins which constructs were transformed into different tissue types and subsequently analysed.

Kumar et al. (2015) analysed the localization of several tomato Aux/IAAs using IAA-YFP fusion protein constructs bombarded in onion peel cells. Many genes were localized in the nucleus, but analyses showed the presence of 10 Aux/IAAs also outside the nucleus, in the cytoplasm. In addition, several reports point to the incomplete or total lack of NLS in some Aux/IAAs as well as their localization outside the nucleus. Audran-Delalande et al. (2012) studied tomato IAA and showed that 2 IAA proteins do not have an NLS signal, another lacks a bipartite structure and some contain a degenerated NLS signal. In tobacco protoplasts, they then monitored the ability of this sequence to transfer the protein to the nucleus. The coding sequences of the selected IAAs were fused to GFP (green fluorescent protein) and their localisation was monitored in tobacco protoplasts. Interestingly, not only proteins containing the NLS signal but also those with a degenerated NLS signal were present exclusively in the nucleus, suggesting that this signal is also sufficient for nuclear localization. Proteins lacking bipartite signal and lacking entire NLS were localized not only in the nucleus but also in the cytoplasm. Aux/IAA fusion with GFP has also been used in study of subcellular localization of IAA maize. C-terminal GFP-fusion proteins of wild-type and two mutated forms were generated and expressed in maize leaf protoplasts. WT (wild type) forms were exclusively located in the nucleus, whereas IAA proteins lacking bipartite signal or the entire NLS were not strictly localized in the nucleus, but also in the cytoplasm (Ludwig et al., 2014). Interesting is the subcellular localization of the IAA26 protein and its change after interaction with the tobacco mosaic virus (TMV). Padmanabhan et al. (2005) created IAA26-GFP fusion construct, which was transiently expressed in either mock-inoculated, WT TMV-infected, tobacco and *Arabidopsis* leaf tissues. In mock-inoculated tissues, the IAA26-GFP fusion protein was found to localize predominantly in the nucleus, whereas in infected leaves the construct was localized only in the cytoplasm, suggesting that TMV disrupts the localization of

IAA26. The precise mechanism remains to be determined. Next, H. Zhang et al., (2019) studied not only localization but also different stability of nuclear versus cytoplasmic localized Aux/IAAs. The results of the analysis of transient expression in tobacco as well as stable expression in *Arabidopsis* roots showed that the *Arabidopsis* IAA17/AXR3 protein is localized not only in the nucleus, but (to a lower extent) also in the cytoplasm, whereas the cytoplasmic localized IAA17/AXR3 was less stable and its signal disappeared more rapidly after auxin treatment. In addition to IAA17/AXR3, signals of other Aux/IAAs outside the nucleus were detected. The localization of Aux/IAAs was also observed in protoplasts. Arase et al. (2012) showed the localization of IAA8 protein not only in the nucleus but also in the cytoplasm using polyethylene glycol-mediated transient expression system in *Arabidopsis* mesophyll protoplasts. In contrast, the IAA17/AXR3 protein was localized exclusively in the nucleus. Using protoplast analysis and fusion with GFP, the IAA12 protein was also localized not only in the nucleus but also in the cytoplasm (Hamann et al., 2002).

In summary, although subcellular localization of Aux/IAAs was first shown to be purely nuclear, many studies now point to extracellular localization, but in many cases the results differ. This area needs further research.

Interactions of Aux/IAAs in plants and their regulation

The modular structure of Aux/IAAs also determines the interactions of these proteins. Overall, the variations in domains may contribute to the diverse functions in the auxin signalling pathway, which further support multiple roles played by Aux/IAAs. A wide variety of interaction as well as Aux/IAA regulation possibilities are known. These data confirm the significant position of these proteins in the plant life cycle.

Interactions of Aux/IAAs in plants

The variety of Aux/IAA functions is also dependent on the existence of many interaction partners. In addition to the components described above of the auxin-regulated transcription process (TIR1/AFBs, TPL/TPRs, ARFs), many components have been identified as interactors of Aux/IAAs. Moreover, these proteins are capable of numerous variations of homo and heterodimerizations.

Luo et al. (2018) carried out various interactome analyses in *Arabidopsis*, a comprehensive physical interactome map of Aux/IAA proteins has been created, which consists of the essential auxin signalling transduction components mediated by Aux/IAA proteins. This map (shown in Figure 4) includes all 29 Aux/IAA from *Arabidopsis* and shows a large number of interactions of these proteins, including not only homodimerization and heterodimerization with ARFs, but also many other interaction partners whose role has been demonstrated in various aspects of plant growth and development or responses to different environmental factors.

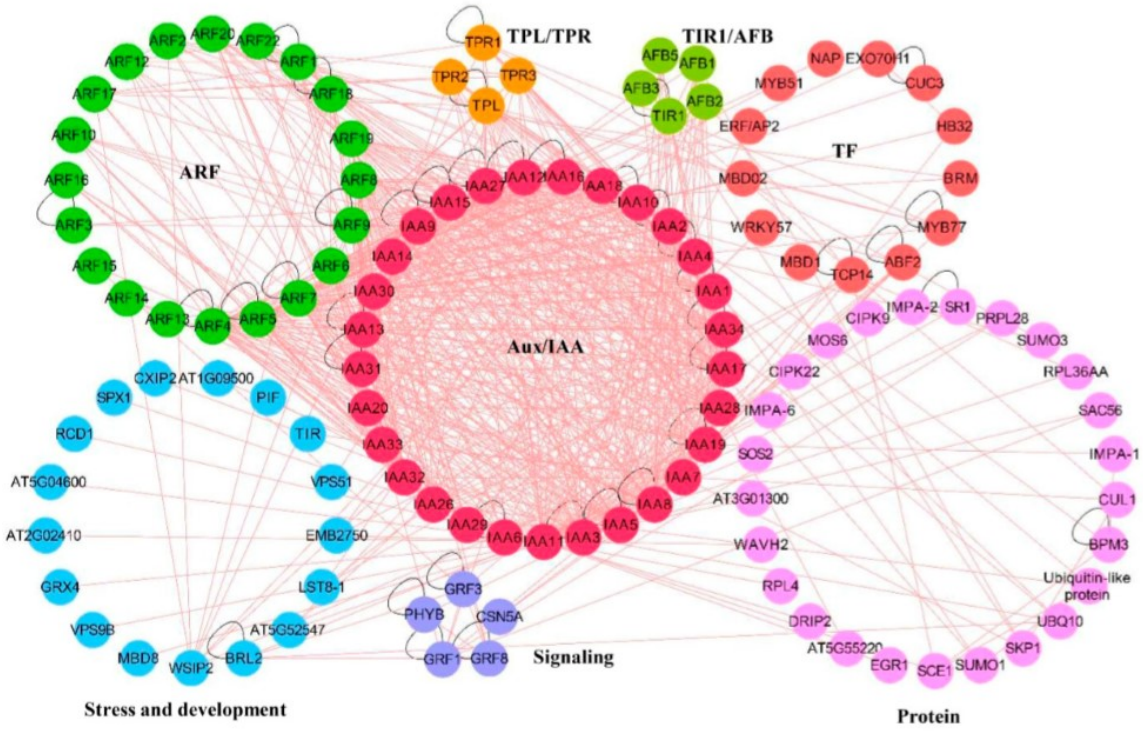

Figure 4) **Aux/IAA protein interaction network.** In silico analysis showed that Aux/IAAs interact not only with each other and with auxin signalling pathway components (ARFs, TIR1/AFBs and TPLs/TPRs), but also with many other proteins, some of which are involved in plant signalling cascades or stress responses and development processes (adapted from Luo et al., 2018).

The most studied and probably most described are the interactions of Aux/IAA proteins with other components of auxin-regulated transcription, such as ARFs, TIR/AFBs and TPL/TPR proteins. As analysed by Luo et al. (2018), 29 Aux/IAA proteins had physical contact with 20 ARF proteins via about 45% of all the interactions described. Most Aux/IAA proteins had physical interactions with four identified TPL/TPR proteins, (except IAA5, IAA6, IAA9, IAA14, IAA15, IAA20, IAA29, IAA30, IAA31, IAA32, IAA33, and IAA34). Moreover, four out of six TIR1/AFB proteins were involved in this

interactome, but only 11 Aux/IAA proteins had direct physical interactions with these four TIR1/AFB receptors. In the context of Aux/IAA protein interactions, it is important to note that each of these 29 proteins interacts with each other to form homo and heterodimers. Oligomerization seems to be another mechanism for regulating the auxin response (Knox et al., 2003). However, most of these results are obtained in vitro and need to be verified in vivo.

Regulation of Aux/IAAs in plants

Protein interactions in living organisms are important not only for their function but also for their regulation. Regulation of gene expression can take place at different levels. Several levels of Aux/IAAs regulation have been demonstrated to date. The results of many scientific papers suggest that Aux/IAAs can be regulated at various levels, such as transcriptional and post-transcriptional regulation, epigenetic modification (reviewed by Luo et al., 2018), or protein turnover regulation. As mentioned above, Aux/IAAs are auxin-regulated genes and their expression increases upon treatment with auxin (Abel et al., 1994).

Probably the most studied level of gene expression regulation is the regulation at the level of transcription. The most widely reported pathway so far is the auxin-mediated transcriptional regulation, including the auxin receptor TIR1/AFB, TPL/TPR corepressors, Aux/IAA transcriptional repressors, which are degraded in the response to auxin, and ARFs response modulators. A detailed description of this process can be found in the previous chapters. Additionally, Aux/IAAs interact with many others transcriptional factors (reviewed by Luo et al., 2018).

Several papers have been devoted to the study of the protein turnover of Aux/IAAs. The study of Gray et al. (2001) showed the importance of Aux/IAA ubiquitination in auxin-regulated transcription. Maraschin et al. (2009) brought evidence for SCF^{TIR1}-mediated poly-ubiquitination of Aux/IAA proteins. Recent studies have also focused on protein turnover as a regulatory mechanism in relation to Aux/IAA proteins. For example, Shi et al. (2017) showed that salt stabilized both IAA17/AXR3 and RGA-LIKE3 (RGL3) proteins (DELLA protein) due to salt-induced NO production. IAA17/AXR3 directly interacted with RGL3 and increased its protein stability, and, consistently, RGL3 stabilized IAA17/AXR3 protein through inhibiting the interaction of TIR1 and IAA17/AXR3 by competitively binding to IAA17/AXR3. Terrile et al. (2012) provide

evidence that NO donors increase auxin-dependent gene expression and NO also enhances TIR1-Aux/IAA interaction, while NO depletion blocks Aux/IAA protein degradation. In addition, according to their results, S-nitrosylation of TIR1 reinforced the TIR1–Aux/IAA interaction and facilitated the turnover of Aux/IAA proteins. Results suggest that TIR1 S-nitrosylation enhances TIR1-Aux/IAA interaction, facilitating Aux/IAA degradation and subsequently promoting activation of gene expression. Tao et al. (2016) described how regulators of 26S proteasome ubiquitination affect Aux/IAA levels and auxin signalling. The study was focused on the Rac GTPases, which stimulate 26S proteasome-dependent degradation of Aux/IAAs. Transformation of protoplasts and their microscopic analysis showed that the components of the SCF/TIR1, COP9 signalosome, and 26S proteasome are colocalized in nuclear protein bodies after auxin application. Auxin also induces Rac GTPases-mediated recruitment of nucleoplasm Aux/IAAs into these proteolytically active nuclear protein bodies. Moreover, it was reported that an E2 conjugating enzyme for Lys63-linked polyubiquitination (UBC13) can regulate the stability of Aux/IAAs to control auxin-mediated root development, and this process may be related to the SCF/TIR1 complex, but it could also be explained by an interaction with other previously unknown interaction partners (Wen et al., 2014). Next, Yang et al. (2016) analysed an *Arabidopsis* homologue of the proteasome inhibitor PI31, PROTEASOME REGULATOR1 (PTRE1). *Ptre1* mutant showed a phenotype typical of auxin mutants, suggesting that auxin signalling could be suppressed in these plants. In addition, this mutant was less sensitive to root growth inhibition, suggesting a positive role for PTRE1 protein in root auxin signalling. Moreover, analysis of Aux/IAA expression level showed that most of them had reduced expression in the *ptre1* mutant while their levels were increased in overexpressed PTRE1 mutant. Analysis by DR5::GFP showed a reduced amount of auxin in the *ptre1* mutant. However, it still remains unclear, why the expression of the Aux/IAA genes was not initially suppressed (it remained unchanged or it was even higher), but it showed reduced expression by extending the auxin treatment time to 3 hours. In addition, they analysed connection between PTRE1 protein and proteasome activity and its localisation after auxin treatment. The summarized results indicate that auxin is able to regulate the change in the localization of the PTRE1 protein - the PTRE1 protein is pulled from the nucleus to the plasma membrane, resulting in a decrease in 26S proteasome activity in the nucleus, thereby regulating the amount of Aux/IAAs. However, the study showed that changes in

proteasome activity are different at the beginning (5/10 min), when these changes happen relatively slowly.

Functional roles of Aux/IAAs in roots

Aux/IAAs are involved in many processes, such as embryo development, hypocotyl growth, tropisms, flower and root organ development, and many other processes (Figure 5). Most stabilizing mutations in Aux/IAA proteins display similar phenotypes in which auxin signalling transduction is hampered, leading to defects in diverse developmental and growth processes (Leyser, 2018). Phenotypes that are more dramatic result from dominant or semi-dominant mutations. The typical phenotype of auxin mutants is dwarfism, which displayed developmental defects, including small and curved leaves, altered shoot apical dominance and gravitropic responses, short siliques, and arrested embryogenesis.

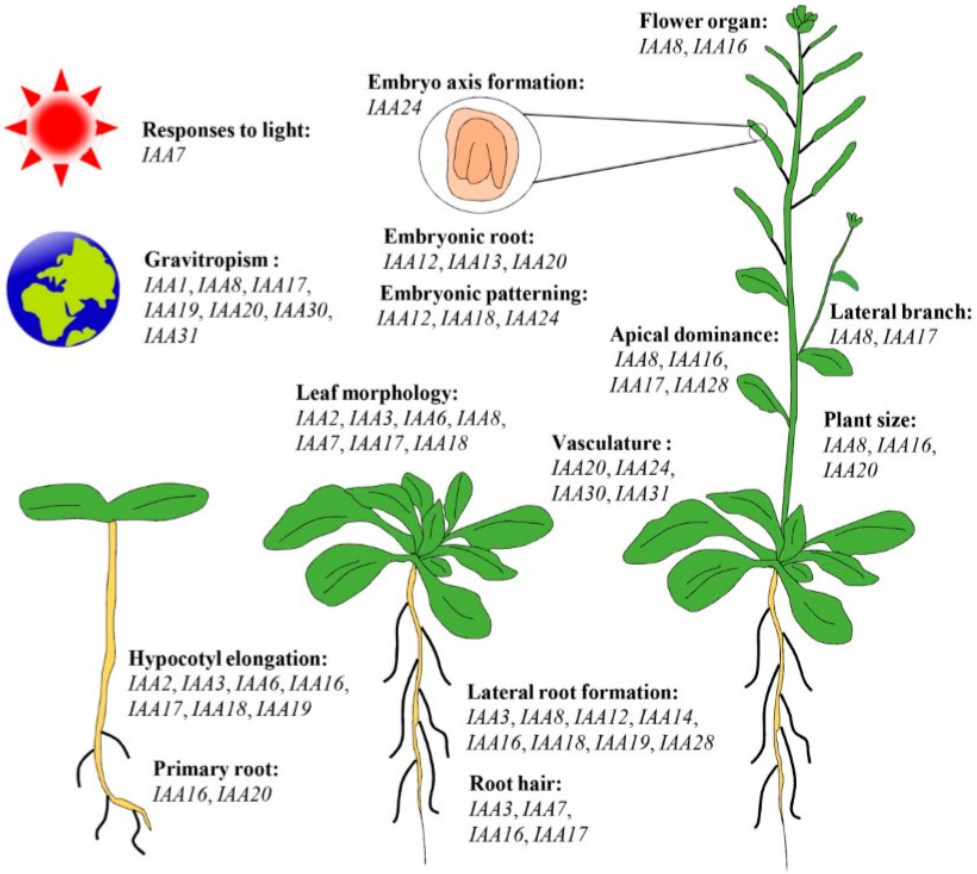

Figure 5) **Summary of the functions of Aux/IAA genes in growth and development processes of *Arabidopsis*** (adapted from Luo et al., 2018). Aux/IAAs are involved in almost all processes of plant life cycle.

Many Aux/IAA mutants and their phenotypes have been described so far, not only in *Arabidopsis* but also in other plant species. The following section describes the root mutants, which are interesting in terms of the topic of this work. Many Aux/IAAs are probably involved in all processes of root growth and development. Mutations in Aux/IAA proteins can result in various developmental changes in the root, e.g. the identity of the founding cells of the root meristem may be changed, and the development and initiation of primary root, lateral roots, and root hairs may be impaired. Mutations also result in changes in plant gravitropism (Arase et al., 2012; Kitomi et al., 2012; Sato & Yamamoto, 2008; Yang et al., 2004).

IAA12 was first characterized IAA involved in embryogenesis. Its interaction with ARF5 is essential for root and embryo patterning in early embryogenesis (Hamann et al., 2002). Primarily the IAA16/20 play a role in the primary root growth (Luo et al., 2018). Regarding the lateral roots, in summary, mutant analyses have shown that Aux/IAA 3/8/12/14/16/18/19/28 play a role in some process from initiation to lateral root formation. Using transcriptomic data and functional studies, De Rybel et al. (2010) characterized GATA23 transcription factor and its role in the process of lateral root founder cell identity. As a negative regulator of this process, IAA28 appears to be in the basal meristem. Guseman et al. (2015) analysed transgenic plants expressing various degradation rate variants of IAA14 and showed that the relative stability of this factor was irreversible to lateral root density. IAA8 can also interact with TIR1 to regulate lateral root formation. Arase et al. (2012) analysed phenotypes of transgenic plants that conditionally overexpressed IAA8, XVE::IAA8, and an IAA8 loss-of-function mutant, *iaa8-1*. In both lines, the root phenotype and the number of lateral roots were altered, decreasing in the former and increased in the latter. Tatematsu et al. (2004) have shown how IAA19 interacts with ARF7, which is essential for the development of lateral roots. In rice, the IAA13 mutant had a reduced number of lateral roots (Kitomi et al., 2012). Interesting, Notaguchi et al. (2012) developed a method that allows tracking of Aux/IAA movement within a plant. They showed that IAA18 and IAA28 are phloem mobile transcripts that are produced in the leaves and are transported to the roots, where they negatively regulate the formation of lateral roots. In addition, Aux/IAA 3/7/16/17 seem to be crucial for the formation and/or extension of root hairs (Luo et al., 2018). The role of these proteins has also been demonstrated in the response of plants to gravitropic stimulation. The IAA13 mutant rice was also agravitropic, indicating the role of this protein not only in lateral root formation but also in the gravitropic response (Kitomi et

al., 2012). Overexpression of IAA8 caused abnormal gravitropism, whereas the loss-of-function mutant had a phenotype comparable to control (Arase et al., 2012). Also plants with IAA20 overexpression showed modified gravitropic root. Overexpression of three non-canonical Aux/IAA genes (IAA20, IAA30, and IAA31) resulted in similar aberrant phenotypes (Sato & Yamamoto, 2008). Likewise, the mutation in the IAA1 protein resulted in disruption of the gravitropism of the above-ground and underground plant parts (Yang et al., 2004).

The complexity of these processes requires precise regulation. A few studies point to various regulatory processes associated with root Aux/IAAs. The transcriptional reprogramming of IAA3, a suppressor of root growth, is directly activated by the basic leucine zipper (bZIP) transcription factor bZIP11, which is essential in the primary root growth (Weiste et al., 2017). To regulate primary root initiation, a nuclear import receptor IMPORTIN-ALPHA 6 (IMPα6) can efficiently take up IAA12 into the nucleus, for maintaining enough short-lived IAA12 (Herud et al., 2016). For the forming of lateral roots in rice, an inositol polyphosphate kinase (IPK2) stabilized IAA11 by interacting with its Domain II, seems to be important (Chen et al., 2017). It has been further shown, that to regulate lateral root initiation by promoting the turnover of Aux/IAAs, OsCYP2 (a cyclophilin gene) directly interacts with its co-chaperone suppressor of the G2 allele of S-phase kinase-associated protein 1 (skp1) - a member of the SCF ubiquitin ligase protein complex (Kang et al., 2013). OsCYP2 can directly interact with C2HC-type zinc finger protein (OsZFP) to regulate lateral root development via the IAA pathway, and OsIAA23 might participate in this OsZFP-mediated auxin signalling process (Cui et al., 2017). miR847, the first miRNA found to cleave Aux/IAA identified in *Arabidopsis*, targets IAA28 mRNA for degradation and positively regulates lateral organ development (Wang & Estelle, 2014).

IAA17/AXR3 protein

As mentioned above, this work focuses on Aux/IAAs, and their role in auxin signalling in the root. One of the 29 Aux/IAA proteins of *Arabidopsis*, namely Aux/IAA17 (Auxin-responsive protein/Indoleacetic acid-induced protein 17), was used as a study tool. Aux/IAA17 (composed of 229 nucleotides) is also called AXR3 (Auxin-responsive protein 3). As its name suggests, the mutant lines are insensitive to auxin and, in addition,

are agravitropic, which are the reasons why it was chosen to study in this thesis. This protein has been studied in many scientific works; summarized information can be found in the following section.

Molecular structure and localisation of IAA17/AXR3

IAA17/AXR3 as a canonical Aux/IAA has identical molecular structure to other canonical Aux/IAAs - it has 4 domains I, II, III and IV, each with their typical function. As far as the tertiary structure is concerned, only the structure of domains III and IV has been experimentally determined (Han et al., 2015). Domain III forms a β−β−α fold as an antiparallel β sheet, whereas domain IV forms a β−β−α−β−α fold as an antiparallel β sheet (Figure 6).

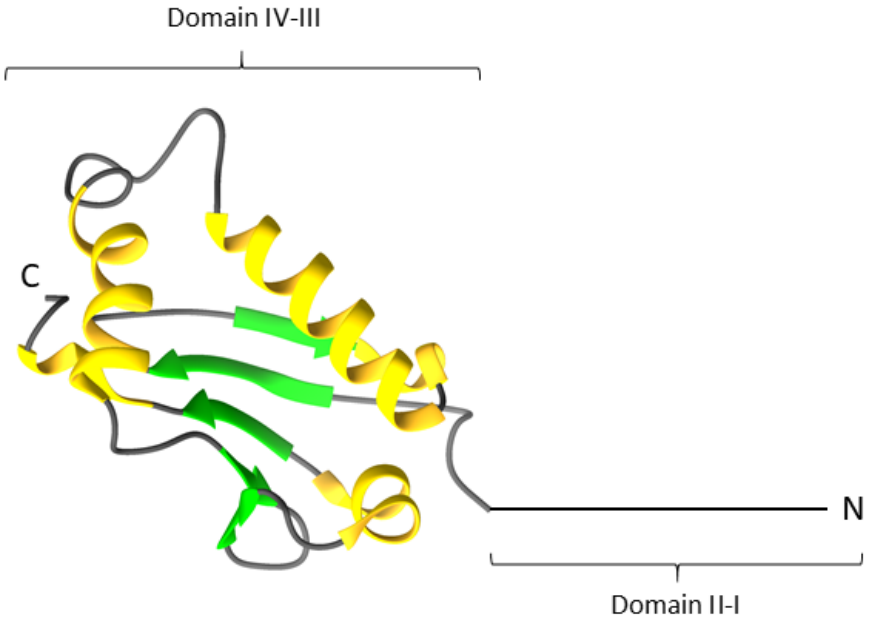

Figure 6) **Structures of domain III−IV of IAA17/AXR3.** PB1 domain of IAA17/AXR3 is comprised of five β strands (green) and four α helices (yellow). The data is taken from the database RCSB PDB, ascension code 2MUK (https://www.rcsb.org/structure/2MUK). The structure was visualized using Chimera software.

Although Aux/IAA proteins are characterized as nuclear localized proteins (Wu et al., 2017). H. Zhang et al. (2019) showed that the IAA17/AXR3 protein is also located outside the nucleus, in the cytoplasm. After the application of auxin to the cells, another degradation rate was observed for nuclear and cytoplasmic localized IAA17/AXR3. The signal of IAA17/AXR3 located in the cytoplasm decreased much more rapidly.

Conversely, there are studies that show the IAA17/AXR3 protein to be located executively in nucleus (Procko et al., 2016). The importance of the NLS signal in the IAA17/AXR3 sequence has already been shown by Ouellet et al. (2001).

Interactions and functions of IAA17/AXR3

The IAA17/AXR3 protein has been shown to possess many molecular and biological functions and has also been shown to be an interaction partner of many proteins. Their overview can be seen in Figure 7.

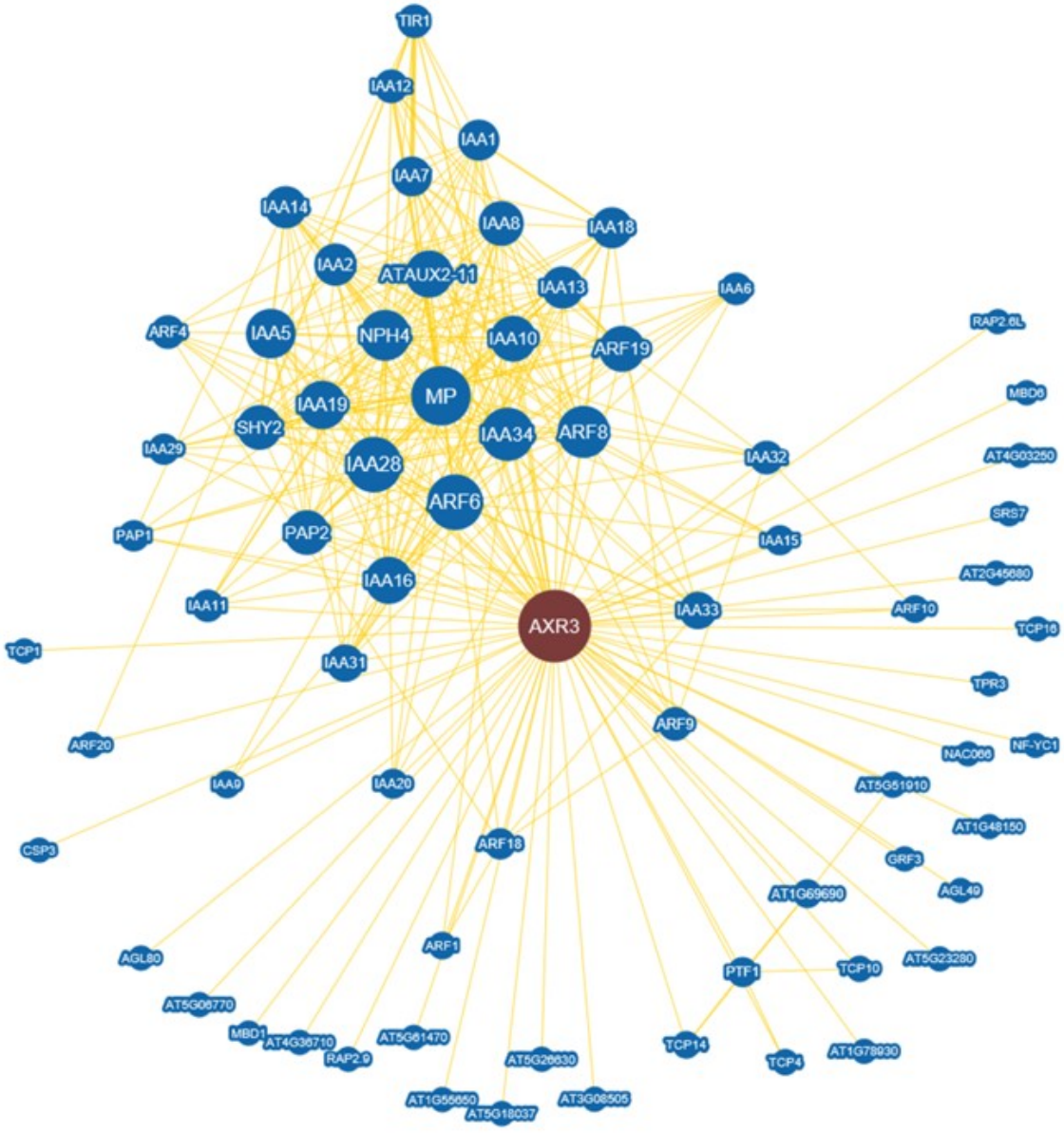

Figure 7) **Interactomic map of IAA17/AXR3 protein.** Interactors of IAA17/AXR3 known to date. A dynamic layout that applies physical forces to repel and attract related nodes. Data taken from Biogrid database (https://thebiogrid.org/24803/table/*Arabidopsis*-thaliana/axr3.html).

According to data obtained from the Biogrid database (https://thebiogrid.org/), the IAA17/AXR3 protein has 72 interactors. As expected, these include not only ARFs, but other known auxin signalling components - TIR1/AFB and TPC/TPL co-receptors. In addition, IAA17/AXR3 interacts with almost all remaining Aux/IAAs in *Arabidopsis*. Moreover, physical interactions with a number of other proteins involved in various processes within plant life have been demonstrated.

IAA17/AXR3 has also been studied in the context of the ubiquitination process. As mentioned above, the level of IAA17/AXR3 is increased in the *ptre1* mutant, conversely, overexpression of the PTRE1 protein involved in proteasome regulation causes a decreased level of IAA17/AXR3 (Yang et al., 2016). Additionally, IAA17/AXR3 protein appears to be affected by changes in atypical Lys63-linked ubiquitination, where the level of IAA17/AXR3 proteins increased after mutation of one gene necessary for the course of this type of ubiquitination (Wen et al., 2014). Other possible interactions of this protein have been mentioned in previous chapters.

Biological function of IAA17/AXR3 protein

In terms of IAA17/AXR3 biological function, it has been so far shown to be involved in some typical phenotypes controlled by auxin signalling. Mutant plants showed changes in many developmental processes, such as hypocotyl elongation, root gravitropism, and root hair and adventitious root formation.

The role of this protein has been studied primarily by creating point mutations. The iaa17/axr3 gene was originally defined by two semi-dominant stabilising point mutations in domain II (Leyser et al., 1996). The two alleles, *axr3-1* (88P → L) and *axr3-3* (89V → G) confer severe phenotypes, largely consistent with an over-response to auxin. Although both mutations had an effect on tropism (photo/gravitropism), the *axr3-1* mutation showed a stronger phenotype. Dominant *axr3-1* mutant plants show dwarf, dark green phenotype, curled leaves, increased apical dominance, decreased adventitious root formation and root growth, agravitropic roots, and no root hairs (Figure 8), indicating an altered auxin response (Leyser et al., 1996).

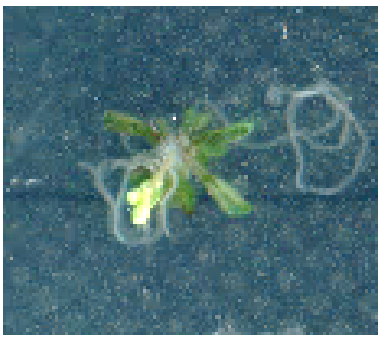

Figure 8) **Dominant *axr3-1* mutant**. The plants show a pleiotropic auxin phenotype.

Knox et al. (2003) used a heat shock inducible system and showed that after activation of *axr3-1* expression, plants showed a defect in root hair formation and gravitropic response. They also pointed out the importance of its interaction with other Aux/IAA proteins.
Swarup et al. (2005) analysed UAS::AXR3-1 lines in relation to gravitropism. After expression of this mutant protein in the epidermis and LRC, the roots were completely agravitropic, suggesting the importance of this protein for the gravitropic response of the root as well as its essential presence in the epidermis and LRC. The same results were obtained by Lucas et al. (2008). Defects in the development of the lateral roots and root hairs of the *axr3-1* mutant were also noted by Kim et al. (2006), which focused on the inclusion of this protein in the brassinosteroid signalling pathway. This proteins cross-linking seems to be essential for root development. In addition, De Smet et al. (2007) studied the effect of a dominant mutation of the IAA17/AXR3 protein on the formation of lateral roots using an inducible GAL4 system and showed that it is necessary for this process.
Li et al. (2009) showed that overexpression of the stable form of IAA17/AXR3 correlates with reduced auxin response, and vice versa, plants constitutively expressing a stabilized version of the IAA17/AXR3 protein that was converted into an activator having high auxin-like phenotypes.
Recently, some papers showed that IAA17/AXR3 was also involved in cytosolic glutamine synthetase-mediated ammonium assimilation in *Arabidopsis* root (Shi et al., 2017). *Axr3-1* mutant was also of major interest in a recent study by Y. Zhang et al. (2019). Based on their results, they proposed a model according to which auxin acts in gravitropism not only by known transcriptional regulation, but the TIR1-AXR3 complex regulates the formation of starch granules by regulating the genes necessary for this synthesis. This suggests that the IAA17/AXR3 protein could also play an indirect role in gravity perception, not just in the gravitropic signal transduction and response. Using the HS::AXR3-1 line, they observed reduced starch grain formation and reduced gene expression after activation.

Only a point mutation in Domain II (Figure 9) has a dramatic effect on the plant phenotype, which is pleiotropic. The *axr3-1* mutation has a dramatic effect on the stability of IAA17/AXR3 but does not abolish its accumulation in the nucleus or its ability to form protein–protein interactions. Pulse–chase experiments showed that the half-life of AXR3-1 is sevenfold longer than the wild-type IAA17/AXR3 (Ouellet et al., 2001). Although

there are two sites of point mutations in domain II, the greatest phenotype change being shown by the mutant plants referred to as *axr3-1* (Figure 8), which have also been used in this work. Since the mutants in this protein showed an altered auxin phenotype including reduced root elongation, no root hairs, increased adventitious rooting as well as an altered gravitropic response, they have been chosen as a suitable means to study the molecular mechanism of plant gravitropism and auxin signalling in the root.

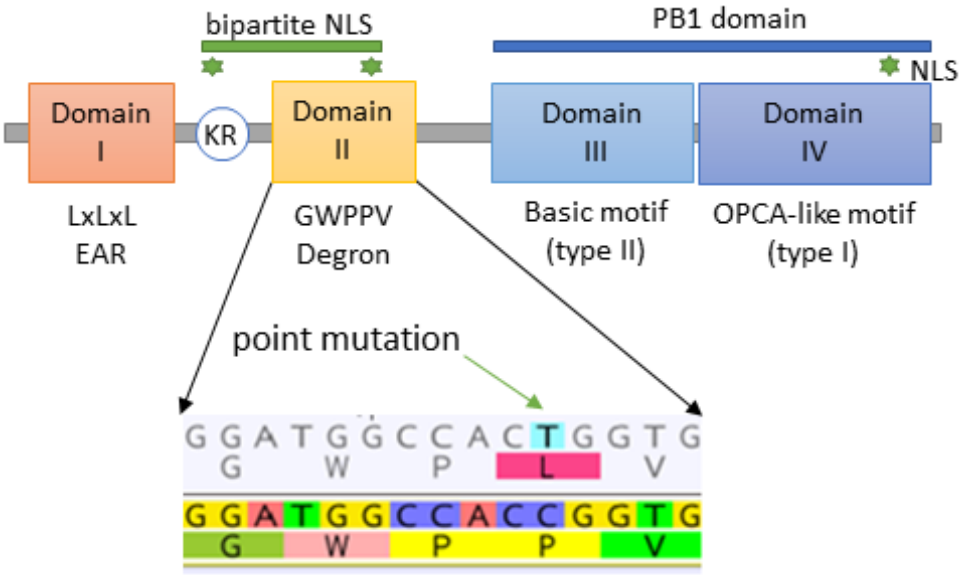

Figure 9) **Point mutation in the domain II degron motif of IAA17/AXR3 protein.** The AXR3-1 mutant contains only a point mutation that causes 88P → L change, resulting in a decrease in auxin affinity.

Analysis of the IAA17/AXR3 protein and its mutants was used to test the hypotheses and achieve the goals set out in this work. We propose that non-ubiquitinated Aux/IAAs promote root growth in a mechanism distinct from the canonical TIR1/AFB–Aux/IAA–ARF dependent transcriptional regulation. This hypothesis is based on several observations:

- Aux/IAA proteins are crucial for the gravitropic response and auxin sensitivity of roots (Rouse, 1998). IAA17/AXR3 is particularly interesting, as it was shown to cause transient agravitropism when expressed in an inducible manner (Knox, 2003).
- The root growth response to auxin is very rapid and likely does not involve the nuclear TIR1/AFB – Aux/IAA dependent transcriptional regulation, yet it is

dependent on the TIR1/AFB receptors (Fendrych et al., 2018; Prigge et al., 2020; Shih et al., 2015).

- Aux/IAA protein levels reflect the intracellular auxin levels; Aux/IAAs are degraded in response to auxin (Woorward et al., 2005). Interestingly, a very tight positive correlation is observed between the amount of Aux/IAAs and the root growth rate (Fendrych, unpublished), when the Aux/IAA levels are approximated by the DII-Venus marker line (Brunoud et al., 2012).

Microscopic analysis of the roots containing the auxin sensor DII-Venus showed a positive correlation between the root growth and the amount of Aux/IAA (Figure 10). DII-Venus is composed of the DII degron domain of Aux/IAA28 and mVenus. With increased auxin level, there is a very rapid loss of DII-Venus signal, indicating degradation of Aux/IAA proteins. The loss of the DII-Venus signal corresponds positively to the decreasing of the growth rate. After removal of auxin, these changes return rapidly - a DII-Venus signal appears and growth rate accelerates. These observations support the hypothesis under study.

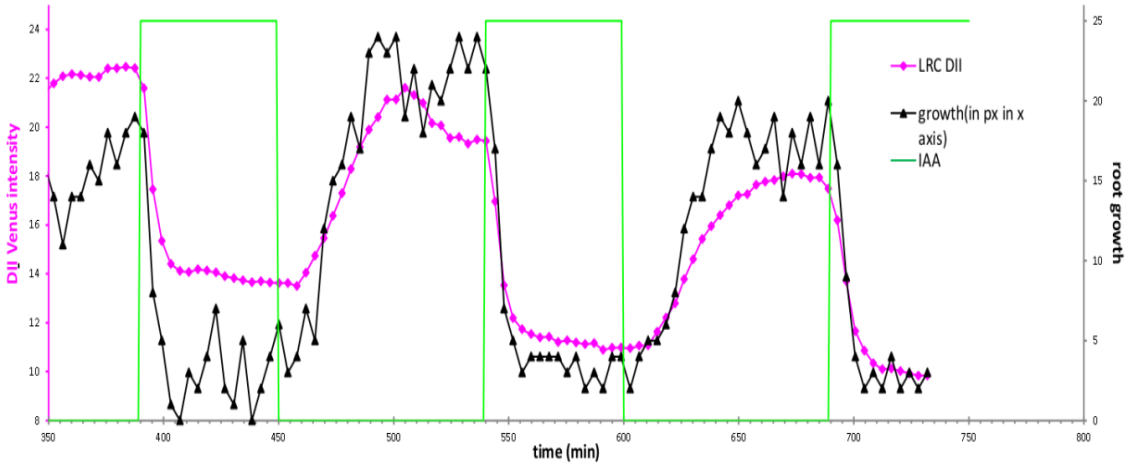

Figure 10) **Dependence between growth rate, DII-Venus intensity and IAA application.** After the addition of auxin, a very rapid reversible inhibition of root growth can be observed corresponding to the intensity of decreased DII-Venus signal. Source: Matyas Fendrych, unpublished.

Methods and materials

Plant lines and growth conditions

Sterilization of the seeds was carried out with chlorine gas: 50 ml household bleach (Savo) + 1.5 ml 37% HCl ; closed in a desiccator that was placed in a fume hood, approx. 4 hours, after that tubes with seeds were placed open into laminar flow hood to remove the chlorine gas.

Different plant lines (listed in the Table 1 and Table 2) after two days stratification were grown in a cultivation room under long day conditions (16/8 hours, 21°C, light intensity approximately 100 µmol m^{-2} sec^{-1}) on vertical MS plates (½ Murashige Skoog (MS) salt mixture (Duchefa) -2.15 g/l, MES (MES.H_2O) - 0.5 g/l, pH 5.8 adjusted with KOH; 1% sucrose, 1% agar (Duchefa plant agar) for 3 – 5 days (according to the requirements of the experiment).

Where appropriate, tobacco or *Arabidopsis* plants were grown in pots containing Jiffy pellets in a cultivation room with automatic water irrigation for long day conditions (same conditions as above).

Table 1) List of plant lines used available from others laboratories.

Line	References
HS::AXR3-1	Knox, 2003
g1090::XVE>>AXR3-1-mCherry	Mähönen et al., 2014
UAS::AXR3-1	Swarup et al., 2005a
UAS::AXR3-1-GR	Swarup et al., 2005a
J2812, J0391, J0951	Haseloff, 1998
DII-Venus	Brunoud et al., 2012

Table 2) List of plant lines prepared in this study.

Line name	Method of preparation
GAL4/UAS system (C24 background) C24>>UAS::AXR3-1-GR J2812>>UAS::AXR3-1-GR J0391>>UAS::AXR3-1-GR J0951>>UAS::AXR3-1-GR C24>>UAS::AXR3-1 J2812>>UAS::AXR3-1 J0391>>UAS::AXR3-1 J0951>>UAS::AXR3-1	Crossing
HS::AXR3-1 x DII-Venus	
g1090::XVE>>AXR3-1-mCherry x DII-Venus	
PIN2::IAA17-mVenus	Molecular cloning
PIN2::mVenus-IAA17	
PIN2::AXR3-1-mVenus	
PIN2::AXR3-1-mScarlet	
PEP::AXR3-1-mScarlet	
GL2::AXR3-1-mScarlet	
GOBL9::AXR3-1-mScarlet	
PIN2::GR::AXR3-1-mVenus	
PIN2::AXR3-1-mVenus8KFarn	
PIN2::AXR3-1-mVenusNESNES	

*All lines contain a mutated form of AXR3-1 protein or WT IAA17/AXR3, which are described in detail in the introductory chapter.

Treatments

The plant lines were subjected to different treatments as required – listed in the following table (Table 3).

Table 3) List of treatments used.

Chemical treatment	Concentration used	Stock concentration	Solvent
Dexamethasone (DEX) (Sigma-Aldrich)	10 µM	10 mM	Dimethyl sulfoxide (DMSO)
Estradiol (Sigma)	5 µM	20 mM	DMSO
Indole Acetic Acid (IAA) (Sigma)	10 nM/ 50 nM	10 mM	Ethanol (EtOH)

* exposure time of the chemical treatments varied depending on the requirements of the experiment, details are given for each experiment separately.

In addition, propidium iodide (Biotium) was used to stain cell wall (roots were immersed in 1 mg/ml propidium iodide solution for 5 min). Other treatments to which the individual lines were exposed include gravistimulation and heat shock. The lines were exposed to 37°C heat shock for about 40-50 minutes and then analysed at room temperature.

Imaging

Root growth was imaged using a flatbed scanner (Epson Perfection v700/v370) and controlled by an AutoIt script that triggered imaging every 20/30 minutes. Plants were placed on the scanning area, covered with black fabric and scanned for 4 hours. Transient expression in tobacco epidermis was imaged using a laser scanning confocal microscope and a vertical spinning disc microscope, which was also used for all other microscopic analyses. A more detailed specification of both types of microscope can be found in the following table (Table 4). mVenus was excited by laser 515 nm, mScarlet and mCherry by laser 561 nm.

Table 4) Technical specification of the microscopes used.

W1 vertical Spinning disk	Zeiss LSM 880
body	
Carl Zeiss Axio Observer.7	Carl Zeiss Axio Observer.Z1
objectives	
EC Plan-Neofluar **5x**/0.16 M27 (FWD=18.5mm) Plan-Apochromat **10x**/0.45 M27 (FWD=2.1mm) Plan-Apochromat **20x**/0.8 M27 (FWD=0.55mm) LD LCI Plan-Apochromat **40x**/1.2 Imm Corr DIC M27 for water, silicon oil or glycerine immersion (CG=0.15-0.19mm) (FWD=0.41mm at CG=0.17mm)	EC Plan-Neofluar **5x**/0.16 M27 (FWD=18.5mm) Plan-Apochromat **10x**/0.45 M27 (FWD=2.1mm) LD LCI Plan-Apochromat **25x**/0.8 DIC Corr, M27 for water, silicon oil or glycerine immersion (CG=0-0.17mm) (FWD=0.57mm at CG = 0.17) C-Apochromat **40x**/1.2 Imm Corr DIC Corr M27 for water, silicon oil or glycerine immersion (CG=0.14-0.19mm) (FWD=0.28mm at CG=0.17mm)
confocal unit	
spinning disk unit: Visiscope Confocal based on Yokogawa CSU-W1-T2 equipped with a VS-HOM1000 excitation light homogenizer	Confocal scanning module**:** 13 fps for 512x512, zoom 0.6 - 40x, max. resolution 8192 x 8192
detection	
PRIME-95B Back-Illuminated Scientific CMOS Camera, 1200 x 1200 Pixel, 11 x 11 um pixel size	Spectral detector 32-channels GaAsP PMT (410-695 nm); 2 standard PMTs („blue “ and „red“; 371-740 nm); 32-channel GaAsP and „red“ PMT enables photon counting mode
lasers	
Laser 405 nm 150 mW Laser 488 nm 100 mW Laser 515 nm 100 mW Laser 561 nm 100 mW	Laser 405 nm 30 mW Laser Argon (458, 488, 514 nm) 25 mW Laser 561 nm 20 mW Laser 633 nm 5 mW

Image analysis

Images were analysed and processed using Fiji (Schindelin et al., 2012). Several procedures were used for processing. The following section lists some of them (less used) with detailed steps.

- growth rate measurement (microscopic images) – plugins >> registration >> correct 3D drift (of root cap) >> measure the changing position of the root tip (as points X and Y)
- intensity measurement – plugins >> registration >> correct 3D drift (of root cap) >> delimit the area in which we want to measure the intensity (the area of the root tip) >> measure the intensity

Calculations

To calculate the root growth after 4 hours, the measurement of the difference in root length between 2 time frames was used using the Fiji program (>> Straight line).

The calculation of the growth rate over time was measured on microscopic time images from which the root tip position (X, Y) was obtained by Fiji. Subsequently, these data were processed in Excel. Growth was calculated according to the formula:

$$\text{Growth at a certain point} = \sqrt{(\Delta X^2+\Delta Y^2)}$$

The vertical growth index was calculated based on the following formula:

$$\text{VGI} = \text{base-tip distance/root length}$$

The signal intensity was calculated either as relative (intensity value in time point x minus value in previous time point) or as absolute (intensity value in time point x minus value in time point 1).

Statistical analysis and data processing were done using Excel, Boxplots (http://shiny.chemgrid.org/boxplotr/) and Anova like test Kruskal Wallis.

Crossing

Unpollinated flowers at an appropriate stage (about 5 weeks old) were emasculated (the anthers were removed) by using tweezers (eye tweezers with a very thin tip) using a binocular microscope (Stemi 305 EDU Microscope Set/ Olympus SZX7). Two days later, healthy, mature and non-pollinated stigmas were pollinated with pollen of the other line. The mature seeds were harvested and used for further analysis in F1 generation.

Molecular cloning

Molecular cloning was used to generate many constructs. Bacterial strains used in experiments: *Escherichia coli* TOP10 and *Agrobacterium tumefaciens* GV3101.

GoldenBraid cloning procedure

Cloning was performed using the GoldenBraid system (Sarrion-Perdigones et al., 2011; https://gbcloning.upv.es/). The GB cloning system uses type II restriction enzymes (BsaI and BsmBI) that cleave several nucleotides downstream of its recognition site. The process of domestication not only removes these restriction sites in our genes of interest, but also adds overhangs that allow for the assembly of the various parts of the transcription units.

Design of cloning was carried out using the Geneious 11.05 (https://www.geneious.com/). This procedure consists of the following parts, the detailed description of which is given in the following paragraphs.

- Creating individual GB-parts.
- Creating transcription units - alpha plasmids level → agroinfiltration into tobacco leaf cells.
- Creating transcription units omega vectors level → stable transformation of *Arabidopsis thaliana.*
- Selection of transgenic plants.

There is also the diagram of the whole course in Figure 11.

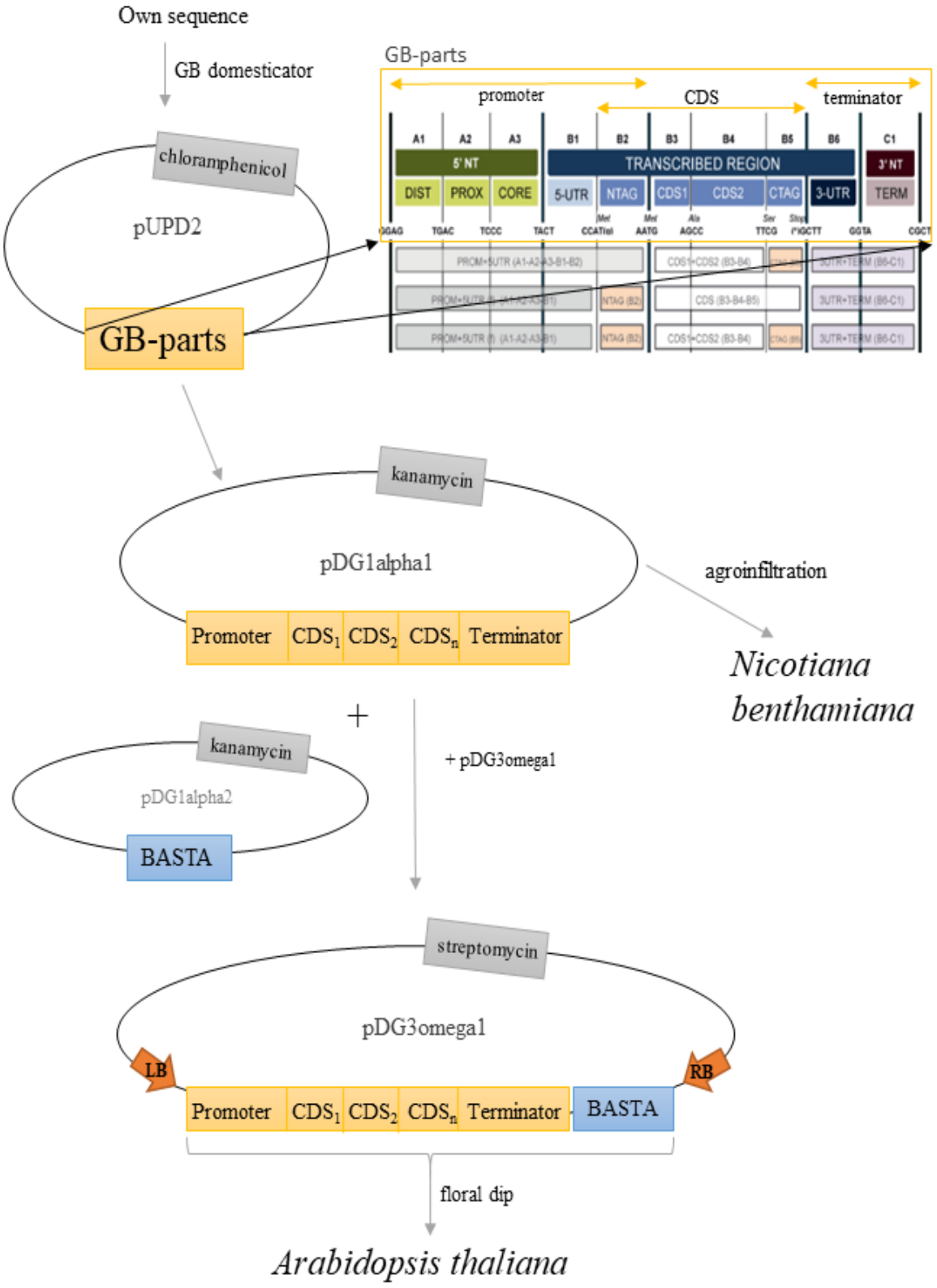

Figure 11) **Schematic principle of GB cloning system**. After domestication, we obtain pUPD2 vectors containing different GB-parts in different positions. These can then be combined into pDG1alpha1 vector, which is suitable for agroinfiltration. In addition, pDG1alpha1 can be ligated with pDG1alpha2 bearing plant-specific resistance (BASTA) and with the pDG3omega1 vector carrying the left and right borders (LB/RB), which are necessary for transformation into *Arabidopsis thaliana.*

Creating individual GB-parts

First, we had template DNA synthesized for mVenus and mScarlet fluorescent proteins (FPs). Individual GB-parts were obtained from the collection or prepared as follows. After designing the primers either through domestication tools (https://gbcloning.upv.es/tools/domestication/) or the Geneious program, we amplified the required DNA fragment by PCR. The chemical components and reaction conditions can be found in Table 5 and Table 6. Amplified DNA was checked by gel electrophoresis (1% agarose (peqGOLD, Universal agarose, VWR), 0,5x TAE buffer, 1.5% GelRed (GelRed™ Nucleic Acid Gel Stains, Biotium); 80 V, 400 mA, approx. 20 min according to gel size). Subsequently, the DNA was extracted from the gel and isolated by means of GeneJET Gel Extraction Kit (Thermo Scientific, according to protocol available on https://www.thermofisher.com/manuals) and its subsequent concentration was determinate by means of nanodrop.

Table 5) Components of PCR.

PCR component	Quantity/concentration (c)
iProof buffer (Thermo Scientific)	4 µl
10µM dNTPs (Thermo Scientific)	0,4 µl
primer forward	c = 1 µM
primer reverse	c = 1 µM
DNA template	1 µl
distilled deionized water	count to a final volume (20 µl)
iProof DNA polymerase (Thermo Scientific, 5U/µl)	0,1 µl

Table 6) PCR cycling conditions.

Step	Temperature (°C)	Time (s)	Number of repetitions
initial denaturation	98	30	1
denaturation	98	5	35
aneling	60	15	
extension	72	15	
final extension	72	300	1

The DNA fragment prepared was ligated with the pUPD2 vector, which contains the chloramphenicol resistance and LacZ gene. The components of this chemical reaction are listed in Table 7. pUPD2 vector and all others used vectors can be found at https://www.addgene.org/browse/article/10316/.

Table 7) Components of ligation reaction with pUPD2 vector.

Reaction component	Total amount
DNA template	40 ng
pUPD2 vector	75 ng
T4 DNA ligase (Promega, 3U/µl)	1 µl
buffer for ligase (10x concentrated, Promega)	1 µl
BsmBI enzyme (Thermo Fischer, 10U/µl)	1 µl
distilled deionized water	count to a final volume (10 µl)

Prepared plasmids were transformed into competent *E. coli* cells, prepared according to the Mix & Go protocol (https://files.zymoresearch.com/protocols/_t3001_t3002_mix_go_e._coli_transformation_kit_buffer_set.pdf), as follows.

1 µl of the ligation mixture was mixed with component cells *E.coli* (TOP10 strain) and left on ice for 10 min. We then added 400 µl of SOC medium (20 g peptone, 5 g yeast extract, 0,58 g NaCl, 0,19 g KCl, 10 ml 1M $MgCl_2$, 10 ml $MgSO_4$, water to total volume of 1 l, pH= 6-7 (adjust with NaOH) + 10 ml 20% (w/v) glucose solution), and allowed to shake for 40 min at 37°C. 100-200 µl of this bacterial suspension was inoculated (spread over the entire surface to dryness) on plates containing LB (Luria-Bertani) medium (4 g peptone; 4 g yeast extract; 4 g NaCl; 6,4 g KOBE agar /Roth/, 400 ml distilled water) and kanamycin (c = 50 µg/ml). 50 µl of 2% X-Gal (5-Bromo-4-chloro-3-indoxyl-beta-D-galactopyranoside; Biosynth) was spread on the surface of the plates before inoculation. Both X-gal and the bacterial suspension were spread to the surface of the medium using a heat sterilized and cooled laboratory glass rod. We allowed the cultures to grow at 37°C overnight.

The next day, appropriate colonies were selected (based on blue-white selection) and reinoculated into 3 ml of liquid LB medium (same antibiotics and components as previous LB medium, except agar). Again, we let the colonies grow overnight at 37°C with continuous shaking. From well-grown colonies, plasmids were isolated (GeneJET

Plasmid Miniprep Kit, Thermo Scientific, according to protocol available on https://www.thermofisher.com/manuals) and measured concentration.
The plasmids were subsequently verified by a restriction reaction. After incubation of all components, listed in Table 8, min. for 1 hour, we verified the accuracy by gel electrophoresis (the same conditions as described above). Subsequently, the plasmids were verified a second time by Sanger sequencing.

Table 8) Components of restriction reaction.

Component	Amount (µl)
DNA	1,5 (of typical concentration)
restriction enzyme (Thermo Fischer/ Biolabs)	0,1
buffer for restriction enzyme (10x concentrated, CutSmartR, BioLabs)	1
distilled deionized water	calculate to the final volume (10 µl)

Creating transcription units – alpha plasmid levels

Selected individual GB-parts were ligated with the pDGB1alpha1 vector with kanamycin resistance (reaction components are listed in Table 9).

Table 9) Components of ligation reaction with pDG1alpha1 vector.

Component	Total amount
gene of interest	75 ng
promoter	75 ng
terminator	75 ng
fluorescent protein	75 ng
pDG1alpha1 vector	75 ng
T4 DNA ligase (Promega, 3U/µl)	1 µl
buffer for ligase (10x concentrated, Promega)	1 µl
BsaI enzyme (Biolabs, 20U/µl)	1 µl
distilled deionized water	calculate to the final volume (10 µl)

The plasmids thus prepared were propagated by transformation into *E. coli* (described in the previous chapter), and the isolated plasmids were transformed into *A. tumefaciens* according to the following procedure.

1 µl of the PCR product was mixed with competent *A. tumefaciens* cells (GV3101 strain with pSOUP helper plasmid), mixed and transferred to the cuvette by pipetting. The bacteria were subsequently transformed by electroporation (Electroporator, Eppendorf; 1000 V). After adding 400 ml of SOC medium the suspension was poured into a tube and cultured at 28°C by shaking. After 2 hours, we inoculated 100-200 µl of suspension on LB media containing antibiotics at the desired concentration listed in Table 10. Cultures were grown for 2 days at 28°C. Prepared colonies were suitable for infiltration into tobacco leaves.

Table 10) List of antibiotics used to select bacteria suitable for agroinfiltration.

Antibiotic	**Concentration used (µg/ml)**
kanamycin (Duchefa)	50
tetracycline (Duchefa)	5
rifampicin (Duchefa)	25
gentamycin (Duchefa)	10

The following tables provide an overview of all used GB-parts, whether used from the collection (Table 11) or prepared by myself in this study (Table 12).

Table 11) List of plasmids used from collection.

Parts	GB part	Description	Notes, origin
35S promoter (long)	A1-B2	derived from cauliflower mosaic virus	created by Shiv Mani Dubey
35S promoter (short)	A1-B1		
PIN2 promoter		promoter of PIN2 - LRC, epidermis, cortex, AT5G57090	
PEP promoter		promoter Aspartyl protease – cortex, AT2G40360	
GL2 promoter		promoter of Glabra-2 – atrichoblasts, AT1G79840	
COBL9 promoter		promoter sequence of Cobra like-9 – trichoblasts, AT5G49270	
35S terminator	B6-C1	derived from cauliflower mosaic virus	
RBCS terminator		ribulose-1,5-bisphosphate carboxylase/oxygenase terminator	created by Nelson Serre
mVenus8KFarn	B5	plasma membrane anchor	created by Shiv Mani Dubey
mVenusNESNES		nuclear export signal	
mScarlet-I		the fluorescent protein sequence used from Bindels et al. (2017)	
	B2		created by Matyas Fendrych
GR		glucocorticoid receptor	created by Shiv Mani Dubey
intron		GUS intron as a linker	available from Tomáš Moravec

Table 12) List of prepared transcriptional parts.

GB part	Notes/ sequence/ primer sequence (Forward/ Reverse)
mVenus	
	CAGGCTGCAATGGTTGACGGCTCCGGATATCAAGTGCATCGAA CAATGCAATTCGAGGATGGAGCTTCCTTGACAGTTAACTATAG GTATACTTATGAAGGGTCACACATCAAAGGAGAAGCACAAGTG AAAGGAACAGGGTTCCCTGCTGATGGGCCTGTCATGACTAACT CACTTACTGCTGCTGATTGGTGCAGATCGAAAAAAACGTACCC TAATGACAAGACGATTATTTCGACGTTTAAGTGGTCTTACACG ACTGGTAACGGTAAACGTTATCGTTCTACGGCAAGAACTACTT ACACTTTTGCCAAGCCTATGGCTGCAAACTATTTGAAAAATCA ACCAATGTACGTCTTCAGAAAGACGGAACTTAAGCATTCGAAG ACTGAGTTGAATTTCAAAGAGTGGCAGAAGGCATTTACGGACG TTATGGGTATGGATGAGTTGTATAAGGGATCTGGTGGCGGGTC T
B2	*F:* GCGCCGTCTCGCTCGCCATGAGCAAAGGCGAGGAACT *R:* GCGCCGTCTCGCTCACATTGATCCTCCTCCAGATCCCTTGTATA GCTCGTC
B5	*F:* GCGCCGTCTCGCTCGTTCGGGAGGAGGAAGCAAAGGCGA *R:* GCGCCGTCTCGCTCAAAGCTTACTTGTATAGCTCGTCCATG
mScarlet	
B2	*F:* GCGCCGTCTCGCTCGCCATGGTGTCTAAGGGGGAGGC *R*: GCGCCGTCTCGCTCACATTGACCCGCCACCAGATCCCTTAT
DII-mVenus	
	DII domain Aux/IAA28 fused to novel fluorescent protein mVenus (mentioned above in this table)
B3-B4	*F:* GCGCCGTCTCGCTCGAATGAAACAAAAAAGCTCG *R:* GCGCCGTCTCGCTCACGAACCGGCCGCTGCAGCCTTG
IAA17/ AXR3-1	
	multiplied from genomic *Arabidopsis* DNA + by the domestication process, the restriction enzyme sites used in the GB cloning system were removed
B3-B4	*F:* GCGCCGTCTCGCTCGAATGATGGGCAGTGTCGAGCT *R:* GCGCCGTCTCGCTGTCTCTGAGAACCCTCTC *F:* GCGCCGTCTCGACAGTTGATCTGAAGCTAAATCTG *R:* GCGCCGTCTCGTAAGACGTAAACGCTTGCATG *F:* GCGCCGTCTCGCTTATGAAAGGATCGGATGCCATTGGTCTTGCT CCGAGG *R:* GCGCCGTCTCGCTGTCTCTGAGAACCCTCTC

GB part	Notes/ sequence/ primer sequence (Forward/ Reverse)
IAA17/ AXR3-1	
B3-B5	*F:* GCGCCGTCTCGCTCGAATGATGGGCAGTGTCGAGCT *R:* GCGCCGTCTCGCTGTCTCTGAGAACCCTCTC *F:* GCGCCGTCTCGACAGTTGATCTGAAGCTAAATCTG *R:* GCGCCGTCTCGTAAGACGTAAACGCTTGCATG *F:* GCGCCGTCTCGCTTATGAAAGGATCGGATGCCATTGGTCTTGCTCCGAGG *R:* GCGCCGTCTCGCTCAAAGCTCAAGCTCTGCTCTTGCACTTCTCCATCGCCCTCGGAGCAAGACCAATG
NLS	
B5	*F:* GCGCCGTCTCGCTCGTTCGGAAGAGCAAGCAAGGAAAGC *R:* GCGCCGTCTCGCTCAAAGCTTACTCTTCTTCTTGATCAGCTTC

Agroinfiltration into tobacco

Plant material used for transient expression is *Nicotiana benthamiana*. Agroinfiltration was carried out as follows (based on Voinnet et al., 2003).

Before the infiltration itself, it was necessary to prepare suitable plants. After sterilization and two days of cold stratification, the seeds of *N. benthamiana* were planted in Jiffy pellets and grown in a cultivation room. After 2 weeks, the small plants were divided into pots containing soil. Leaves of healthy 2-3 week-old plants were used for infiltration.

The agroinfiltration into *N. benthamiana* itself consisted of several days. Colonies of transformed *Agrobacteria* were inoculated into 3 ml of liquid LB medium containing the antibiotics, listed in Table 10, and left on a shaker at 28°C overnight. Next day, the OD600 of each culture was measured (1:5 dilution with water was used). Subsequently, the required amount of bacterial suspension was spun down to obtain OD600 = 0,3 in a final volume of 2 ml. The pellet was resuspended in 2 ml of infiltration buffer (10 mM $MgCl_2$, 100 µM acetosyringone) /aliquots should be frozen in -20°C, do not refreeze, add always freshly prior to use/ and incubated 2-3 hours at room temperature in dark.

This was followed by infiltration into the leaves of 3-4 week old plants. The inoculation was performed using a syringe, where the tip is placed close to the underside of the leaf and the medium containing *Agrobacteria* is pressed into the mesophilic cells. The

tobaccos were then cultured for another two days in a culture room and then analysed microscopically.

Creating transcription units – omega plasmid levels

To transform into *Arabidopsis*, it was necessary to ligate pDGB1alpha1 (containing kanamycin resistance and our gene of interest), pDGB1alpha2 (containing kanamycin and a plant-specific BASTA resistance cassette) and pDGB3omega1 (containing spectinomycin and LB/RB sites). The exact components of this ligation reaction are listed in Table 13. Again, multiplication occurred in *E. coli* as in the previous chapters (however, the antibiotic is spectinomycin, c = 50 µg/ml).

Table 13) Components of ligation reaction with pDG3omega1 vector.

Component	Total amount
DNA (pDG1alfa1 vector with our gene of interest)	75 ng
pDG3omega1 vector	75 ng
pDG1alpha2 vector with BASTA resistance cassete	75 ng
BsmBI enzyme (Thermo Fischer, 10U/µl)	1 µl
buffer for ligase (10x concentrated, Promega)	1 µl
T4 DNA ligase (Promega, 3U/µl)	1 µl
distilled deionized water	calculate to the final volume (10 µl)

pDG3Omega1 vectors thus prepared and isolated were transformed into *Agrobacteria* (procedure described above, but the strain without helper plasmid is used). The transformed bacteria were inoculated onto plates containing LB medium with the antibiotics listed in Table 14. Selected plasmids were used for stable transformation into *Arabidopsis thaliana*.

Table 14) List of antibiotics used to select bacteria suitable for stable transformation into *Arabidopsis.*

Antibiotic	Concentration used (µg/ml)
gentamycin (Duchefa)	10
spectinomycin (Duchefa)	50
rifampicin (Duchefa)	25

Stable transformation of *Arabidopsis thaliana*

Arabidopsis thaliana ecotype Col-0 (NASC ID: N70000) was used for stable expression. The transformation was based on Clough & Bent (1998) and carried out as follows.

Again, it was necessary to first prepare suitable plants, we cut away all siliques and fertilized flowers, left just the young, non-fertilized flowers.

Subsequently, we inoculated *Agrobacterium* carrying the desired plasmid into 1 ml of liquid LB medium (in a 50 ml falcon tube, without antibiotics) and allowed to grow for 6 hours shaking at 28°C. After this time we added another 10 ml of LB media and let overnight shaking grow at 28°C.

The next day we added 40 ml of dip media (1 l H_2O, 100 g sucrose, 500 µl Silwet (AgroBio Opava)) into the same falcon tube to well-grown *Agrobacterium* culture and mixed. We dipped *Arabidopsis* flowers in this bacterial suspension for approximately 30 seconds. After dipping, we attached the plants to a stick and placed them in a dark and humid room/box, where we left them until the next day, when we transferred them to the culture room.

Mature seeds were harvested and subsequently selected.

Selection of transgenic plants

T1 seeds of *Arabidopsis* plants containing all newly-prepared constructs were grown on vertical plates containing ½ MS medium and the BASTA (glufosinate ammonium, phosphinothricin) antibiotic (15 µg/ml, Cayman chemical) after sterilization and 2-3 days stratification. Only green, viable plants were selected for further microscopic analysis. Plants with clear signal of the desired fluorescent proteins were kept and transplanted into Jiffy pellets and grown. After approximately 2 to 3 weeks T2 seeds were harvested and used for further analysis.

Statistics and reproducibility

- *Figure 13)* ***Comparison of Col-0 and HS::AXR3-1 roots after heat shock.*** - analysed in 3 replicates, each with a minimum of 15 roots for each treatment; results reported from a single replication; statistics not applied
- *Figure 14)* ***Growth of HS::AXR3-1 x DII-Venus after heat shock.*** - analysed in at least 5 replicates, in each of at least 7 roots for each treatment; results reported from a single replication; statistics on growth rate were applied - standard deviation, relative intensity was measured from approximately 3 roots, repeated 3x
- *Figure 15)* ***HS::AXR3-1 x DII-Venus and DII-Venus lines without heat shock.*** - analysed in 3 replicates, each with a minimum of 7 roots for each treatment
- *Figure 17)* ***Microscopic analysis of g1090::XVE>>AXR3-1-mCherry line.*** - analysed in 3 replicates, each with a minimum of 7 roots for each treatment
- *Figure 18)* ***g1090::XVE>>AXR3-1-mCherry induction, and quantification of growth and signal intensity.*** - analysed in at least 5 replicates, in each of at least 7 roots for each treatment; results reported from a single replication; statistics were applied - standard deviation, absolute intensity was measured from approximately 3 roots, repeated 3x
- *Figure 19)* ***The response of g1090::XVE>>AXR3-1-mCherry to auxin.*** - analysed in 3 replicates, each with a minimum of 15 roots for each treatment; results shown from all replicates together; statistics not applied
- *Figure 20)* ***g1090::XVE>>AXR3-1-mCherry x DII-Venus line.*** - analysed in 2 replicates, each with a minimum of 9 roots for each treatment
- *Figure 23)* ***Microscopic analysis of GAL4-GFP driver lines.*** - analysed in 1 replicate, each with a minimum of 5 roots for each treatment
- *Figure 24)* ***Comparison of GAL4>>AXR3-1, GAL4>>AXR3-1-GR with and without DEX.*** - analysed in 3 replicates, each with a minimum of 12 roots for each treatment
- *Figure 25)* ***VGI of the UAS::AXR3-1 line and the UAS::AXR3-1-GR lines crossed with J2821, J0591 and J0391 lines.*** - analysed in 3 replicates, each with a minimum of 5 roots for each treatment; results shown from all replicates together; Anova like Kruskal Wallis test statistics was applied

- *Figure 26)* ***Localization of IAA17 and AXR3-1 versions with N- and C-terminal fluorescent protein fusions in tobacco leaf epidermis.*** - infiltration repeated at least 2x, at least 3 microscopic images from each construct
- *Figure 27)* ***GR-AXR3-1/IAA17 and its response to DEX treatment in tobacco leave cells.*** - infiltration repeated at least 2x, at least 3 microscopic images from each construct
- *Figure 28)* ***AXR3-1 or IAA17 proteins containing NESNES and 8KFarn in tobacco leaf epidermal cells.*** - infiltration repeated at least 2x, at least 3 microscopic images from each construct
- *Figure 30)* ***DII-mVenus-mScarlet construct infiltrated into tobacco***. - infiltration repeated at least 2x, at least 3 microscopic images from each construct
- *Figure 31)* ***Expression of IAA17 and AXR3-1 fused with mVenus and controlled by the PIN2 promoter.*** - repeated 1x, analysed at least 7 roots from each line
- *Figure 33)* ***Arabidopsis root tips expressing AXR3-1 fused with GR, 8KFarn and NESNES under the control of PIN2 promoter***. - repeated 1x, analysed at least 7 roots from each line
- *Figure 36)* ***Expression of AXR3-1-mScarlet under the control of different tissue-specific promoters.*** - repeated 1x, analysed at least 7 roots from each line
- *Figure 38)* ***4 day old plants containing AXR3-1 and driven by PIN2 promoter.*** - repeated 1x, analysed at least 15 roots from each line
- *Figure 39)* ***PIN2::AXR3-1-mVenus analysis.*** - repeated 1x, analysed at least 10 roots, VGI analysed 1x, at least 12 roots for each treatment, statistics not applied
- *Figure 40)* ***Growth rate analysis of the PIN2::AXR3-1-mVenus line.*** - repeated 1x, analysed at least 10 roots
- *Figure 41)* ***Microscopic analysis of the PIN2::GR-AXR3-1-mVenus line.*** - repeated 2x, analysed at least 10 roots for each treatment
- *Figure 42)* ***Time series of the PIN2::GR-AXR3-1-mVenus line after DEX/DMSO application.*** - repeated 2x, analysed at least 10 roots for each treatment
- *Figure 43)* ***Microscopic analysis of the PIN::AXR3-1-mVenus8KFarn line.*** - repeated 1x, analysed at least 10 roots
- *Figure 44)* ***Microscopic analysis of the PIN2::AXR3-1-mVenusNESNES line.*** - repeated 1x, analysed at least 10 roots

Results

Inducible AXR3-1 expression and effect on root growth and auxin response

The *axr3-1* mutant was chosen as a suitable study tool. However, as described in the previous chapters, its dominant mutant has a pleiotropic phenotype, which would make observing and obtaining the data necessary to test the established hypotheses very difficult (e.g. changes in root meristem do not allow monitoring of cell elongation). Therefore, predominantly inducible system lines were used. In addition, the use of inducible systems make it possible to monitor the effect of this mutation on the initial responses of the root (whether it is growth or gravitropic response). Each section includes a detailed description of the particular mutant line used.

HS::AXR3-1 and HS::AXR3-1 x DII-Venus line

In the initial experiments, I used HS::AXR3-1 line alone or a crossed combination with an auxin sensor. HS::AXR3-1 line contains a mutated AXR3-1 protein expressed under the heat shock (HS) promoter, allowing inducible expression by heat shock treatment (Figure 12, A). After this activation, the protein is produced for a period of time during which the effect of its expression on the phenotype of the root is observed (Knox, 2003). To be able to monitor auxin response levels in the cells, we crossed into the HS::AXR3-1 line the auxin perception sensor DII-Venus. Brunoud et al. (2012) fused the fast maturing monomeric yellow fluorescent protein (mVenus) to the auxin and TIR1 interaction domain (domain II) of Aux/IAA28 and expressed it under the control of the constitutive 35S promoter (Figure 12, B). Due to the presence of domain II, the fusion protein forms a complex with auxin and the TIR1/AFB receptor, and in turn is ubiquitinated by the activity of the SCF^{TIR1} complex and degraded in response to auxin (Figure 12, C). This allows us to obtain a reverse map of auxin response presence (Figure 12, D).

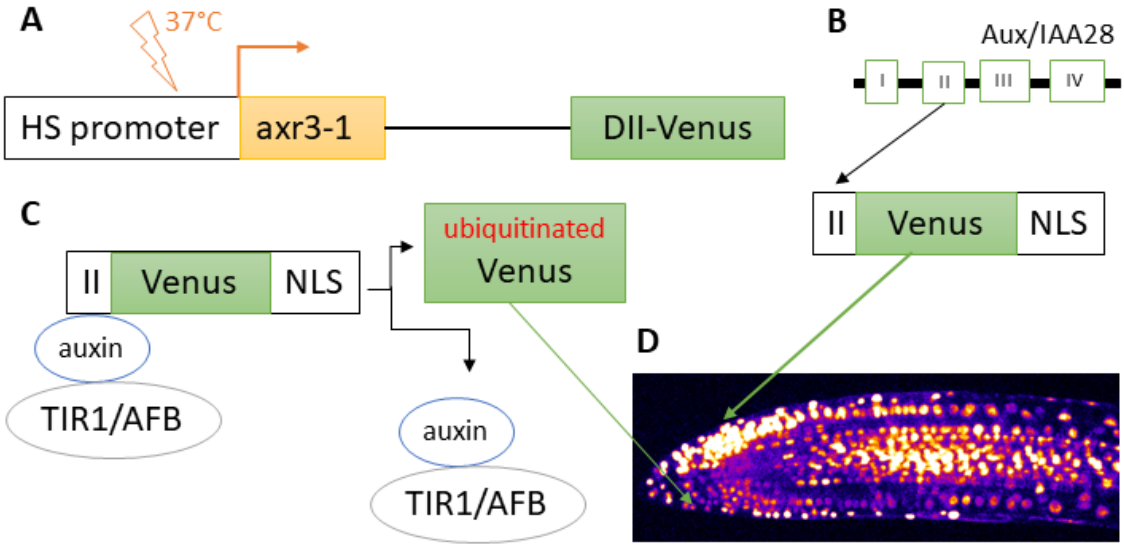

Figure 12) **The principle of the HS::AXR3-1 inducible line and the DII-Venus auxin reporter line.** A) The AXR3-1 gene is under the control of the heat shock promoter. DII-Venus, which is composed of Aux/IAA28 domain II and Venus fluorescent protein (B), that is crossed into the HS::AXR3-1 line. In the presence of auxin, ubiquitination and subsequent degradation of DII-Venus occur (C), resulting in a reversal map of the presence of auxin (D). D) A gravitropically stimulated root. A strong signal at the top of the root indicates the absence of auxin, while at the bottom of the root, there is a weak signal indicating the presence of auxin.

It was shown that induction of HS::AXR3-1 leads to a transient agravitropism (Knox, 2003), and that degradation of Aux/IAAs correlates with root growth rate (Figure 10). Therefore I analysed the growth kinetics of HS::AXR3-1 and Col-0 lines in response to a heat shock treatment (37°C, 40 min). As expected, the HS::AXR3-1 line became agravitropic, while the control line remained positively gravitropic (Figure 13, B). The growth rate of the HS::AXR3-1 was higher than growth rate of the Col-0 (Figure 13, A). The explanation of the loss of gravitropism could be the loss of gravity perception in the cells of columella, loss of auxin transport or the inability to respond to auxin (Sato et al., 2015). Therefore, I analysed the response of the lines to increasing concentrations of IAA (10/50 nM IAA). The growth rate of the control line decreased with increasing auxin concentration. In contrast, mutant lines grew faster and the auxin inhibition of growth was less noticeable (Figure 13, A). The results indicate that the mutant line is partially auxin insensitive.

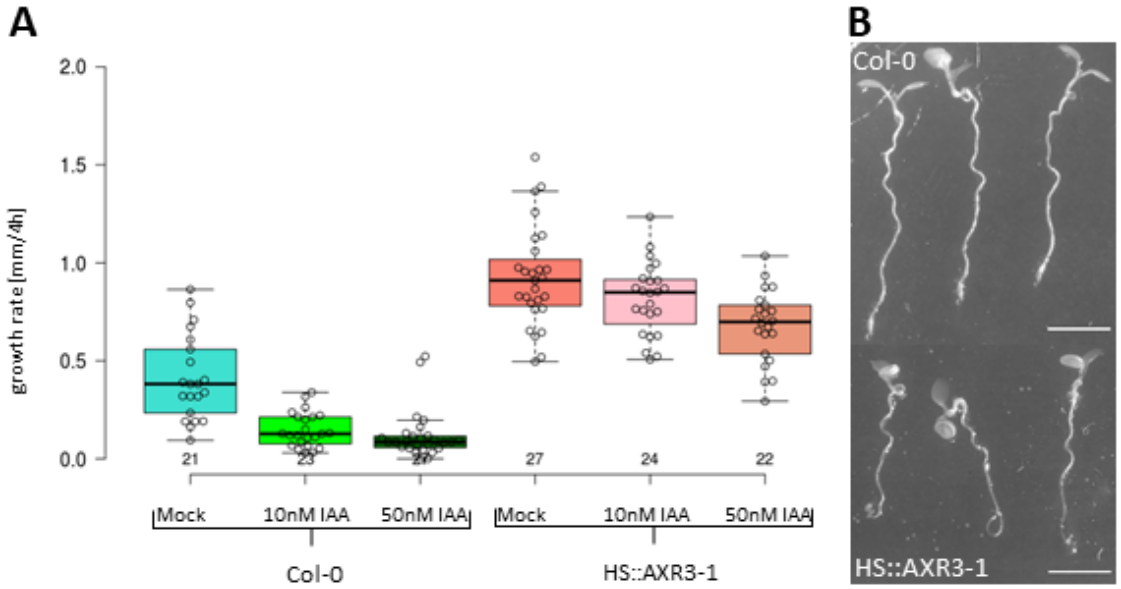

Figure 13) **Comparison of Col-0 and HS::AXR3-1 roots after heat shock.** A) Growth rate after 4 hours. Mutant plants grew faster and their response to auxin was reduced. Both lines showed decreased growth rate after auxin treatment, in respect to auxin concentration. Both lines were treated with 0/10 and 50 nM IAA. Numbers of analysed plants are indicated. B) Phenotype of control and mutant plants. The HS::AXR3-1 line showed agravitropic roots, while the Col-0 was gravitropic. Scale bars = 5 mm.

To test the presence of auxin gradient during gravitropism, we observed the DII-Venus marker in the HS::AXR3-1 line and Col-0 after heat shock induction. Both growth rate and intensity of DII-Venus were analysed.

Surprisingly, the mutant line showed a sharp increase in growth upon activation of the promoter. The growth rate gradually decreased over time, and then we observed a decrease of growth (approximately 8 - 10 hours after heat shock). Such growth changes were not observable in control lines that have been exposed to the same conditions (Figure 14, B).

Next, it could be seen that the DII-Venus signal was well observable in the control line, and formed a gradient during gravitropic response, while the signal of DII-Venus in the HS::AXR3-1 x DII-Venus lines gradually disappeared with time (Figure 14, A). The intensity of DII-Venus was unchanged or slightly increased in the control lines, in contrast to the HS::AXR3-1 x DII-Venus relative intensity, which decreased rapidly (Figure 14, C).

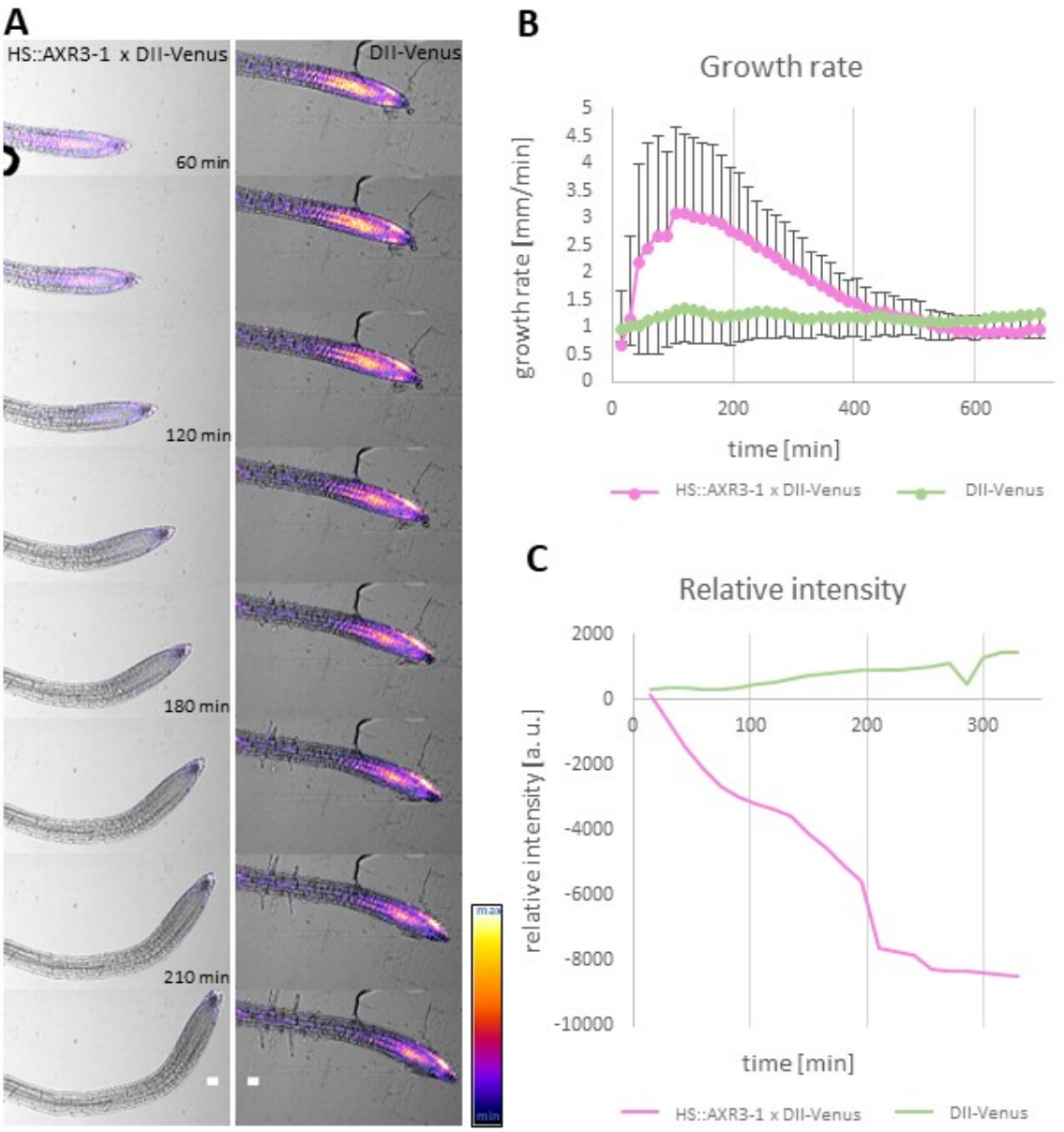

Figure 14) **Growth of HS::AXR3-1 x DII-Venus after heat shock.** A) Auxin gradient and root growth over time. Mutant lines grew faster, were agravitropic, and did not form root hairs. In the mutant line, the DII-Venus signal was gradually lost. Microscope settings and image processing is the same for both lines. Time since the beginning of the heat shock is indicated. The calibration bar on the right shows the fluorescence signal intensity. Scale bars = 50 µm. B) Growth rate of HS::AXR-1 and Col-0 over time. The mutant line first accelerated and then slowed. Error bars represent standard deviation. C) The relative intensity of the DII-Venus in the control and the HS::AXR3-1 lines in which this signal was gradually lost. Average of 3 roots is shown. Plants were gravistimulated.

To confirm that the AXR3-1 expression causes the decrease of the DII-Venus signal, I performed an additional control experiment, where I analysed the HS::AXR3-1 line without applying heat shock. In this case the DII-Venus signal was comparable to control (Figure 15) and accordingly, roots of both lines were gravitropic.

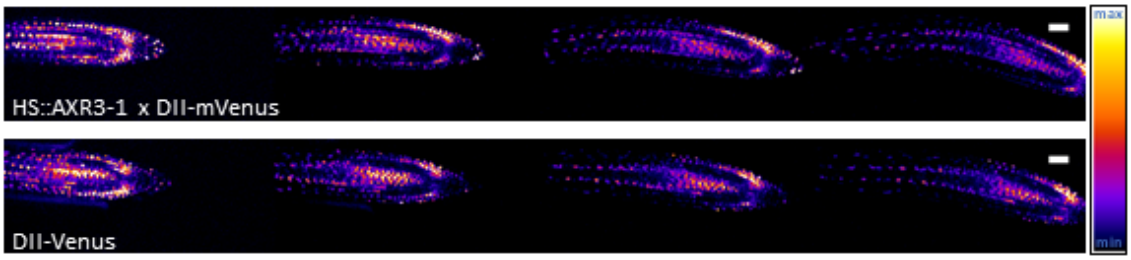

Figure 15) **HS::AXR3-1 x DII-Venus and DII-Venus lines without heat shock.** A time series was taken immediately after gravistimulation and imaged every 30 min. There were no differences in signal intensity and distribution of DII-Venus signal. Both lines were gravitropic. The calibration bar on the right shows fluorescence signal intensity. Scale bars = 50 µm.

In summary, induction of AXR3-1 protein expression resulted in faster growth and partial insensitivity to auxin. In addition, the DII-Venus pattern was disrupted in mutant lines. The fact that the DII-Venus signal was not disturbed in the DII-Venus plants after the heat shock suggests that the loss of signal was not due to elevated temperature. However, the signal was not altered in mutant lines that have not been activated, suggesting that the presence of the mutated form of AXR3-1 protein is responsible for DII-Venus signal loss.

Estradiol-inducible AXR3-1 expression

The heat shock induction is a rather harsh treatment that will trigger the expression of a large set of genes (Wang et al., 2016). Therefore I used XVE, estradiol induction system, which should be more specific than heat shock (Siligato et al., 2016).

g1090::XVE>>AXR3-1-mCherry line

The available g1090::XVE>>AXR3-1-mCherry inducible line (Mähönen et al., 2014), represents a modified use of the classical XVE system. This construction principle was used to insert a modified version of the XVE inducible system (Zuo et al., 2000) to replace constitutive promoters. The chimeric transcriptional activator XVE is expressed under constitutive synthetic promoter (in our case g1090), and terminated by two terminator sequences: e9T and nosT. Upon estradiol treatment, the XVE binds to multiple copies of XVE-binding sites in LexA operator sequence fused with a minimal cauliflower mosaic virus 35S promoter (together called pLexA) to promote the transcription of *axr3-1* only in the tissues where the promoter of interest is active (Siligato et al., 2016) (Figure 16).

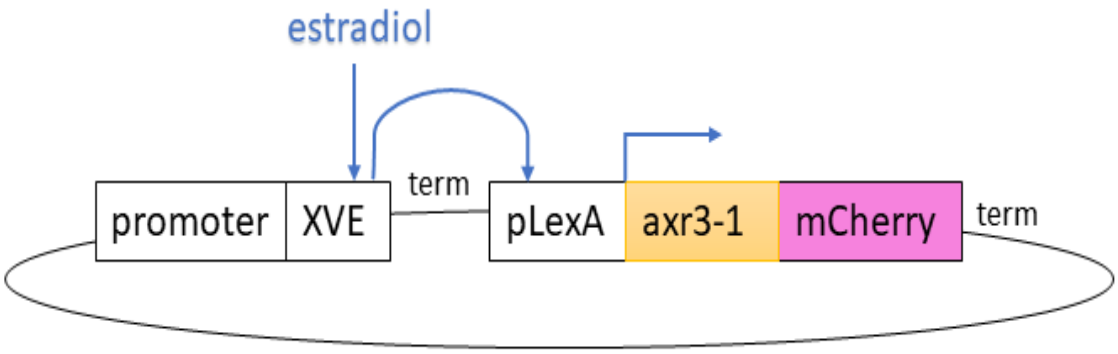

Figure 16) **Principle of regulation of XVE system by estradiol.** After estradiol treatment, estradiol is bound to XVE and the product binds to pLexA operator resulting in the expression of *axr3-1* gene fused to mCherry.

Approximately 4 day old plants were transferred to estradiol containing medium and subsequently analysed. After 1.5 hours we could see the AXR3-1-mCherry signal, roots were agravitropic, they grew faster and did not create root hairs (Figure 17, A). The signal was observed mainly in the nucleus (Figure 17, B).

Growth rate and intensity of mCherry fluorescence were also analysed. The growth rate of the mutant lines after activation was increased, gradually decreasing until the root grew slower than the control (Figure 18, B). The intensity of mCherry fluorescence gradually increased over time, while we have not observed any signal in the control line. No changes in absolute intensity or growth rate were observed in the control line (Figure 18, C).

As mentioned, the signal was observed as early as 1.5 hours after estradiol treatment, gradually increasing its intensity over time (Figure 18, A). Since the roots increase their growth rate even earlier, we assume that the mutant protein is expressed earlier, but signal detection is technically limited.

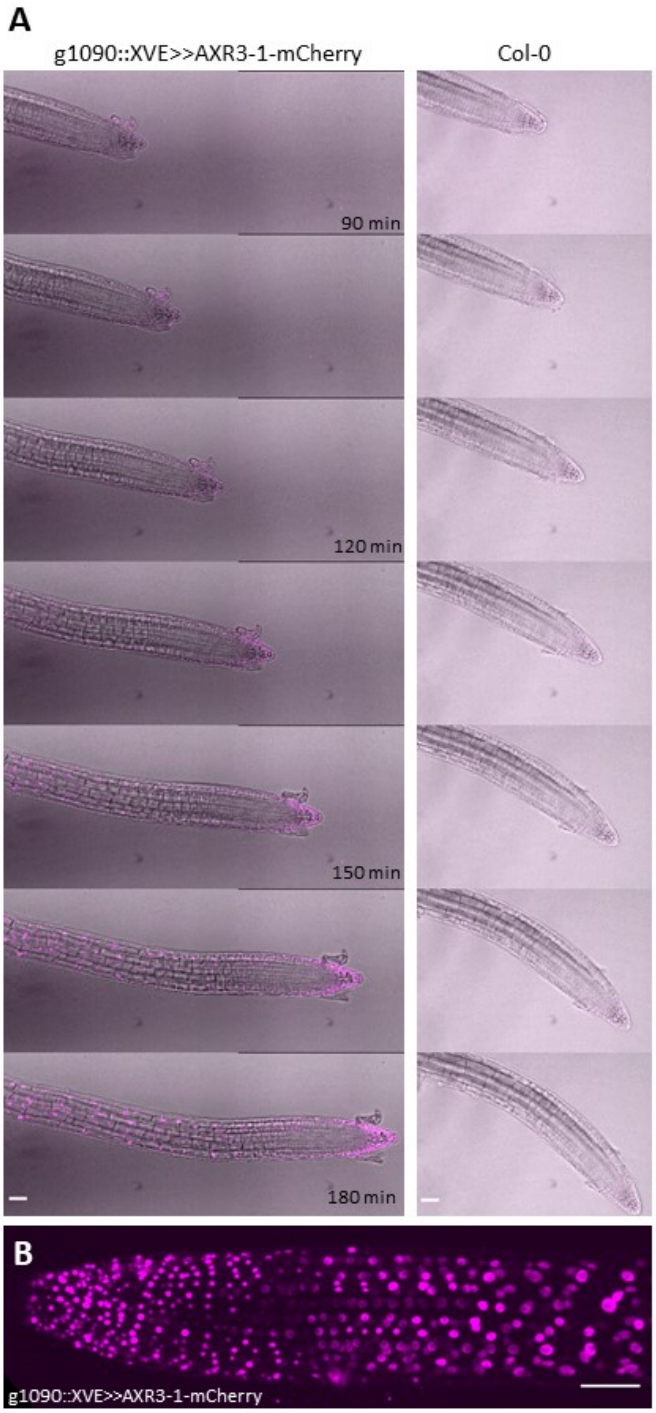

Figure 17) **Microscopic analysis of g1090::XVE>>AXR3-1-mCherry line.** A) Comparison of growth rate and gravitropic response of the g1090::XVE>>AXR3-1-mCherry line and the control (Col-0). Both lines were transferred to estradiol-containing medium and after 1.5 hours gravistimulated. Mutant roots grew faster, were agravitropic and did not form root hairs. Time after transfer to the estradiol-containing medium is indicated. B) Root tip of g1090::XVE>>AXR3-1-mCherry plant after approximately 3 hours on estradiol containing medium. The AXR3-1 protein fused to mCherry was predominantly localized to the nucleus, A maximum projection of confocal z-sections. Scale bars = 50 µm.

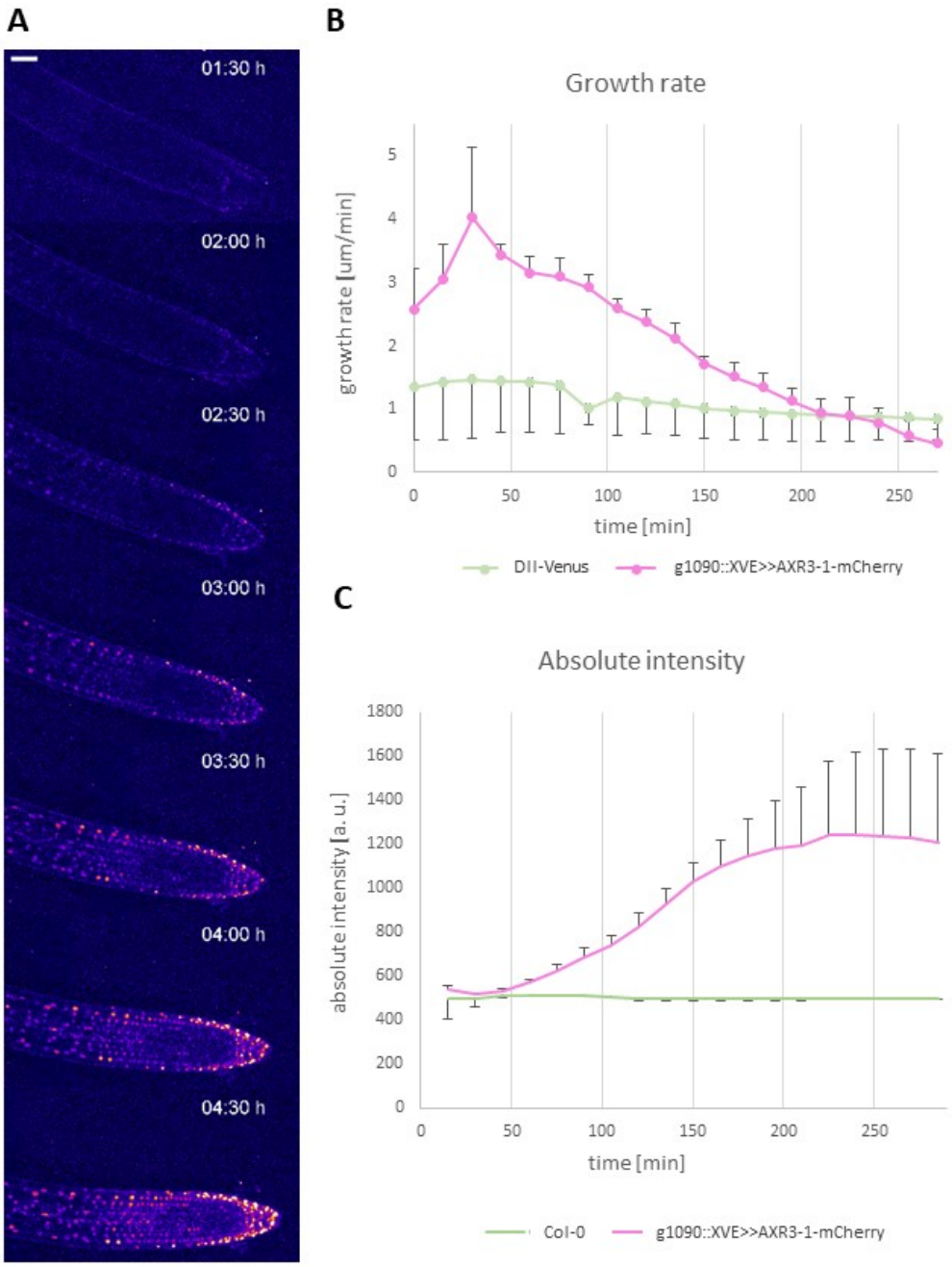

Figure 18) **g1090::XVE>>AXR3-1-mCherry induction, and quantification of growth and signal intensity.** A) Gradual induction of the mCherry signal after estradiol treatment showed the localization of the AXR3-1 protein. Time after transfer to estradiol-containing medium is indicated. Scale bar = 50 µm. B) Growth rate. The g1090::XVE>>AXR3-1-mCherry mutant line increased the growth rate, but in time it began to decrease until the rate was less than the growth rate of the control line, which level had barely changed throughout the experiment. Analysis started 1.5 hours after estradiol treatment. On the x-axis, 0 represents the beginning of the microscopic analysis. Error bars represent standard deviation. C) Signal intensity of AXR3-1-mCherry. The intensity of mCherry gradually increased in the mutant line. Mean of 3 mutant and 3 control roots were measured. Error bars represent standard deviation.

The phenotypes described above could be due to alterations in auxin perception. To verify that, mutant lines were treated with different concentrations of auxin and the root length increment was measured after 4 hours (Figure 19). In one case, the Col-0 plants was used as control line, subjected to the same conditions as the mutant lines (Figure 19, A) and in the second case, the control was a mutant line that was not exposed to estradiol, thus AXR3-1 was not expressed at all (Figure 19, B).

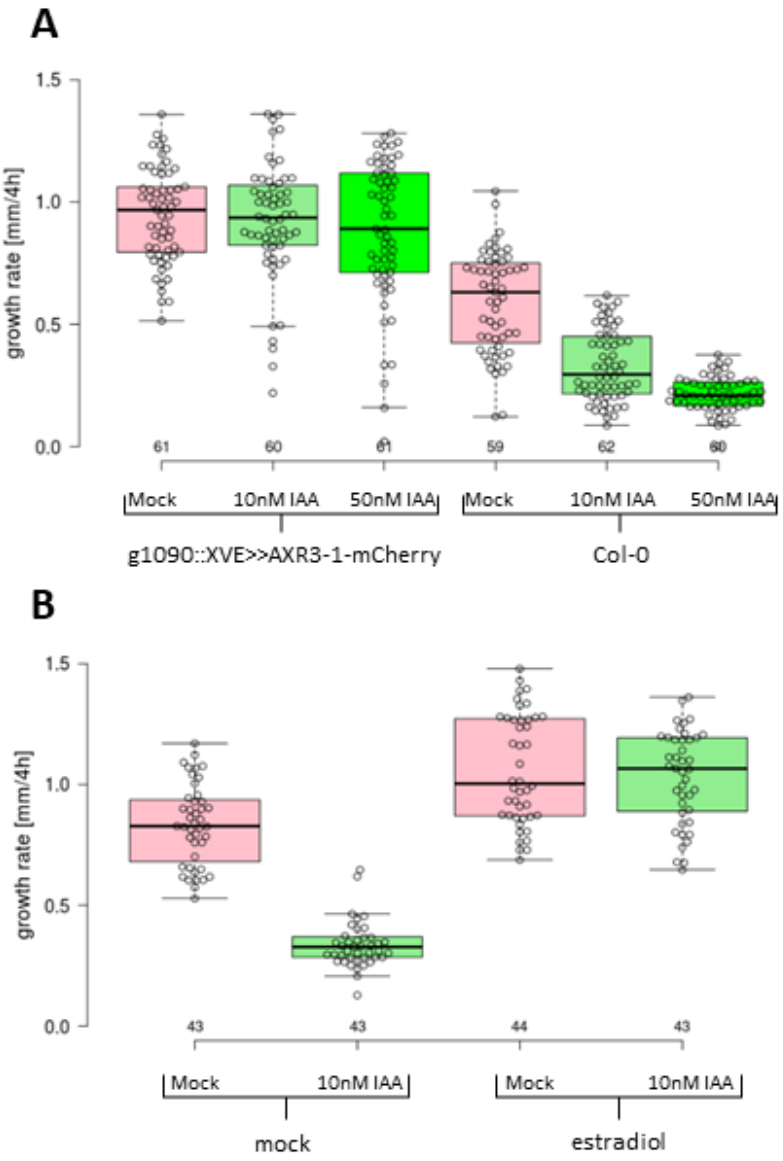

Figure 19) **The response of g1090::XVE>>AXR3-1-mCherry to auxin.** A) Effect of increasing concentration of IAA on g1090::XVE>>AXR3-1-mCherry and comparison of growth rate versus control. Mutant lines grew faster and showed insensitivity to auxin. Numbers of analysed plants are indicated. B) The effect of auxin treatment on g1090::XVE>>AXR3-1-mCherry lines used as a control plants that were not activated by estradiol treatment. Estradiol-activated g1090::XVE>>AXR3-1-mCherry lines grew faster and again showed insensitivity to auxin.

Both attempts yielded the same result. In the first case, dose-dependent inhibition of root growth in control lines after auxin treatment could be observed, whereas mutant lines grew more rapidly and showed auxin insensitivity. Similar conclusion could be deduced from the second experiment.

Altogether, the results suggest that the AXR3-1 protein is localized in the nucleus and its mutation results in faster root growth, which slows down over time and gradually stops. This confirms the role of AXR3-1 in regulation of root growth. In addition, mutant lines show auxin insensitivity, confirming involvements of AXR3-1 protein in the auxin signalling pathway.

g1090::XVE>>AXR3-1-mCherry x DII-Venus

Analysis of the HS::AXR3-1 x DII-Venus line showed that the DII-Venus signal and its gradient were disrupted after activation. Since this signal was comparable to the control line in non-activated mutant lines, I aimed to verify the reason for the loss of the DII-Venus signal. For that purpose, I crossed the DII-Venus into g1090::XVE>>AXR3-1-mCherry line. The explanation for the loss of signal could be the presence of high concentrations of auxin or its impaired signalling. This line could allow us to find out more information.

In the time series of g1090::XVE>>AXR3-1-mCherry x DII-Venus line, we observed how the intensity of DII-Venus has gradually weakened and at the same time the presence of the mCherry signal has increased (Figure 20, A). Interestingly, in cells where the AXR3-1 protein expression started (which induces the mCherry signal), the DII-Venus signal was turned off (Figure 20, B). Changes in DII-Venus intensity were not observed in the control line (Figure 20, A).

This observation is consistent with the results of previous experiments and suggests again on a link between the AXR3-1 protein and auxin signalling disruption.

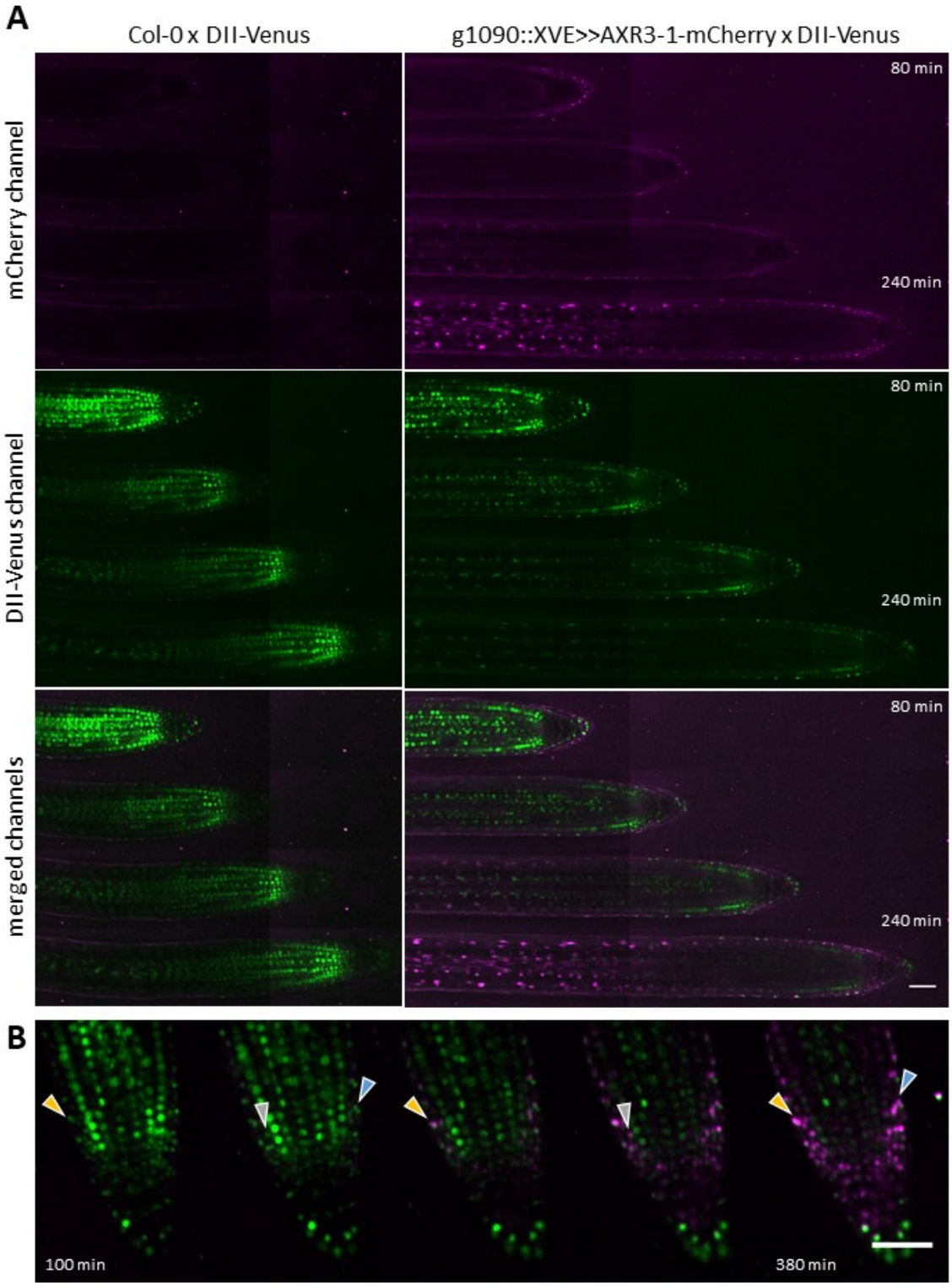

Figure 20) **g1090::XVE>>AXR3-1-mCherry x DII-Venus line.** A) Time series analysis of the control (left side) and the mutant line (right side of the image), first with split channels for mCherry and DII-Venus and then with their overlap. In mutant line, the DII-Venus signal gradually disappeared while the mCherry signal gradually appeared. B) Detail on the root tip of the g1090::XVE>>AXR3-1-mCherry x DII-Venus line. Arrows indicate cells in which the DII-Venus signal was turned off gradually after the mCherry signal was detected. The time indicates the time from the start of the transfer of plants to the estradiol-containing medium. The roots were not gravistimulated. Scale bars = 50 μm.

Root tissue-specific expression of AXR3-1 and AXR3-1-GR using the GAL4 activator lines

Another aim of this diploma thesis was to analyse the effect of tissue-specific expression of *axr3-1* gene, for which the GAL4/UAS lines (Haseloff, 1998) were used at the beginning of the project.

GAL4/UAS system

The GAL4/UAS system is commonly used to drive expression of a gene of interest. Tissue-specific promoters drive expression of GAL4 protein, derived from yeast, that results in transcriptional activation from the GAL4 binding sites - Upstream Activation Sequence (UAS) to drive expression of a gene of interest (Brand & Perrimon, 1993), in our case it is *axr3-1* gene. In addition, our system employs a glucocorticoid receptor (GR) sequence fused in frame to stabilized AXR3-1. This system will be used for transactivation of UAS::AXR3-1-GR to modify the location of the AXR3-1 protein, which will depend on the presence of dexamethasone (DEX) in the medium. In the presence of DEX, this protein will be located in the nucleus. If there is no DEX in the medium, the AXR3-1-GR complex will be located in the cytoplasm (Schmitt & Stunnenberg, 1993) (Figure 21).

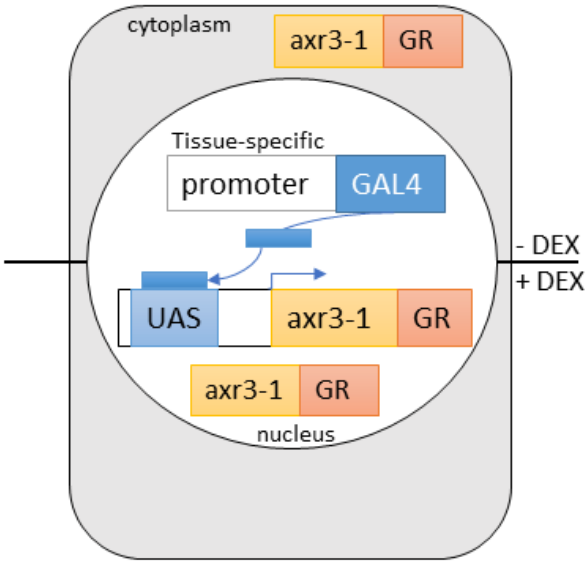

Figure 21) **Schematic principle of the GAL4/UAS system.** The tissue-specific promoter drives expression of the GAL4 protein that binds to its binding site (UAS), thereby driving the expression of the AXR3-1-GR complex. Due to the presence of GR it is possible to change the localization of this complex. In the absence of DEX, AXR3-1-GR complex is localized in the cytoplasm, but in the presence of DEX, the complex moves to the nucleus.

I used the GAL4 activation lines from the Haseloff collection (Haseloff, 1998) that drive the expression of GAL4 in tissues of interest and contain UAS::ER-GFP as a control for the transactivation activity. I selected those lines that drive expression in the epidermis, cortex, pericycle, endodermis and elongation zone. The native expression of the iaa17/axr3 gene was characterized in the meristematic zone, parts of elongation and maturation zone of the root, with the highest level of expression being seen in the meristematic zone (data is taken from http://bar.utoronto.ca/eplant/). High level of expression was determined primarily in the cortex, but also in the epidermis, endodermis and pericycle of the meristematic zone (Figure 22). The mutant lines we used follow this pattern.

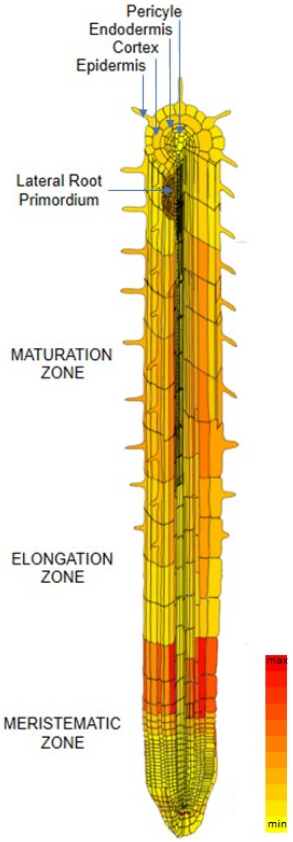

Figure 22) **Expression of the iaa17/axr3 gene in the root.** iaa17/axr3 is most expressed at the crossing of the meristematic and elongation zones, also in the elongation and maturation zones. On the cross-section of the root tissues, iaa17/axr3 is expressed in the epidermis (particularly in the trichoblasts), in the cortex, endodermis, phloem companion cells and the pericycle. Data is taken from http://bar.utoronto.ca/eplant/ and obtained by Effective Fragment Potential (EFP) method.

Individual mutant lines were subjected to microscopic analysis where we could see the expression of GFP in various tissues. J2821 expressed GFP in the epidermis, cortex, endodermis and pericycle. The elongation zone and epidermis specific promoter appeared to be used in the J0391 line. The signal in the lateral root cap and epidermis cells, probably in trichoblasts, could be observed in the line designated as J0951 (Figure 23). The C24 line serves as a control, which also represents the background for the other lines but did not contain the GFP construct.

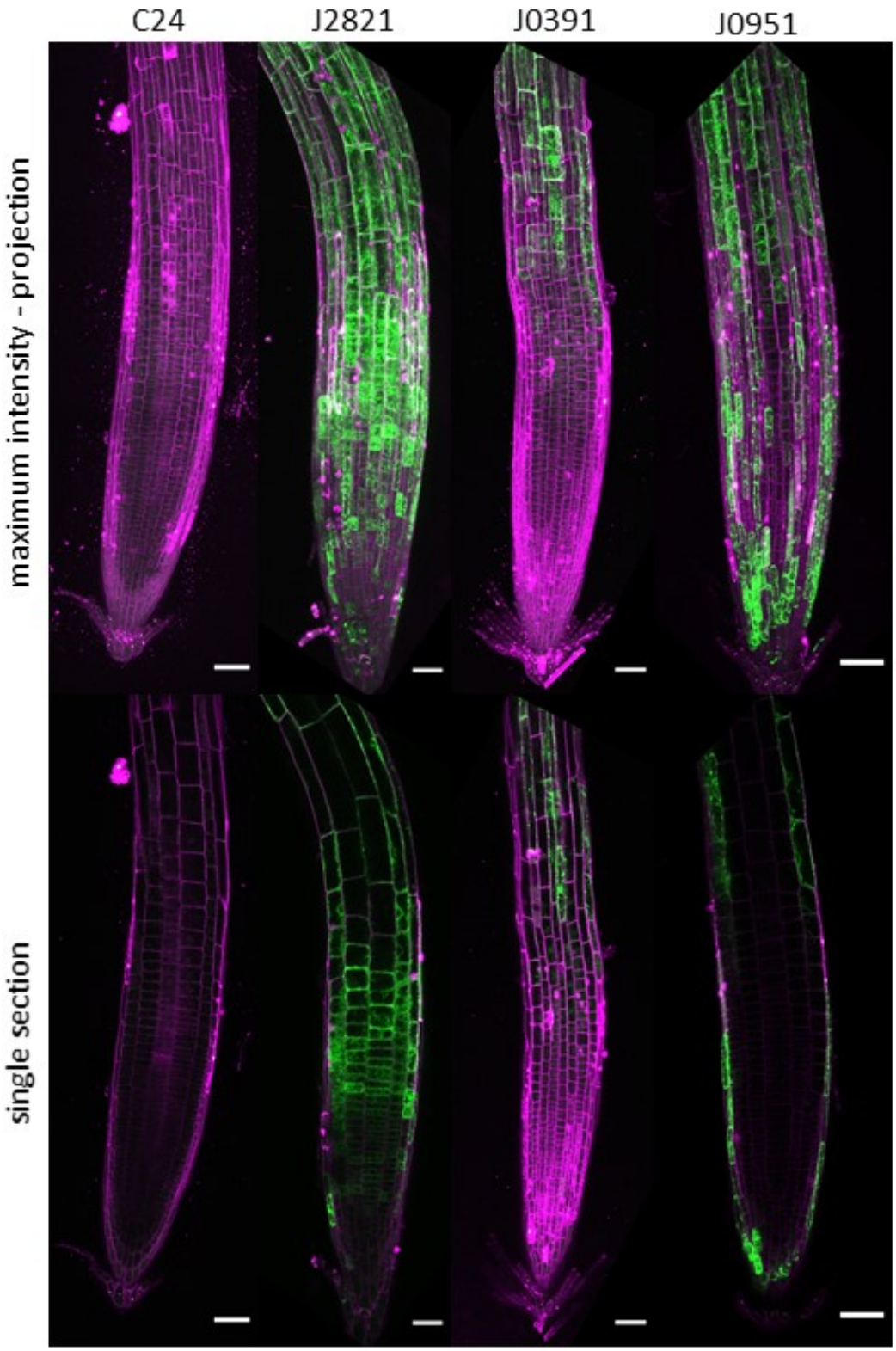

Figure 23) **Microscopic analysis of GAL4-GFP driver lines**. In the upper part of the picture is the maximum intensity of created z-stacks and in the bottom is the single z-section. The signal in the J2821 line was observed in the pericycle, endodermis, cortex, and epidermis within both the meristematic and elongation zones. The signal in the elongation zone and epidermis was observed in line J0391. J0951 line had a GFP signal in the epidermis, probably in trichoblasts, and in the LRC. Cell walls were stained with propidium iodide (magenta colour). Scale bars = 50 μm.

F1 crosses were analysed macroscopically. Plants were grown 3-4 days on MS media and subsequently transferred to media containing the DEX or mock (DMSO). DEX should cause the GR construct to be released from the complex in the cytoplasm, and move to the nucleus (Figure 21). In this case, we could see that the plants were, to varying degrees, agravitropic. The degree of agravitropism varies in intensity between different lines, suggesting the effect of the mutant protein expression site on the phenotype. The presence of the AXR3-1 protein in the cortex, epidermis, endodermis and pericycle (J2821 line) had the greatest effect, less effect if AXR3-1 was present in elongation zone + epidermis (J0391) and epidermis + LRC (J0951) (Figure 24). If we compared DEX-treated UAS::AXR3-1-GR to UAS::AXR3-1 plants, i.e. the same driver lines, but we did not change the subcellular localization of AXR3-1 protein in any way, we could see that UAS::AXR3-1 plants were more agravitropic. There may be many reasons for this, and more information can be brought to us by experiments described in other parts of this work.

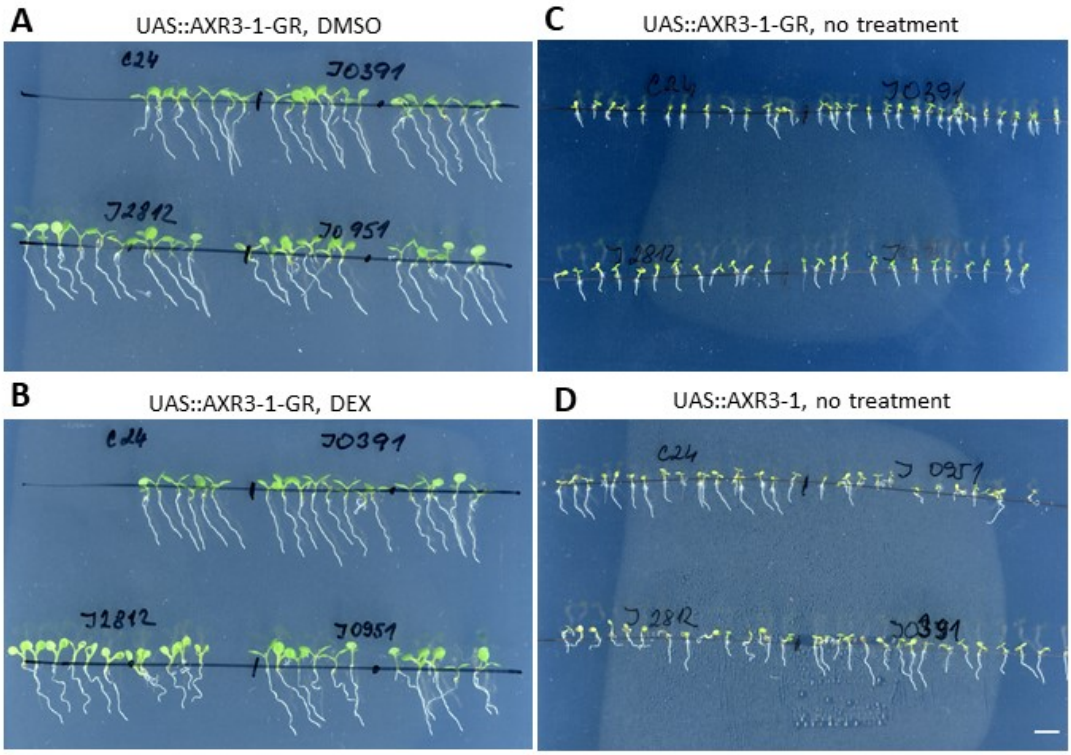

Figure 24) **Comparison of GAL4>>AXR3-1, GAL4>>AXR3-1-GR with and without DEX.** A) Approximately 7 days UAS::AXR3-1-GR treated with DEX. B) Approximately 7 days UAS::AXR3-1-GR treated with DMSO (mock). C) 3 days UAS::AXR3-1-GR without treatment. D) 4 days UAS::AXR3-1 without treatment. On the right, UAS::AXR3-1-GR plants could be seen without treatment, all lines showing the same phenotype as the control. The UAS::AXR3-1-GR plants transferred to the DMSO plates did not differ significantly from the control. Plants transferred to DEX-containing medium showed varying degrees of agravitropism. UAS::AXR3-1 were also agravitropic. Scale bar = 5 mm.

This experiment was repeated in various forms: plants were grown to the 2-day stage and then transferred to DEX-containing media and scanned after the following 4 days. Alternatively, they were grown immediately on DEX-containing plates. The results were very similar.

To quantify the degree of agravitropism in the different lines the vertical growth index of the root (VGI) was measured. VGI was defined as a ratio between the root tip ordinate and the root length (Grabov et al., 2004). The roots of approximately 4-5 days old plants from several replicates were measured and data was subsequently evaluated. Anova like test Kruskal Wallis was used for data processing, comparing the significant lines for each line compared to the control, as well as for each line separately within the different treatments.

Analysis of the UAS::AXR3-1 line showed a significant change in VGI of all lines compared to the control ($p\ value_{J2821} < 0.0487$; $p\ value_{J0391} < 0.0319$; $p\ value_{J0951} < 0.008$) (Figure 25, A). Next, UAS::AXR3-1-GR plants were further analysed, treated with DEX (=AXR3-1-GR in the nucleus) and DMSO (=AXR3-1-GR in the cytoplasm) (Figure 25, B and C). After DEX treatment, only J2821>>UAS::AXR3-1-GR showed significant changes compared to control (p value < 0.0077), suggesting the importance of AXR3-1, being in the epidermis, cortex, endodermis and pericycle, in the gravitropism process. Line J0391>>UAS::AXR3-1-GR and J0951>>UAS::AXR3-1-GR did not show significant change in VGI after DEX/DMSO treatment (Figure 25, B). In general, DMSO-treated lines showed very little agravitropism compared to control (the data do not show a significant difference) (Figure 25, C). By comparing UAS::AXR3-1-GR lines after DEX and DMSO treatment (Figure 25, B and C), only changes of the J2821>>UAS::AXR3-1-GR line could be considered statistically significant (p value < 0.0022), suggesting the importance of nuclear localization of AXR3-1 if present in epidermis, cortex, endodermis and pericycle.

When comparing the UAS::AXR3-1 (Figure 25, A) and UAS::AXR3-1-GR lines treated with DEX (Figure 25, B), we could see that the degree of agravitropism was different for J0391>>UAS::AXR3-1-GR vs J0391>>UAS::AXR3-1 lines (p value < 0.0003), while the VGI of the J0591 and J2821 line appeared to be comparable (the data do not show a significant difference).

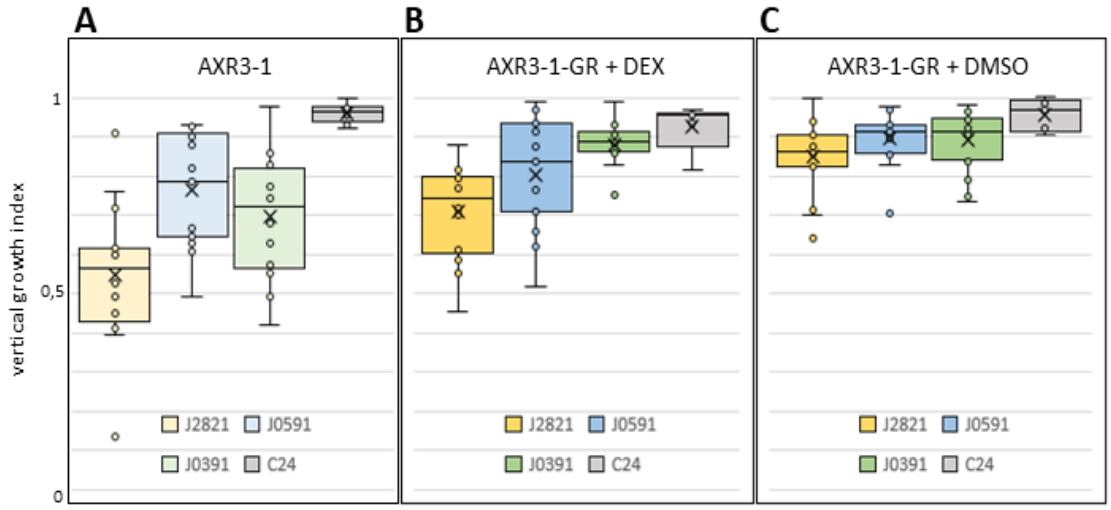

Figure 25) **VGI of the UAS::AXR3-1 line and the UAS::AXR3-1-GR lines crossed with J2821, J0591 and J0391 lines.** C24 serves as a control. A) VGI of UAS::AXR3-1 line crossed with C24, J2821, J0591 and J0391 lines without treatment. All lines showed a significant change in VGI compared to control. B) VGI of UAS::AXR3-1-GR lines crossed with the J2821, J0591 and J0391 and C24 lines and treated with DEX, in which case the most agravitropic line J2821 expressing our AXR3-1 in the epidermis, cortex, endodermis and roots pericycle. C) VGI of UAS::AXR3-1-GR lines crossed with J2821, J0591 and J0391 lines and treated with DEX solvent - DMSO. The AXR3-1-GR complex should be held in the cytoplasm. Compared to control, all three lines showed a small and comparable level of agravitropism. The VGI of J2821 line is clearly different for different treatments (DEX and DMSO), lines were more agravitropic after application of DEX. VGI of J2821>>UAS::AXR3-1-GR after DEX treatment and J2821>>UAS::AXR3-1 was comparable. Anova like test Kruskal Wallis was applied.

As a result, it can be concluded that the AXR3-1 protein, in order to function, must not be held in the cytoplasm and should be present in the nucleus. However, unless we change AXR3-1 localization in these two ways (addition of GR and thus a possible change in the localization between the nucleus and the cytoplasm), the AXR3-1 protein appeared to have a stronger effect. The results also suggest the importance of the epidermis, cortex, endodermis and pericycle in the agravitropism process. When expressed in these tissues, AXR3-1 had the greatest effect on gravitropism. Conversely, when the AXR3-1 protein was expressed in the elongation zone and epidermis, the UAS::AXR3-1 plants showed some degree of agravitropism, but this was not observed in the UAS::AXR3-1-GR lines (independent of treatment). The AXR3-1 protein expressed in the epidermis and LRC had an effect on gravitropism compared to the control, but the cross-linking of this protein to the nucleus or cytoplasm (UAS::AXR3-1-GR treated with DEX or DMSO) reduced this effect.

Preparation of new IAA17/AXR3 (WT) and AXR3-1 (mutant) protein fusions

We can draw some conclusions from previous experiments that need to be verified – in particular that the AXR3-1-GR protein is (probably) not active without application of DEX. The major disadvantage of the transactivation lines is that we could not directly visualize the localization of AXR3-1 (we could not see where exactly the protein is, we could just assume this according to the GFP signal), and that it is not clear whether the GR-fused protein can be active when DEX is not present.

Another aim of this thesis is to visualize the natural localization of the IAA17/AXR3 protein. It is well known that Aux/IAA proteins show very short life times (Rouse, 1998). To visualize the IAA17/AXR3 protein, constructs containing both the WT (designated IAA17) and the mutant (designated AXR3-1) form fused (through the both C- and N-end) with two different fluorescent proteins - the rapidly maturing mVenus-NB (Balleza et al., 2018, further named mVenus) and mScarlet-I (https://www.fpbase.org/protein/mscarlet-i/, further named mScarlet) were prepared. The version of mVenus that we use is supposedly even faster than the commonly used mVenus in plant research (Balleza et al., 2018).

Furthermore, I prepared constructs that modify the localization of AXR3-1 within the cell. These constructs contained GR, 8KFarn and NESNES parts. The function of GR has already been described in previous chapters (see Root tissue-specific expression of AXR3-1 and AXR3-1-GR using the GAL4 activator lines). 8KFarn serves as an anchor that anchors our protein of interest to the plasma membrane (Simon et al., 2016). NESNES in turn serves as a signal for transport out of the core (Schwarzerová et al., 2019).
The prepared constructs were first verified by agroinfiltration into tobacco leaf cells. A detailed list of used transcriptional parts for generating the constructs can be found in the Material and Methods chapter (see Molecular cloning).

Expression of the fusion constructs in *Nicotiana benthamiana*

To verify the correctness and functionality of the prepared constructs, I used the *Nicotiana benthamiana* transient expression system. In the following table you can see an overview of the prepared constructs through the GoldenBraid cloning system (Table 15). The exact procedure is given in the Material and Methods chapter (see Molecular cloning).

Table 15) The transcriptional parts ligated into pDG1alpha1 vector.

<table>
<tr><th>A1-B1</th><th>B2</th><th>B3</th><th>B4</th><th>B5</th><th>B6-C1</th></tr>
<tr><td colspan="2" rowspan="2">35S promoter (long)</td><td colspan="2">IAA17 (WT)</td><td>mVenus</td><td rowspan="5">35S terminator</td></tr>
<tr><td colspan="2">AXR3-1 (mutant)</td><td>mScarlet</td></tr>
<tr><td rowspan="2">35S promoter (short)</td><td>mVenus</td><td colspan="2" rowspan="2">IAA17</td><td>mVenus</td></tr>
<tr><td>mScarlet</td><td>mScarlet</td></tr>
<tr><td rowspan="2">35S promoter (short)</td><td>mVenus</td><td colspan="2" rowspan="2">AXR3-1</td><td>mVenus</td></tr>
<tr><td>mScarlet</td><td>mScarlet</td></tr>
<tr><td colspan="6"></td></tr>
<tr><td rowspan="2">35S promoter (short)</td><td rowspan="2">GR</td><td colspan="2">IAA17</td><td>mScarlet</td><td rowspan="4">35S terminator</td></tr>
<tr><td colspan="2">AXR3-1</td><td>mVenus</td></tr>
<tr><td colspan="2" rowspan="2">35S promoter (long)</td><td colspan="2">IAA17</td><td>mVenus8KFarn</td></tr>
<tr><td colspan="2">AXR3-1</td><td>mVenusNESNES</td></tr>
<tr><td colspan="6"></td></tr>
<tr><td colspan="2">35S promoter (long)</td><td colspan="2" rowspan="2">DII-mVenus</td><td rowspan="2">NLS</td><td rowspan="2">35S terminator</td></tr>
<tr><td>35S promoter (short)</td><td>mScarlet</td></tr>
</table>

In the leaves of *N. benthamiana*, the IAA17/AXR3 signal was observed predominantly in the nucleus, and a small signal level was also observed in the cytoplasm (Figure 26, A-H). There were no obvious differences when I fused mVenus or mScarlet to N- or C-terminus of IAA17/AXR3 (Figure 26, A-H). Differences in the activity of individual constructs on representative images can be explained by different infiltration efficiencies. From several repetitions could also be concluded that both FPs used were equally suitable for the visualization of this type in tobacco and C/N-tag did not have effect on visualization.

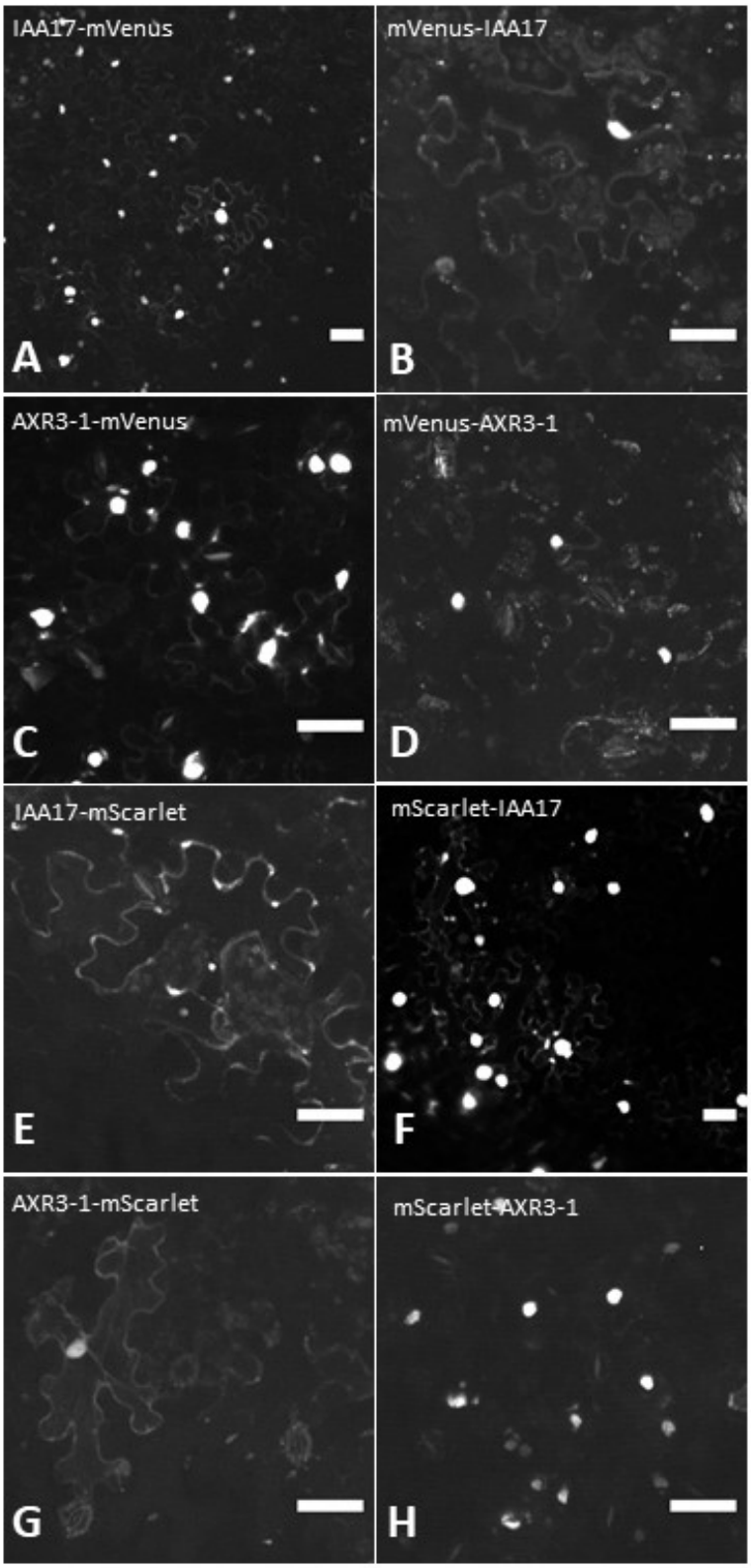

Figure 26) **Localization of IAA17 and AXR3-1 versions with N- and C-terminal fluorescent protein fusions in tobacco leaf epidermis**. Figure shows representative images of tobacco leaf epidermis expressing the respective constructs. The signal was observed predominantly in the nucleus, but with varying degrees the signal was detected in various constructs outside the nucleus. Images were adjusted in brightness contrast to visualize the signal in order to the localisation not to the intensity comparison. Images are in grey scale. Scale bars = 50 μm.

Further I analysed the localization of the constructs that manipulate subcellular localization of AXR3-1. Constructs containing GR make it possible to observe a change in the subcellular localization of IAA17/AXR3 and AXR3-1: in the absence of DEX, the signal was predominantly present in the cytoplasm for both IAA17/AXR3 and AXR3-1 (Figure 27, A-D). Interestingly, the protein appeared to form aggregates in the cytoplasm. After application of DEX, we observed the transfer of this protein to the nucleus (Figure 27, E-H).

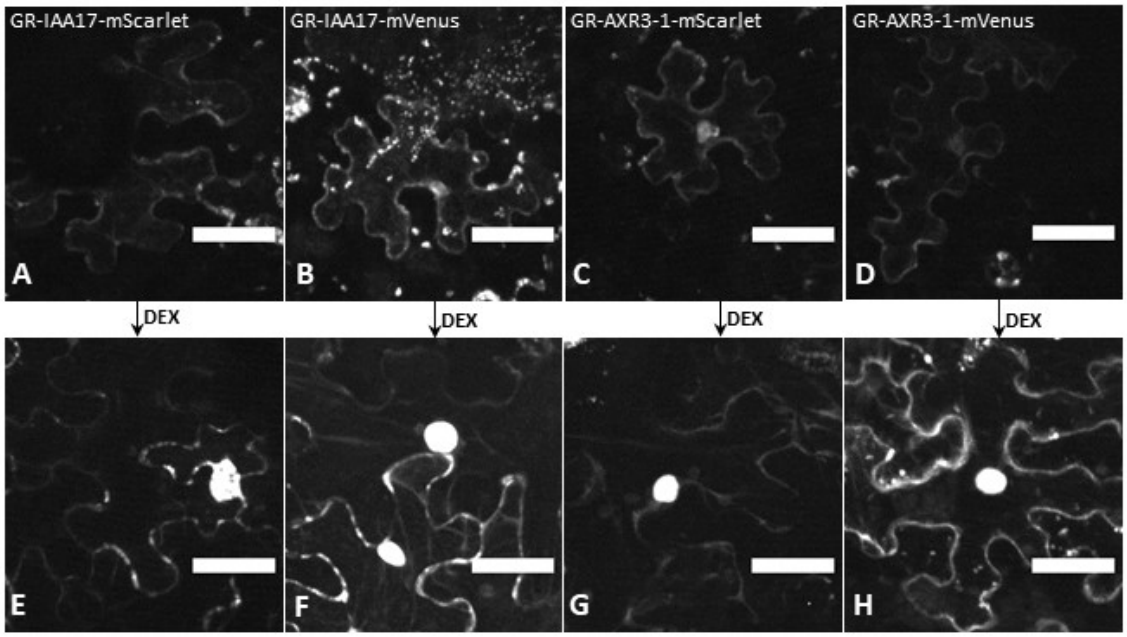

Figure 27) **GR-AXR3-1/IAA17 and its response to DEX treatment in tobacco leave cells**. A-D) GR-AXR3-1/IAA17-mScarlet/mVenus without treatment. E-H) The same constructs after DEX treatment. In the absence of DEX, GR-AXR3-1 constructs were present in cytoplasm, where they formed complexes with other proteins. After the application of DEX, signal returned to the core after a certain time (E-H). Images are in grey scale. Scale bars = 50 μm.

Since using GR binds to a HSP90 chaperon in the cytoplasm and is released after binding of DEX (Schmitt & Stunnenberg, 1993), we could not be sure that the AXR3-1 can be active in the cytoplasmic clusters. Therefore, I prepared protein fusions that keep AXR3-1 protein out of the nucleus by different means (Table 15) first one, AXR3-1-mVenusNESNES containing the nuclear export signal, and second AXR3-1-mVenus-8KFarn. The cationic probe 8KFarn farnesyl anchor is supposed to bind strictly to the plasma membrane based on electrostatic interactions (Simon et al., 2016). NESNES is multiple leucine-rich nuclear export sequences (NESs) found in plant, which are recognized by the receptor of the export pathway and actively exported from the nucleus

(Schwarzerová et al., 2019). In both cases, after infiltration into tobacco leaves, we observed a change in localization to the predicted site within the cell, but a significant portion of the signal still remained in the nucleus (Figure 28, A). Comparison of the 8KFarn fusion to the mutated or WT form of the IAA17/AXR3 protein showed no differences (Figure 28, B and C).

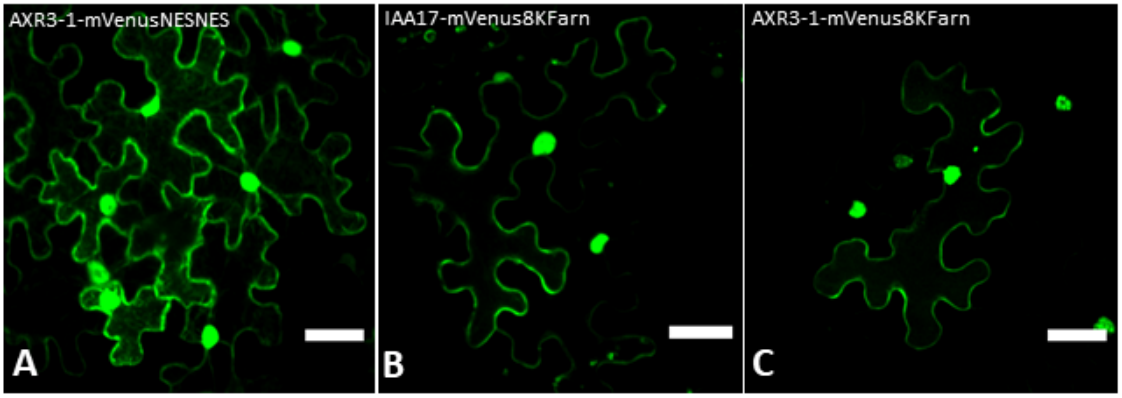

Figure 28) **AXR3-1 or IAA17 proteins containing NESNES and 8KFarn in tobacco leaf epidermal cells.** These cells had different signal ratios inside and outside the nucleus. A) NESNES construct leaded to higher localization of the fusion protein in the cytoplasm compared to the control. No differences were seen between the mutated and WT form of IAA17 fused with 8KFarn (B and C). Compared to the control (Figure 26, A), the presence of 8KFarn anchor changed the ratio of the IAA17 localization between the nucleus and the membrane in favour of the membrane. Scale bars = 50 μm.

DII-mVenus fast maturing auxin sensor

In the previous chapters, it can be seen an experiments with plants containing DII-Venus. In another series of experiments, constructs were prepared containing the DII domain of Aux/IAA28 fused to the rapidly maturing FP mVenus. Due to the shorter maturation time and in combination with the short half-life of Aux/IAAs, this sensor could potentially be even more sensitive than conventional DII-Venus (Brunoud et al., 2012). In addition, I created constructs containing two fluorescent proteins: DII-mVenus and mScarlet. DII-Venus is used as an auxin sensor and allows to obtain a reverse auxin map. As mentioned above, the problem of Aux/IAA protein visualization is primarily related to their short half-life, which in combination with the time it takes to mature FPs limits their visualization. The DII-Venus sensor works well in cells that have a very low concentration of auxin (Brunoud et al., 2012), but in cells of the root epidermis, for example, there is almost no DII-Venus signal. If the sensor maturation time would be

further minimized, the auxin response range could be broadened and so the sensor could be used also in cells with higher auxin levels. To minimize the maturation time, we merged the DII domain of Aux/IAA28 with the rapidly maturing FP mVenusNB. The signal after infiltration of these constructs was present mainly in the nucleus, a small fraction of the signal is also visible in the cytoplasm (Figure 29).

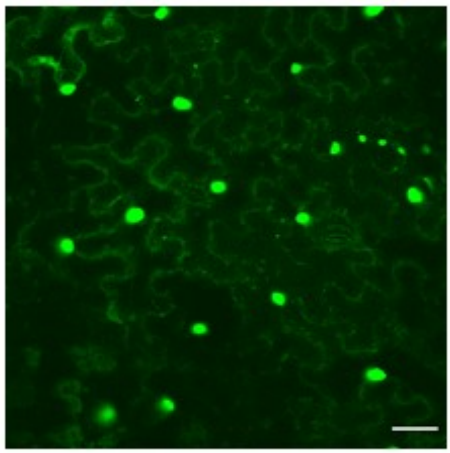

Figure 29) **DII-mVenus-NLS construct infiltrated into tobacco** (max intensity of z-stacks). Signal is predominantly in the nucleus. Scale bar = 50 μm.

Next, I created a construct containing two different FPs (DII-mVenus and mScarlet) with different maturation kinetics, which would allow to monitor the lifetime of the mScarlet-DII-mVenus protein. Both DII-mVenus and mScarlet colocalized (Figure 30). Observing this construct over time could bring interesting results. An extremely small amount of auxin would be observed as green + magenta, little auxin level as green, and a large amount of auxin would not be seen due to the degradation of mScarlet-DII-mVenus.

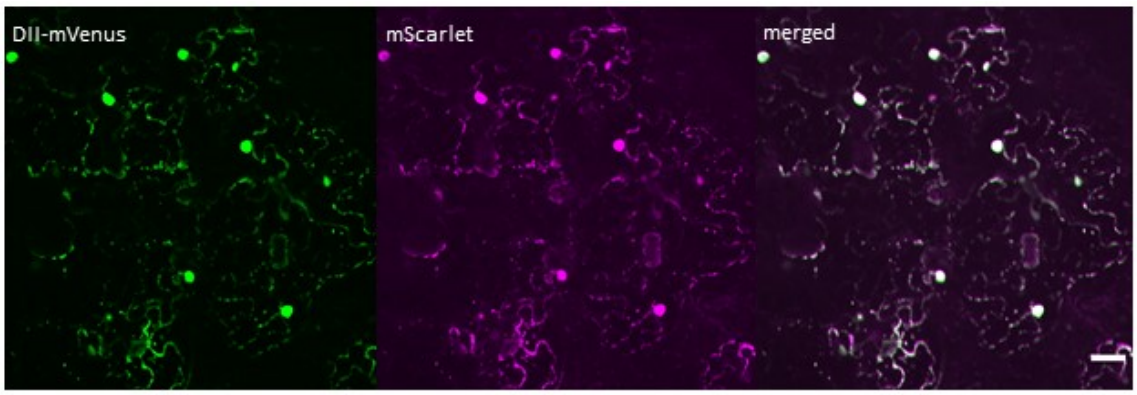

Figure 30) **DII-mVenus-mScarlet construct infiltrated into tobacco** (max intensity of z-stacks). The expression pattern of both FPs is almost the same as can be seen in the right part of the figure (merged channels). Scale bar = 50 μm.

Influence of AXR3-1 subcellular/tissue-specific localization on its effect on growth in *Arabidopsis* roots

After testing expression and localization of the constructs in tobacco, I prepared vectors for stable transformation of *Arabidopsis thaliana*, where their effects on root growth, gravitropism and auxin responsiveness can be tested. Several constructs have been prepared to test dynamic and subcellular and tissue-specific localization (Table 16). PIN2::IAA17-mVenus and PIN2::AXR3-1-mVenus allowed to monitor the dynamics of IAA17/AXR3 protein directly in the *Arabidopsis* root and compare the subcellular dynamics of mutant and WT forms of IAA17/AXR3. Transformants containing GR, NESNES and 8KFarn fusions (whose effect is described above) were created to change the subcellular localization and analyse its effect on root growth and auxin responsiveness. Further, I used different tissue-specific promoters (PIN2, PEP, GL2 and COBL9 - see Figure 35) to address the effect of AXR3-1 protein expression in different root tissues.

Table 16) Transcriptional units ligated into pDG3omega1 vector suitable for transformation into *Arabidopsis*.

<table>
<tr><th>A1-B1</th><th>B2</th><th>B3-B4</th><th>B5</th><th>B6-C1</th></tr>
<tr><th>promoter</th><th>N-tag</th><th>CDS</th><th>C-tag</th><th>terminator</th></tr>
<tr><td rowspan="5">PIN2 (LRC, epidermis and cortex)</td><td>intron</td><td>IAA17</td><td>mVenus</td><td rowspan="10">RBCS</td></tr>
<tr><td>mVenus</td><td colspan="2">IAA17</td></tr>
<tr><td rowspan="4">intron</td><td rowspan="5">AXR3-1</td><td>mVenus</td></tr>
<tr><td rowspan="3">mScarlet</td></tr>
<tr><td>PEP (cortex)</td></tr>
<tr><td>GL2 (atrichoblast)</td></tr>
<tr><td>COBL9 (trichoblast)</td></tr>
<tr><td rowspan="3">PIN2</td><td>GR</td><td>mVenus</td></tr>
<tr><td rowspan="2">intron</td><td>mVenus8KFarn</td></tr>
<tr><td>mVenusNESNES</td></tr>
</table>

The following chapters provide an analysis of the T1 generation of transformants. The root morphology of these plants is altered, but this may be affected by growth on antibiotic-containing medium. Eliminating the (presumed) effect of the antibiotic on root morphology will be possible in the next generation.

I prepared different transformants containing construct of the fluorescently labelled our gene of interest. IAA17/AXR3 fused to the rapidly maturing fluorescent protein mVenus should allow analysing of protein behaviour directly in the *Arabidopsis* root. Transformants with C- and N-terminal fusions were generated (Figure 31, A and B). The effect of C- or N-terminal fusion on protein localization or signal intensity needs to be analysed in the next generation of plants. With the same microscope settings and the same image adjustments, we could see that the signal strength of the AXR3-1 (Figure 31, C) was apparently higher than that of IAA17/AXR3 (Figure 31, A and B), confirming the known fact that AXR3-1 point mutant protein is degraded slower than the WT form. In both cases, we could observe the signal in the nuclei, a very weak signal in the cytoplasm, which, however, when compared to the control (Figure 31, D), could be marked as an autofluorescence.

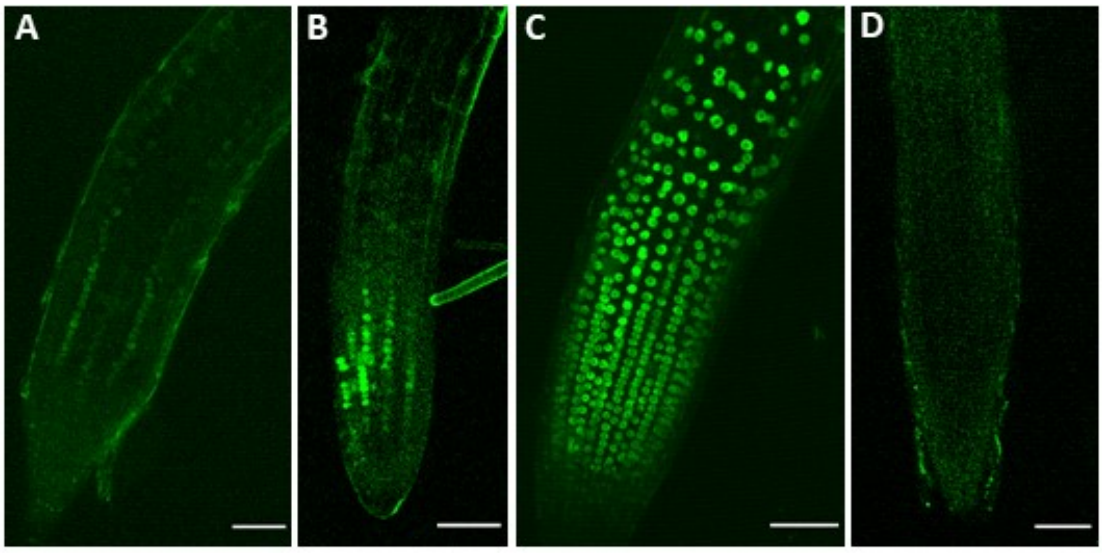

Figure 31) **Expression of IAA17 and AXR3-1 fused with mVenus and controlled by the PIN2 promoter.** A) IAA17-mVenus. B) mVenus-IAA17. C) AXR3-1-mVenus. D) control – Col-0. In the WT form (A and B), a weak signal was mostly in the nucleus. The effect of C- or N-tag fusion on visualization was not visible. The mutant form of this protein (C) was localized predominantly in the nucleus, with a clearly stronger signal compared to WT form. Comparison with the control plant (D) suggested autofluorescence in cytoplasm. A, B, D are single z-stacks. C is maximal projection of z-stacks. Scale bars = 50 μm.

After microscopic analyses, plants with good mVenus signal were transplanted into soil to grow the next generation of seeds. The phenotype of the above-ground part varied depending on the type of transformed plasmid.

Regarding the overall state of transformants and their viability, we could observe differences between constructs. Figure 32 shows a comparison of transformants containing fluorescently labelled IAA17/AXR3 (Figure 32, A and B). The plants looked phenotypically normal. Transformants containing AXR3-1 protein had significantly reduced viability and altered morphology of aboveground parts (Figure 32, C), despite the fact that the PIN2 promoter should be active in the root only.

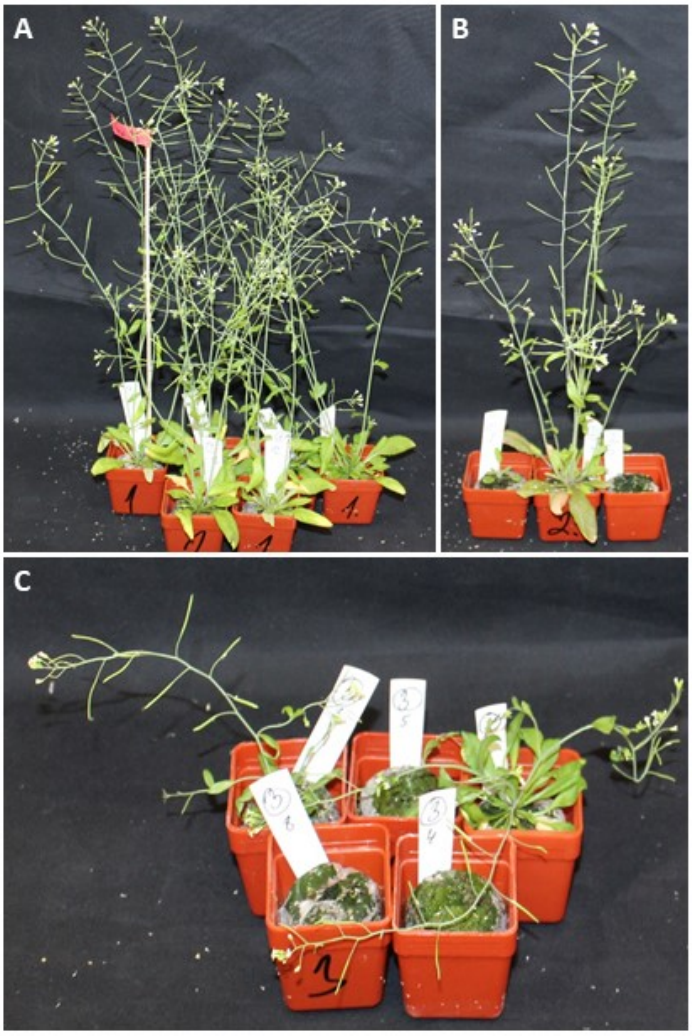

Figure 32) **33-36 days old *Arabidopsis* thaliana T1 transformants.** A) PIN2::intron-IAA17-mVenus-RBCS B) PIN2::mVenus-IAA17-RBCS C) PIN2::intron- AXR3-1-mVenus-RBCS . For scale, see the size of the upper edge of pot, which is 4,5 cm wide.

Subsequently, T1 generations of lines altering the subcellular localization of the AXR3-1 protein were analysed (line containing GR, 8KFarn and NESNES).

Without treatment, PIN2::GR-AXR3-1-mVenus line showed signal predominantly in the cytoplasm (Figure 33, A), as expected. PIN2::AXR3-1-mVenus8KFarn line showed clear signal at the plasma membrane, but signal could be seen also in the nucleus (Figure 33, B). In PIN2::AXR3-1-mVenusNESNES line, the signal was observed outside the nucleus, as expected (Figure 33, C).

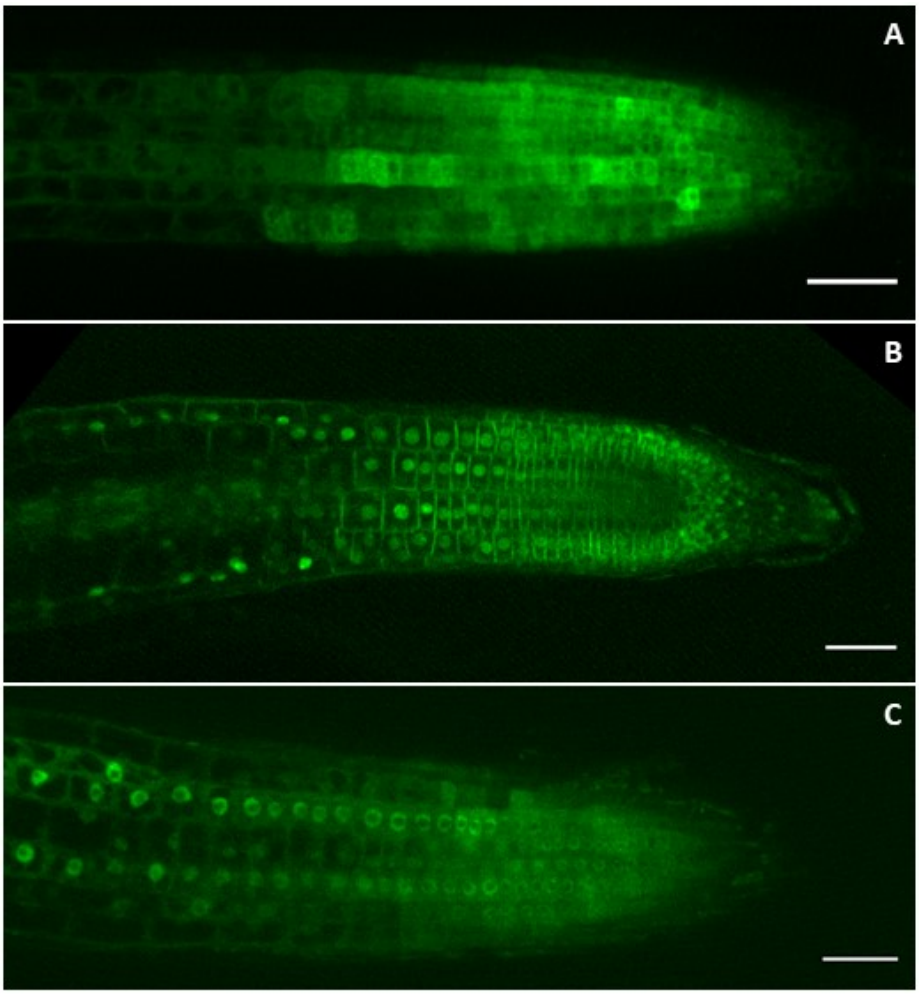

Figure 33) ***Arabidopsis* root tips expressing AXR3-1 fused with GR, 8KFarn and NESNES under the control of PIN2 promoter**. A) PIN2::GR-AXR3-1-mVenus. The signal was visible mostly outside the nucleus - in the cytoplasm. B) PIN2::AXR3-1-mVenus8KFarn. AXR3-1 partially localized to the nucleus and partly on the plasma membrane. C) PIN2::AXR3-1-mVenusNESNES. Signal was outside the nucleus. All pictures represent single z-sections and scale bars correspond to 50 μm.

T1 plants PIN2::GR-AXR3-1-mVenus (Figure 34, A), PIN2::AXR3-1-mVenus8KFarn (Figure 34, B) PIN2::AXR3-1-mVenusNESNES (Figure 34, C) did not show changes in the phenotype of the aboveground part.

Figure 34) **36 days old *Arabidopsis* T1 transformants expressing** A) PIN2::GR-AXR3-1-mVenus-RBCS. B) PIN2::intron-AXR3-1-mVenus8KFarn-RBCS. C) PIN2::intron-AXR3-1-mVenusNESNES-RBCS. For scale, see the size of the upper edge of pot, which is 4,5 cm wide.

The results of previous experiments (see Root tissue-specific expression of AXR3-1 and AXR3-1-GR using the GAL4 activator lines) already point to the influence of tissue-specific expression of the AXR3-1 protein on the severity of the root phenotype. As mentioned earlier, transformants containing AXR3-1 fused to the fluorescent protein mScarlet expressed under various tissue-specific promoters (PIN2, GL2, PEP and

COBL9) were generated. The characteristic expression of PIN2, PEP, GL2 and COBL9 mRNAs in the root can be seen in Figure 35.

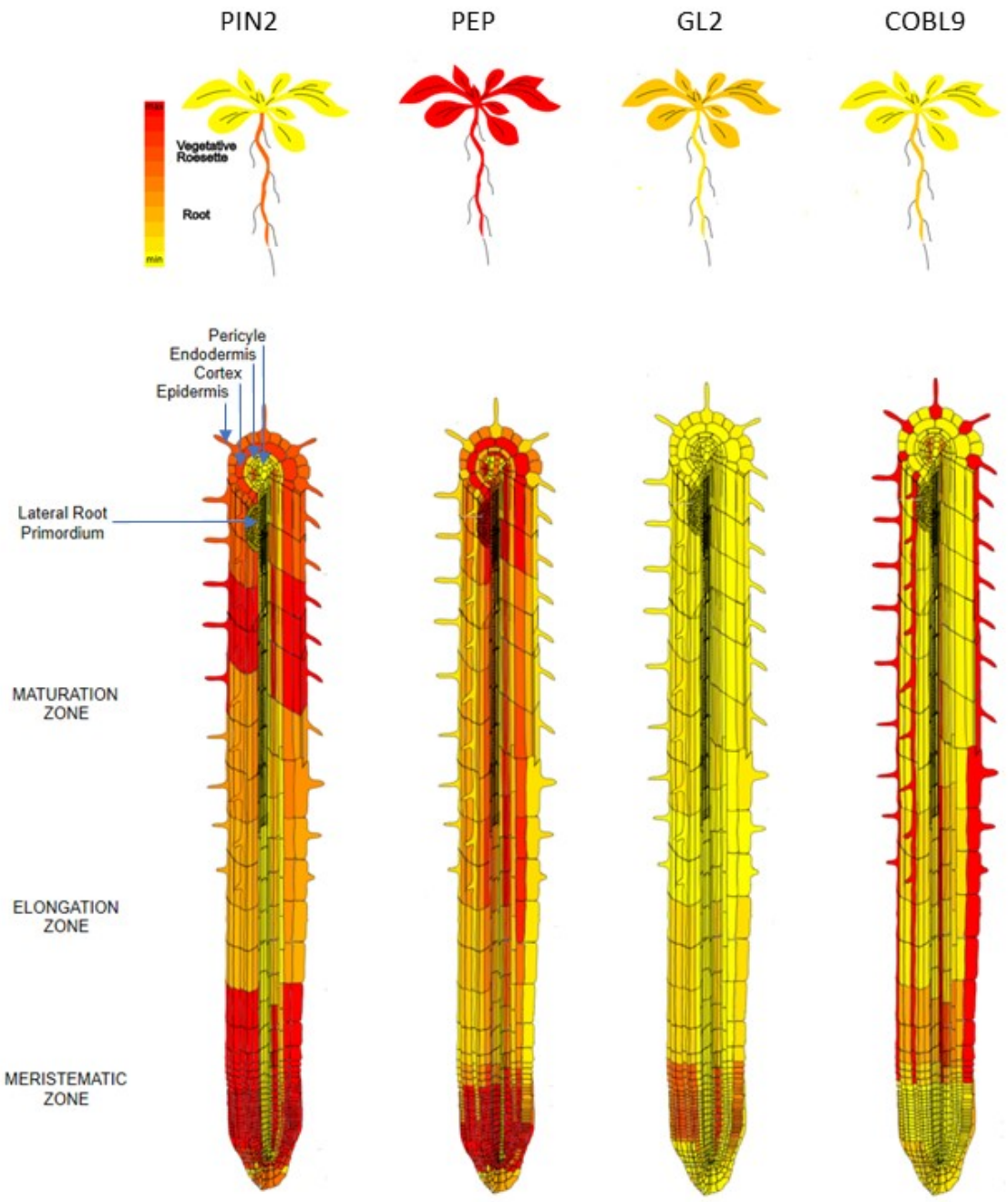

Figure 35) **Characteristic expression of PIN2, PEP, GL2 and COBL9 mRNAs focusing on the roots and young plants.** Data is taken from http://bar.utoronto.ca/eplant/. Expression of selected mRNA within young plants with details for expression in root cells. All selected proteins are expressed in the root, PEP1 and GL2 as well as in the above-ground part of the plants, in vegetative rosette. The PIN2 is expressed only in the root, with the highest expression in the lateral root cap, the epidermis and the cortex. PEP1 is also expressed in the cortex. In the root, GL2 is expressed predominantly in atrichoblasts, whereas COBL9 expression is typical in trichoblasts.

In plants expressing AXR3-1-mScarlet driven by different promoters, microscopic analysis showed that the signal was just partially visible where we expected it. The PIN2 promoter is supposed to be active in the lateral root cap, epidermis, and cortex. This also corresponded to our observation (Figure 36, A), however, what is unusual in our case is the expression in the above-ground part of plants (Figure 36 , B). In addition, some roots had changed morphology (Figure 36, C). GL2 expression was observed in atrichoblasts and partly also in the aboveground part, as we expected (Figure 36, D). COBL9 is supposed to be expressed in the trichoblast cells. In our case, we observed signal not only in the trichoblast, but also in the vascular cylinder (Figure 36, F) and in the aerial part of the plant. Expression of the protein controlled by the PEP promoter (Figure 36, E) was expected in the cortex. Also in this case, the presence of the signal in the vascular cylinder could be seen, suggesting the transport of the AXR3-1 protein. The following attempts to verify compliance between phenotype and genotype are necessary.

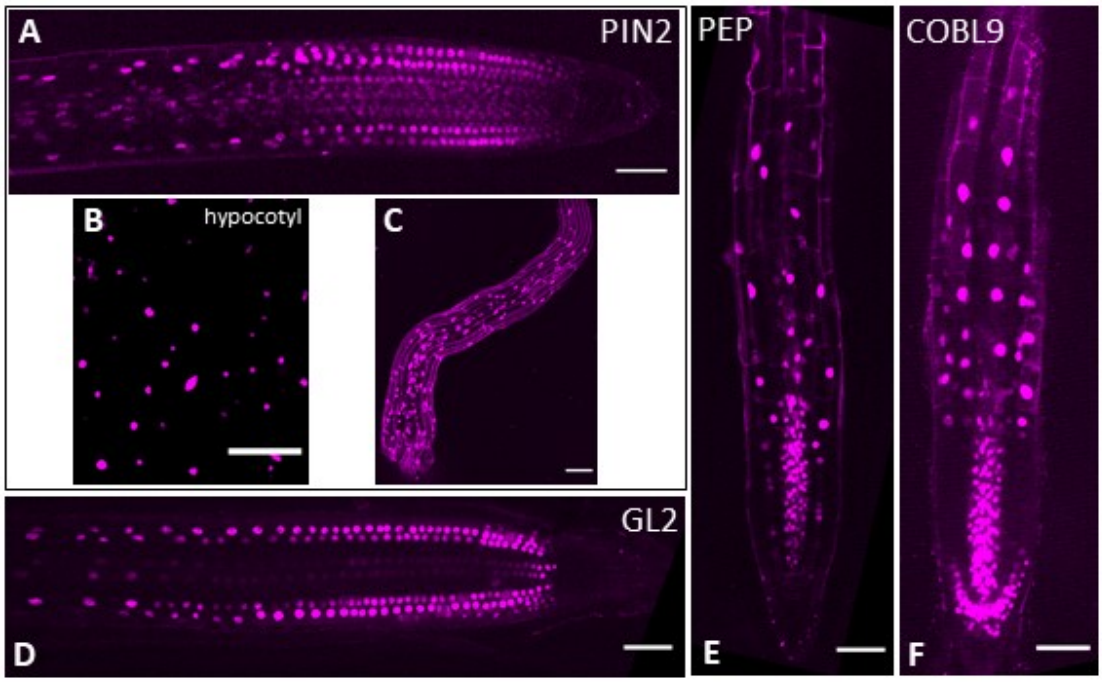

Figure 36) **Expression of AXR3-1-mScarlet under the control of different tissue-specific promoters.** A) Primary root tip of PIN2::AXR3-1-mScarlet. B) GL2::AXR3-1-mScarlet. C) PEP::AXR3-1-mScarlet. D) COBL9::AXR3-1-mScarlet. In all cases, protein expression in the expected cell types could be seen, i.e. the construct under the control of the PIN2 promoter in LRC, cortex and epidermis, the construct under the control of GL2 promoter in atrichoblasts, the construct under the control of COBL9 promoter in trichoblasts and the construct under PEP promoter is expressed in cortex. In all constructs was the signal predominantly in the nucleus. However, in all these transformants, additional signal in the vascular cylinder was observable. Interestingly, in the case of the PIN2 promoter shoot expression of AXR3-1 was visible. Single z-sections, scale bars represent 50 μm.

Regarding the morphology of the above-ground parts of these transformants (Figure 37), we could see a different effect on plant phenotype and viability. Plants expressing AXR3-1-mScarlet under the PIN2 and PEP promoters (Figure 37, A and B) were small and had reduced viability. Plants expressing AXR3-1-mScarlet from the GL2 and COBL9 promoters (Figure 37, C and D) were larger and more viable compared to previous two lines.

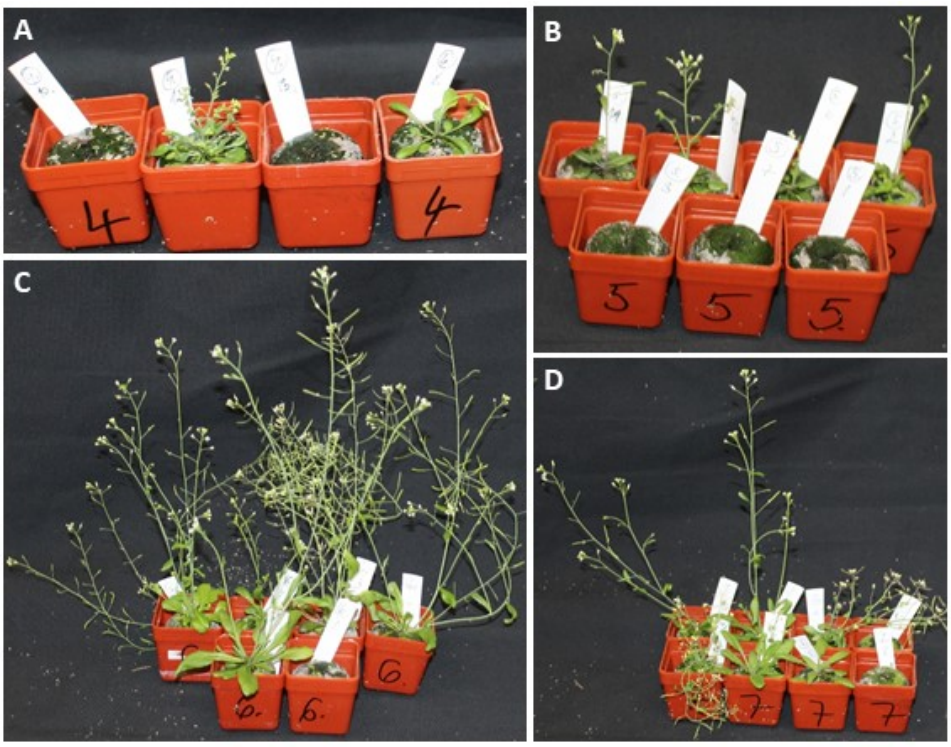

Figure 37) **36 days old *Arabidopsis* transformants**. A) PIN2::intron-AXR3-1-mScarlet-RBCS. B) PEP::intron-AXR3-1-mScarlet-RBCS. C) GL2::intron-AXR3-1-mScarlet-RBCS. D) COBL9::intron-AXR3-1-mScarlet-RBCS. For scale, see the size of the upper edge of pot, which is 4,5 cm wide.

In many of the above-mentioned plant lines, the plants showed an altered phenotype at both microscopic and macroscopic levels. This can be explained by the expression of protein in places where this is not expected, or by the movement of AXR3-1 protein to other parts of the plant. T2 generation analyses could provide further results. Due to time constraints, we underwent analysis only lines driven by PIN2 promoter. The results can be found in the next chapter.

T2 generation: AXR3-1 and IAA17/AXR3 driven by PIN2 promoter

In the final part of the completion of my diploma thesis, T2 seeds lines were first planted on MS media and analysed macroscopically (Figure 38). Lines expressing GR-AXR3-1 not treated with DEX appeared similar to the control line (Figure 38, B vs. A), whereas the other lines showed an altered phenotype (Figure 38, C-F). AXR3-1-mVenus was stunted, and together with AXR3-1-mVenusNESNES and AXR3-1-mVenus8KFarn lines grew poorly and were agravitropic. The AXR3-1-mScarlet line was not viable.

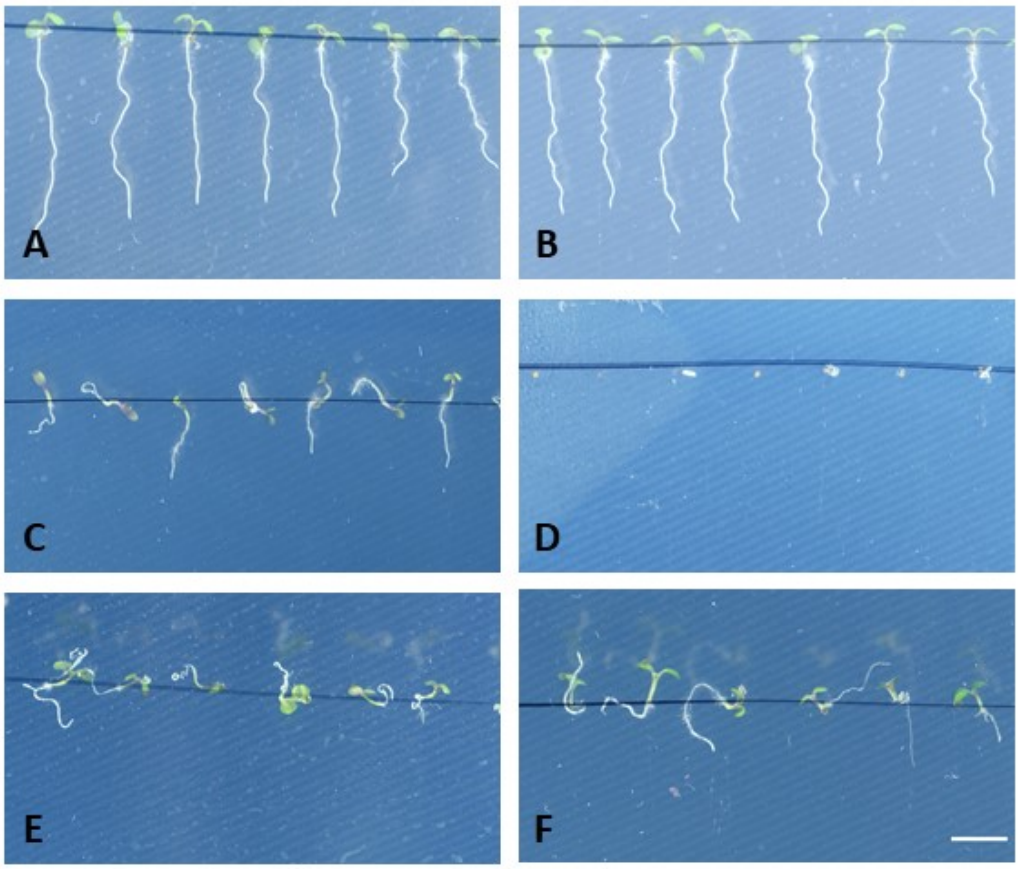

Figure 38) **4 day old plants containing AXR3-1 and driven by PIN2 promoter.** A) Col-0. B) PIN2::GR-AXR3-1-mVenus line without visible changes compared to the control. C) PIN2::AXR3-1-mVenus plants were dwarfs with varying degrees of agravitropism. D) PIN2::AXR3-1-mScarlet line was not viable. E) PIN2::AXR3-1-mVenusNESNES line. F) PIN2::AXR3-1-mVenus8KFarn line. The last two lines had changed phenotype. Scale bar = 5 mm.

To determine the dynamics and role of the AXR3-1 protein, these lines were subjected to microscopic analysis and further experiments. 4 lines were analysed, in most of them we observed the signal in expected tissues. By microscopic analysis of the PIN2::AXR3-1-mVenus line, we observed the localization of AXR3-1 protein in the nucleus, but interestingly, it was again possible to observe the signal in the vascular cylinder (Figure 39, A) and hypocotyl (Figure 39, C), which indicates again a possible transport of AXR3-1 mRNA or protein. VGI analysis showed varying degrees of agravitropism of mutant plants. PIN2::AXR3-1-mVenus line had a larger degree of agravitropism compared to the control line (Figure 39, D).

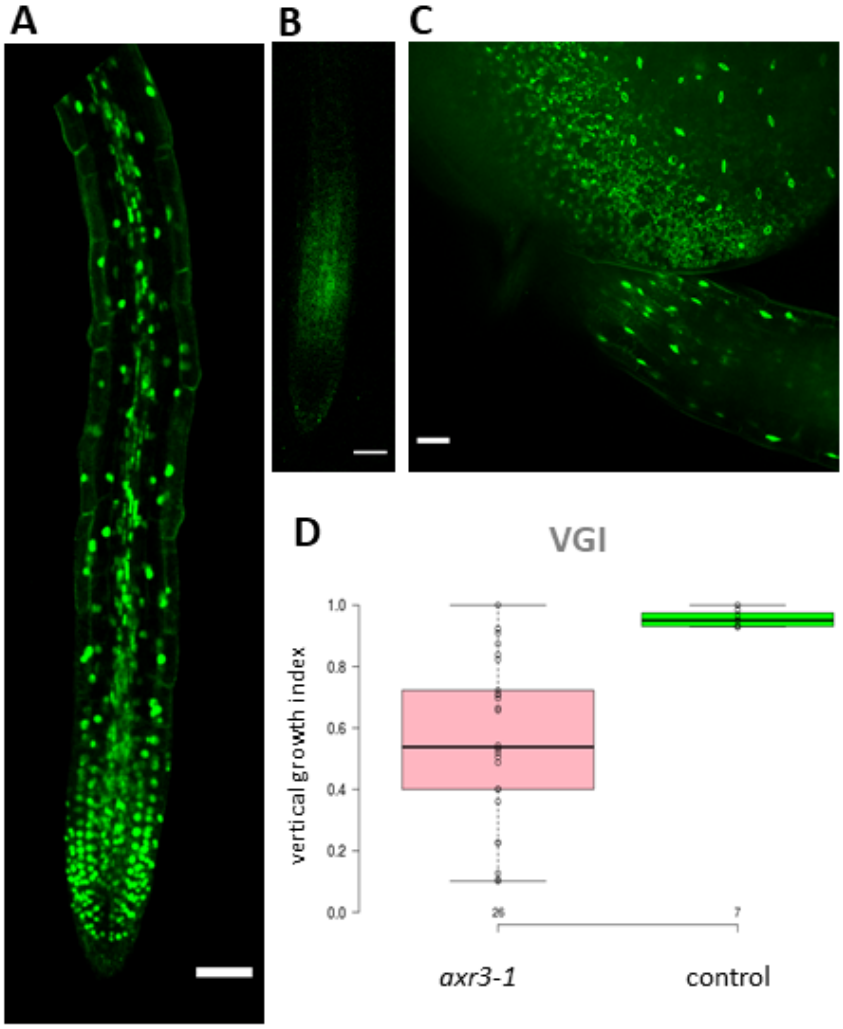

Figure 39) **PIN2::AXR3-1-mVenus analysis.** A) Primary root tip of the PIN2::AXR3-1-mVenus line showed nuclear signal in epidermis, cortex and lateral root cap, but also in vascular cylinder. B) Col-0. C) Hypocotyl and cotyledon of PIN2::AXR3-1-mVenus line demonstrated that the signal was also present in the aboveground part. Single z-stacks, scale bars = 50 µm. D) Analysis of vertical growth index showed that PIN2::AXR3-1-mVenus plants were agravitropic compared to control.

To test auxin responsiveness, the PIN2::AXR3-1-mVenus line was exposed to 50 nM IAA and growth rate was measured after 4 hours. The results showed that PIN2::AXR3-1-mVenus alone grew slower than the control. However, after auxin application, the growth of the mutant line was stimulated in contrast to the control that showed growth inhibition (Figure 40).

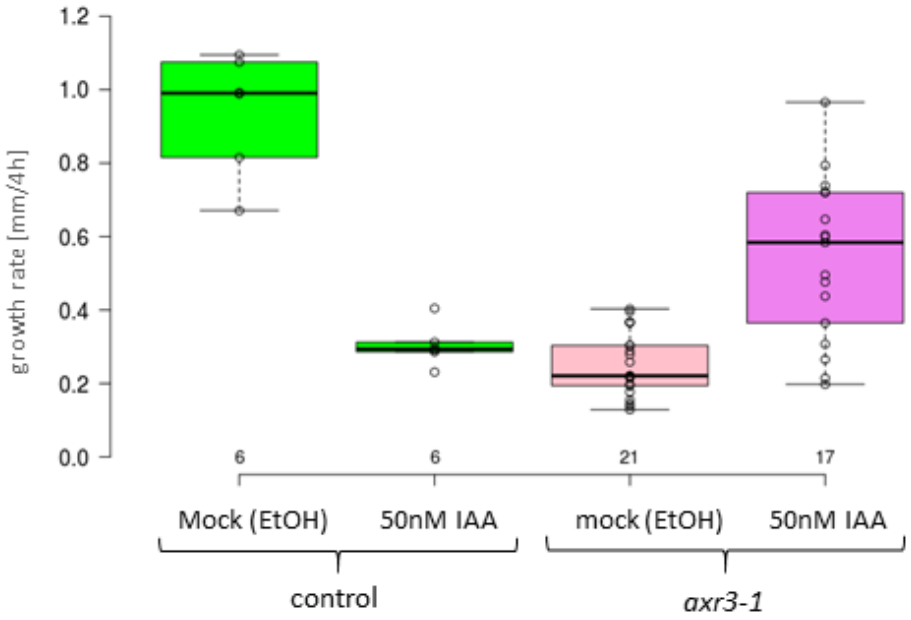

Figure 40) **Growth rate analysis of the PIN2::AXR3-1-mVenus line**. The PIN2::AXR3-1-mVenus line grew slower than the control. In mutant line, growth was stimulated after application of 50 nM auxin. Numbers of analysed plants are shown.

Figure 41 shows the PIN2::GR-AXR3-1-mVenus line and the localization of the AXR3-1 protein predominantly in the cytoplasm of epidermis, LRC and cortex (Figure 41, A and B), as expected. Four lines were analysed and the signal was present in the expected subcellular structures as well as in the expected tissues. However, in some plants, even without any treatment, the signal was weakly present in the nucleus. After adding DEX, it was possible to see how the signal moved to the nucleus (Figure 41, D). Surprisingly, in some plants of this line it was possible to monitor the signal transfer to the vascular cylinder as well, which could not be observed when the AXR3-1-GR complex was exclusively present in the cytoplasm (Figure 41, A).

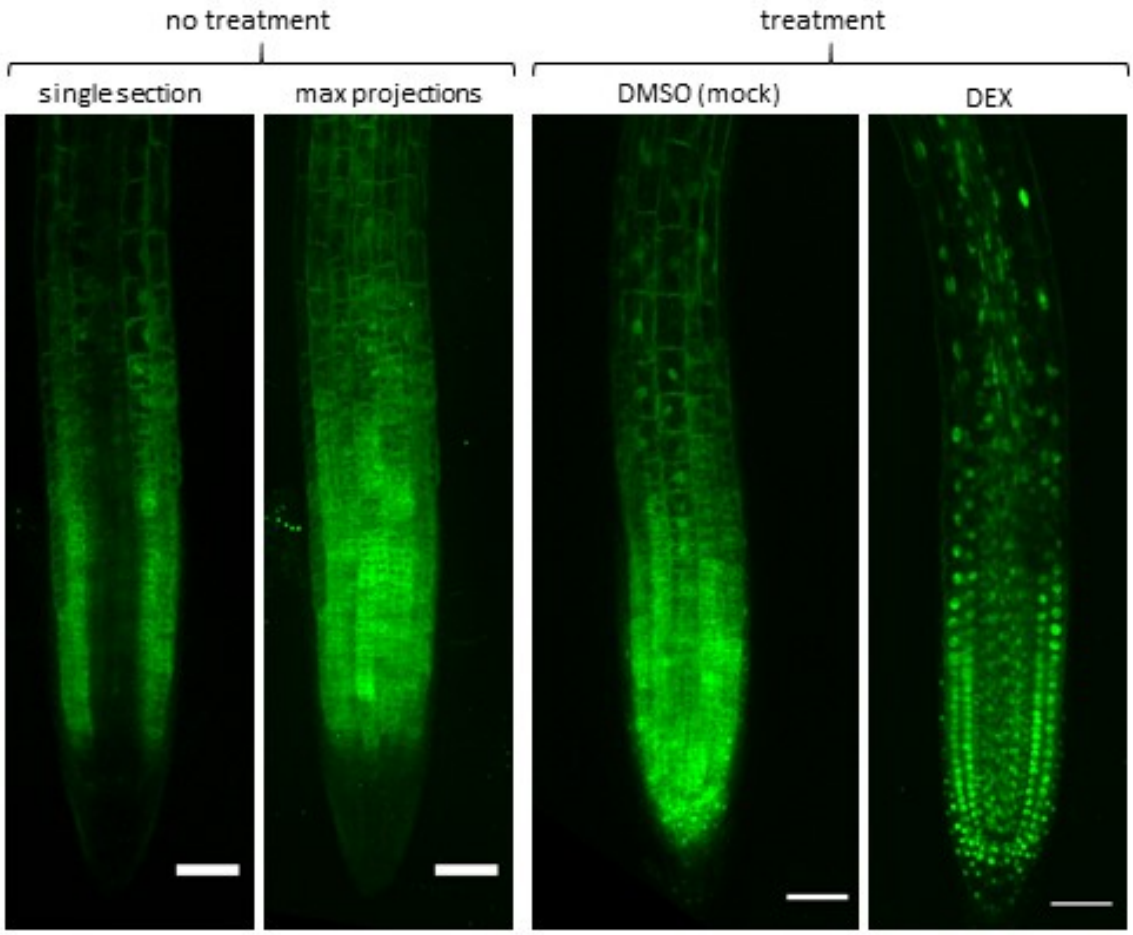

Figure 41) **Microscopic analysis of the PIN2::GR-AXR3-1-mVenus line**. Untreated roots had a signal present predominantly in the cytoplasm (A, B). After adding DEX (D), the signal was present in the nucleus. The signal is also present in the vascular cylinder. These changes could not be observed after DMSO (mock) treatment (C). Scale bars = 50 μm.

After transferring the plants to DEX-containing medium and subsequent microscopic analysis, we monitored the transfer dynamics of the signal to the nucleus. After 15 minutes of DEX treatment, a change in the signal ratio between the nucleus and the cytoplasm was visible (Figure 42, A) (this time is given by the time required to shift the plants and set up the microscope). Plants growing on DMSO showed no changes in signal localization - the signal remained in the cytoplasm (Figure 42, B).

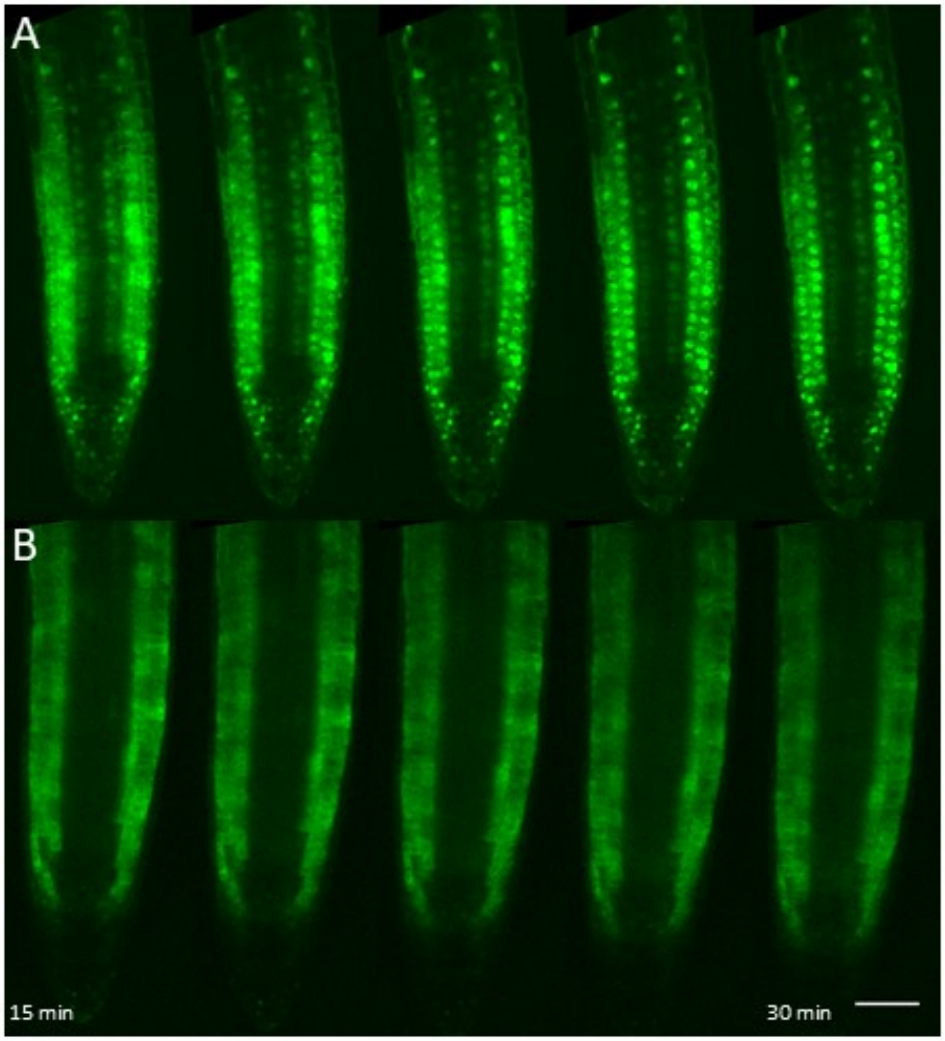

Figure 42) **Time series of the PIN2::GR-AXR3-1-mVenus line after DEX/DMSO application.** A) After transfer to DEX-containing medium, a gradual and relatively rapid transfer of the signal to the nucleus could be seen. B) After DMSO treatment, the signal still remained in the cytoplasm. Time frames represents every 3 minutes. The time after transfer to treatment is indicated. Scale bars = 50 μm.

PIN2::AXR3-1-mVenus8KFarn was localized on the plasma membrane, but part of the signal could still be observed in the nucleus (Figure 43, A and B). Interestingly, this line formed root hairs even though AXR3-1 expression could be observed in trichoblast cells (Figure 43, C). We did not observe expression in the above-ground part, however the signal in most of the analysed plants was still observable in the vascular cylinder (data not shown). It is important to note that we analysed only one line and therefore it is not possible to determine whether the phenotype is really the result of an AXR3-1 mutation or whether this phenotype is affected by the course of the transformation.

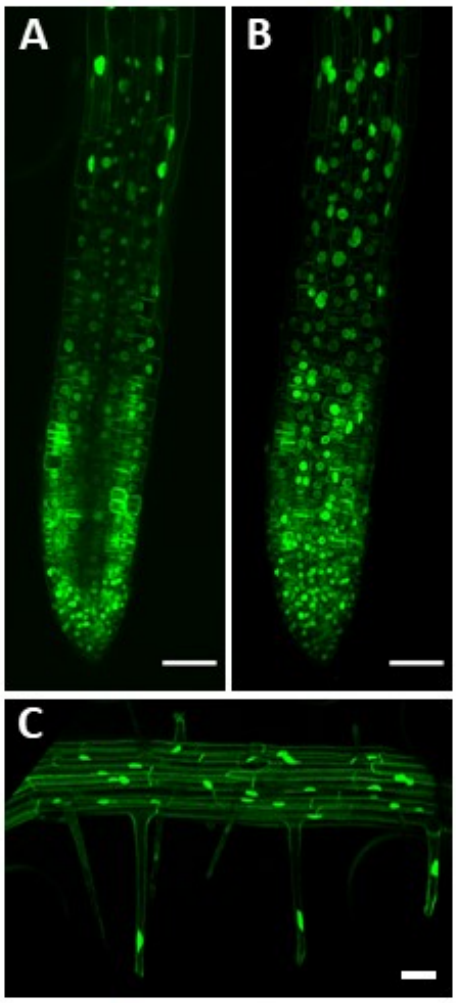

Figure 43) **Microscopic analysis of the PIN::AXR3-1-mVenus8KFarn line.** A) Single z-section. B) Max projection of z-stacks. The signal was predominantly present on the plasma membrane, but also observable in the nucleus. C) Max projection of z-stacks. The signal could also be observed in root hairs. Scale bars = 50 μm.

In the case of the PIN2::AXR3-1-mVenusNESNES line, I did not notice expression in the aboveground part . AXR3-1 signal was mostly observed outside the nucleus, although in some cells it is still observable probably still in the nucleus (Figure 44, A). The signal was again observable in the vascular cylinder (Figure 44, B).

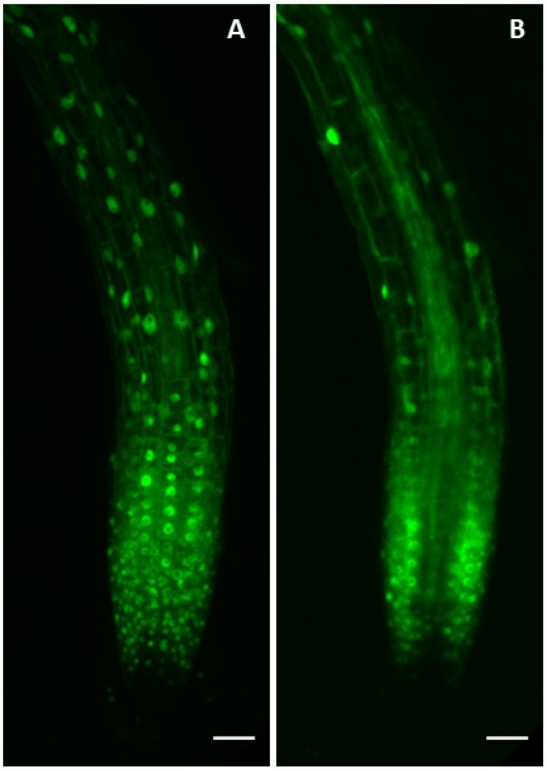

Figure 44) **Microscopic analysis of the PIN2::AXR3-1-mVenusNESNES line.** A) Max projection of z-stacks. The signal could be observed not only around the nucleus, but in some cells also in the nucleus. B) Single section. The signal was present also in the vascular cylinder. The brightness and contrast settings have been set individually for optimal visualization rather than image comparison. Scale bars = 50 μm.

After successful transformation of all the above-mentioned lines and analysis of the T2 generation, it will be necessary to obtain T3 homozygous lines, which will be further analysed in the near future.

Discussion

During the completion of my diploma thesis, I analysed the dynamics and possible role of IAA17/AXR3 protein in the root. Several inducible systems were used in the experiments, and in the second part I created constructs that helped verify, refine or supplement current knowledge.

Analysis of inducible systems

I managed to analyse several plant lines that contain an inducible system that could heat or chemically trigger AXR3-1 protein production. I subsequently crossed these lines with DII-Venus plants, which allowed us to follow a reverse map of auxin. All lines were analysed and yielded interesting results.

What are the growth responses of plants after activation of AXR3-1 protein production?

Heat shock-inducible system was used in the initial experiments. The HS::AXR3-1 line was one of the first tools used to understand how Aux/IAAs can affect auxin responses (Knox et al., 2003). The IAA17/AXR3 protein in its mutated form is not able to bind auxin, which has been confirmed in several studies. Gray et al. (2001) analysed the IAA17/AXR3 protein in both its WT and mutant forms driven by the HS promoter and fused to GUS. These studies were the first that demonstrated the importance of Aux/IAAs in the $TIR1^{SCF}$ auxin pathway and the role of ubiquitination. The same line, HS::AXR3NT-GUS, was also studied by Oono et al. (2003), who showed that AXR3-1 levels in mutant line did not change at all after application of both auxin and antiauxin. Similar to previous studies (Knox et al., 2003), the results of our experiments showed that the roots of mutant plants were agravitropic and insensitive to auxin.

For simultaneous monitoring of auxin signalling, I crossed this inducible system with the DII-Venus auxin sensor (Brunoud et al., 2012). These lines were also agravitropic after the treatment. Their growth accelerated in the initial stages and gradually began to slow down. The time during which root growth rate is increased could correspond to the time during which AXR3-1 protein was produced after heat shock. It could theoretically suggest that free AXR3-1 (unable to bind auxin, thus ubiquitination is not possible)

promotes root growth. Since both Aux/IAAs (Luo et al., 2018) and IAA17/AXR3 itself (see Interactions and functions of IAA17/AXR3) have been shown to have many interactors, the growth response may be the result of an interaction with some unknown interactor. In addition, there could be changes in the meristem of plants after AXR3-1 production, as will be discussed below.

Although the heat shock inducible system is widely used, non-specific activation of many genes can occur during the heat shock (Wang et al., 2016), so we used another type of inducible system – estradiol-inducible system - in further experiments. Arase et al. (2012) used the classical XVE system to the study of IAA8 protein in the root. Using the same expression system, Bishopp et al. (2011) analysed the role of the AXR3-1 protein in xylem formation. The g1090::XVE>>AXR3-1-mCherry system we used contains a constitutive promoter, and mutated form of the IAA17/AXR3 protein fused to mCherry, which allowed us observation of studied protein localization. The signal was predominantly localized in the nucleus, confirming the designation of the IAA17/AXR3 protein as nuclear (Procko et al., 2016; Rouse, 1998). According to our results, activated g1090::XVE>>AXR3-1-mCherry lines did not form root hairs, were agravitropic and insensitive to auxin, corresponding with the analysis of the previous line (HS::AXR3-1) and with the results in previous literature as well (Knox et al., 2003; Siligato et al., 2016). Our results showed that after activation, the growth rate increased, similarly to the previous line (HS::AXR3-1). This could support the hypothesis that free Aux/IAAs (in our case free IAA17/AXR3) promote growth, at least in the early stages of root growth. Although rapid root growth responses have been described previously (Fendrych et al., 2018; Prigge et al., 2020; Shih et al., 2015), the exact molecular mechanism remains unclear. The increase in root growth rate indicates the importance of AXR3-1 protein in the early stages of root growth regulation, and the insensitivity of mutant plants after activation confirms the inclusion of AXR3-1 protein in auxin signalling.

In contrast with our results, previous studies analyses of g1090::XVE>>AXR3-1-mCherry line showed that upon activation, the growth of XVE::AXR3-1 plants stopped (Mähönen et al., 2014; Siligato et al., 2016). According to our results, growth first accelerated sharply then it gradually slowed down until it stopped. However, previous studies did not focus on the initial phase, with measurements taken only after a long time (min. 7 hours). Growth arrest might have several explanations: the meristem was consumed, the cells in the meristem divided less and the cells stop growing into the

elongation zone after a certain time. Mähönen et al. (2014) associated this growth pattern with the importance of auxin signalling for the creation of a PLT gradient in the root, which is essential for proper root zoning, thus for proper cell division and expansion. The interaction of the IAA17/AXR3 protein with WOX5 root meristem regulator has previously been demonstrated (Tian et al., 2013), supporting the idea of disrupting meristem maintenance in the AXR3-1 roots.

Interestingly, the mCherry signal appears about 1,5 hours after the start of estradiol treatment, but growth changes could be observed earlier. However, mCherry requires a minimum of 40 min to mature in optimal conditions and 37°C (Balleza et al., 2018), suggesting that the AXR3-1 protein accumulates in the root earlier, but cannot be seen. Analysis of the increasing intensity of mCherry suggests an accumulation of AXR3-1 protein, suggesting another theoretical possibility of arresting root growth - a too high concentration of AXR3-1 could inhibit growth.

Does auxin signalling change after activation of AXR3-1 protein production?

Crossing the above mentioned lines with the DII-Venus auxin sensor (Brunoud et al., 2012) could give us approximate information about the distribution and approximate amount of auxin (although it still only shows how the DII domain is degraded).

Surprisingly, the DII-Venus signal was gradually lost in the HS::AXR3-1 x DII-Venus lines after their activation. Since the DII-Venus signal and the associated monitoring of the auxin gradient could be seen not only in the control but also in the mutant lines that were not subjected to heat shock activation, the AXR3-1 protein and its interactions, high auxin concentration, or disrupted auxin signalling could be responsible for the signal loss in activated line. Results on this topic vary in the literature. Prát et al. (2018) showed, based on the change in signal intensity, that the localization of PIN1 and PIN2 proteins changed after activation of the HS::AXR3-1 line (although the change was very small), suggesting that changes in auxin flux could occur. On the other hand, Y. Zhang et al. (2019) analysed HS::AXR3-1 lines in relation to starch grain formation and thus its essentiality for the gravitropic perception. Transcriptional analysis of PIN1 and PIN2 proteins showed that their level did not change after heat shock activation. The differences may be due to the use of a different method or may be a regulation at a level other than the transcriptional one.

In addition, interactions between AXR3-1 protein and components of the auxin signalling pathway could occur and affect auxin signalling. Many interaction and regulatory partners of the IAA17/AXR3 protein have been reported (reviewed in Luo et al., 2018). Further experiments are needed to reveal why the DII-Venus signal is lost in the HS::AXR3-1 lines after their activation, e.g. endogenous auxin levels would need to be measured.

In the next part of the project, I crossed plants containing the auxin sensor DII-Venus (Brunoud et al., 2012) and the estradiol-inducible system g1090::XVE>>AXR3-1-mCherry, which allowed us to simultaneously monitor the presence of AXR3-1 protein and DII-Venus intensity suggesting the present of auxin. Microscopic analysis of these lines showed that the presence of AXR3-1 in the cells turns off DII-Venus signal. Explanations may be similar to the HS::AXR3-1 x DII-Venus analysis. Upon activation of the *axr3-1* gene expression, the amount of auxin could increase in the cells, leading to the DII-Venus degradation. Since auxin signalling is a highly regulated system (Woodward et al., 2005) by turning on a strong negative regulator, the pathway enters a new state, which could result in overproduction of auxin. Alternatively, AXR3-1 could interact with some component of the auxin pathway and thus affects auxin signalling. Purely theoretically, there could also be some interaction between AXR3-1 and DII-Venus that results in the degradation of DII-Venus.

Moreover, to eliminate the influence of non-specifically induced genes by chemical or heat treatment, it will be interesting to analyse transcriptomic data (data not shown) obtained during completion of this work. Analysis of the transcriptome of the HS::AXR3-1 line, XVE::AXR3-1mCherry and Col-0 treated with auxin and antiauxin will allow the selection of genes that are specific for the gravitropic response.

What effect does tissue-specific expression of the *axr3-1* gene have on the plant phenotype?

To determine the effect of tissue-specific expression, GAL4 driven lines (Haseloff, 1998) were first analysed. Lines containing specific promoters copying tissues of typical IAA17/AXR3 protein expression were selected for analysis. Using these lines, we were able to obtain information in which tissues AXR3-1 protein needs to be present to affects gravitropism. According to our results, the mutated protein present in the pericycle, endodermis, cortex, epidermis, LRC and their combination within different root zones, had the greatest influence on gravitropism. By analysing and comparing the VGI of the

UAS::AXR3-1 and UAS::AXR3-1-GR lines (with DEX and DMSO treatment), we observed different effects of the AXR3-1 presence in specific root tissues. If we applied DMSO to the plants, thus the AXR3-1-GR complex should be located in the cytoplasm, all lines showed only a very small change in gravitropism compared to the control line (nonsignificant differences). Moreover, if DEX is applied to plants, thus the AXR3-1-GR complex should be released from the complex in the cytoplasm and transferred to the nucleus, the degree of agravitropism will change, however, the only line, J2821>>UAS::AXR3-1-GR, showed significant changes compared to control. According to our results, only this line showed significant changes when we compared different treatments (DEX and DMSO). It suggests the need for AXR3-1 presence in epidermis, cortex, endodermis, and pericycle and in the nucleus as well to function in gravitropism. The importance of nuclear localization could be confirmed by comparing J2821>>UAS::AXR3-1-GR after the DEX application and J2821>>UAS::AXR3-1 (presumed natural subcellular localization), where there is no significant difference between these two lines. Likewise, there is no significant difference between J0951>>UAS::AXR3-1-GR after the DEX application and J0951>>UAS::AXR3-1, which suggests the role of the epidermis and LRC in the gravitropic response and, at the same time, once more, the need for nuclear localization of AXR3-1. In contrast to the previous two lines, J0391>>UAS::AXR3-1 showed the lowest effect (this could be affected by the small number of analysed plants). However, the elongation zone has previously been demonstrated as a tissue included in the gravitropic response (Sato et al., 2015). For these lines, it is important to mention the strength of expression, which may not be the same and therefore could have an effect on the differences between the lines. All examined tissues so far have been shown to be included in gravitropism (Sato et al., 2015), however, their correct combination is also important. Swarup et al. (2005) showed that the AXR3-1 presence in LRC alone is not sufficient to cause agravitropism. The results suggest that the AXR3-1 protein must be present in the nucleus in order to perform its function.

In this line, it is important to mention that the AXR3-1 protein is fused with GR. Using this receptor, which allows the target to move between the nucleus and the cytoplasm, we wanted to verify the possibility of extranuclear function of AXR3-1. Prigge et al. (2020) showed that the rapid root growth response might be carried out in the cytoplasm. However, GR forms complexes with HSP proteins in the cytoplasm in the absence of DEX. When DEX is added, GR is released from the complex and is targeted to the place

which is dictated by its sequence (Schmitt & Stunnenberg, 1993). The IAA17/AXR3 protein is thought to be a nuclear protein, and Ouellet et al. (2001) has shown that disruption of the NLS signal in its sequence resulted in localization within the whole cell. Because proper conformation and interactions with other proteins are essential for the protein function, the binding to HSP complexes in the cytoplasm could hinder/prevent the activity of AXR3-1 protein in the cytoplasm. For that reason, it is not clear whether the AXR3-1 protein held in the cytoplasm is able to perform its theoretical function. Therefore, I prepared additional constructs to provide more information not only about the possible effect of GR on AXR3-1 protein, but also constructs were prepared that could provide additional information on tissue-specific AXR3-1 expression.

Is it possible to reduce the visualization limitation of short living proteins such as Aux/IAAs?

During the completion of this work, I also prepared and verified by agroinfiltration in tobacco a construct containing DII-mVenusNB - a faster maturing protein compared to DII-Venus (Brunoud et al., 2012), and mScarlet. This construct appears to be functional and will be further used after transformation into *Arabidopsis*, which will be done in the near future. Its stable transformation and subsequent analysis can bring beneficial results, in particular by reducing the time limitation of protein visualization given by the maturation time of FPs. Depending on the maturation time of these proteins, it could be possible to monitor sites with higher auxin content using this construct. A similar system using two FPs fused to the IAA17/AXR3 protein was used previously (H. Zhang et al., 2019).

Preparation and analysis of new transgenic plants

By analysing various inducible systems available from other laboratories, we obtained a lot of information, which we supplemented and refined by analysing the transgenic plants we created. The analysis of these reporter lines could provide answers to the questions and goals asked in this thesis. In the first part of the project, I prepared series of constructs that allow not only the visualization of IAA17/AXR3 or AXR3-1 proteins, but also the change of their subcellular localization. I first verified all constructs in a transient tobacco

expression system. Next, several constructs were modified for the possibility of transformation into *Arabidopsis*.

Extranuclear localization of IAA17/AXR3 or AXR3-1 protein?

We were able to analyse both T1 and T2 generation of transformants containing IAA17/AXR3 protein and its mutant form AXR3-1. In tobacco epidermal cells, we could test the functionality of all constructs. Both used FPs seemed to be equally suitable for visualization, as did the C- or N-terminal fusion. In tobacco epidermal cells, constructs with IAA17/AXR3 or AXR3-1 protein were localized predominantly in the nucleus, but a weak signal was also observed in the cytoplasm. The localization of the AXR3-1 protein has also been analysed in other studies, which yielded various results. Several papers point to a purely nuclear localization of the IAA17/AXR3 or AXR3-1 protein (Arase et al., 2012; Procko et al., 2016). This is supported by the presence of a bipartite NLS signal in IAA17/AXR3 sequence (Rouse, 1998). In contrast, H. Zhang et al. (2019) showed that IAA17/AXR3 is found in both the nucleus and the cytoplasm. Different results could be caused by using another method (protoplasts versus transient expression in tobacco leaves). Additionally, H. Zhang et al. (2019) showed different stability of nuclear and cytoplasmic IAA17/AXR3 protein. The rapid degradation of cytoplasmic IAA17/AXR3 after auxin application could correspond to IAA17/AXR3 involvement in the rapid root growth response, which is also supposed to take place in the cytoplasm (Prigge et al., 2020). According to microscopic analyses of PIN2::AXR3-1-mVenus, PIN2::IAA17-mVenus and g1090::XVE>>AXR3-1-mCherry, our results suggested the nuclear localization of the AXR3-1 protein as well.

What does the *axr3-1* mutant look like at the macroscopic level?

At the macroscopic level, we observed differences between the T1 generation plants containing WT and the mutated form, with IAA17/AXR3-labeled lines showing a phenotype indistinguishable from the Col-0 background. Regarding the phenotype of the aboveground part of T1 AXR3-1-labeled plants, the plants were stunted, as well as the T2 generation of PIN2::AXR3-1-mVenus line. The phenotype of the aboveground part correlates to some extent with the phenotype of the dominant *axr3-1* mutant (Leyser et al., 1996). For AXR3-1 lines, it is important to mention that T2 generation varies

depending on the FP used. T2 generation of PIN2::AXR3-1-mScarlet plants were non-viable, but in order to draw conclusions, more lines need to be analysed.

What is the subcellular dynamics of the IAA17/AXR3 protein in its WT and mutant form?

To monitor the dynamics of the IAA17/AXR3 and AXR3-1 protein directly in the root of *Arabidopsis*, I used several constructs. We were able to detect a low signal of IAA17/AXR3 (which is understandable given its very short half-life (Abel & Theologis, 1996)). We could observe the mutated form of the protein with a sufficiently strong signal, mainly in the nucleus. The subcellular localization of the mutated and WT forms of the protein was not different. Microscopic images showed the signal present in certain parts of the nucleus. Tao et al. (2016) point to the accumulation of $TIR1^{SCF}$, COP9 signalosome, and 26S proteasome (and thus also Aux/IAAs) in nuclear protein bodies after auxin application. However, this hypothesis is based on the interaction of Aux/IAAs with auxin, which is not possible with AXR3-1, indicating that localization in certain parts of the nucleus is not dependent on auxin. In the following experiments it will be interesting to monitor the dynamics of IAA17/AXR3 and AXR3-1 protein after the application of auxin or after gravistimulation.

Does a change in the localization of AXR3-1 protein at the subcellular level affect the plant phenotype?

Furthermore, we were able to create and transform constructs that could change the localization of the mutated form of IAA17/AXR3 protein. We observed that transformants containing GR without treatment had AXR3-1 protein outside the nucleus, i.e. in the cytoplasm. As mentioned earlier, GR forms complexes with HSP proteins in the cytoplasm, which corresponds to our results - in epidermal tobacco leaf cells we observed cluster formation. T1 and T2 PIN2::GR-AXR3-1-mVenus has been analysed and the transformation appeared to be successful. In the absence of DEX, or in the presence of DMSO, we observed a signal present in the cytoplasm, in some lines a weak signal was also observed in the nucleus. Different localization of the signal in the same lines could be explained by the site of T-DNA incorporation (for example, if our gene of interest was inserted into the transcriptionally strong active region, the signal could be

stronger and therefore present also in the nucleus). After the application of DEX, we observed how the signal shifted relatively quickly to the nucleus. This line is a tool to study the change in the localization of the AXR3-1 protein and its effect over time.

In T1 and T2 generations, we could also observe a partial effect of nuclear export signal (PIN2::AXR3-1-mVenusNESNES) and plasma membrane anchor (PIN2::AXR3-1-mVenus8KFarn). However, in both cases, we still monitored the signal in the nucleus, but to a lesser extent. After microscopic analysis, the T2 generation showed that in these lines there is no detectable protein in the aboveground part, which also coincided with the phenotype of the aerial part of T1 plants, which did not appear to be different from the control.

T2 PIN2::AXR3-1-mVenus8KFarn plants were poorly growing and agravitropic. Interestingly, this line forms root hairs (signal is detected in them as well). Only the presence of root hairs (although shorter or otherwise deformed) on roots containing AXR3-1 protein is strange and this result has not yet been observed. The role of IAA17/AXR3 protein in root hair formation is known (Knox et al., 2003). Since only one line was analysed, it is not possible to draw final conclusions. If analyses of other PIN2::AXR3-1-mVenus8KFarn lines will show the same results it could mean that, theoretically, partial withdrawal of the AXR3-1 protein from the nucleus could mean that it is less active (and thus not able to inhibit root hair growth). However, in this case, the same phenotype would be observed in the PIN2::GR-AXR3-1-mVenus and PIN2::AXR3-1-mVenusNESNES lines (whereas in both AXR3-1 is also pulled out of the nucleus). Alternatively, it could be purely theoretically possible that the AXR3-1 protein must be at least partially on the membrane in order to form root hairs, and this process is not dependent on auxin binding (since in our case we used AXR3-1 protein, which is not able to bind to IAA). Verifying that this process is auxin dependent would be possible by PIN2::IAA17-mVenus8KFarn analysis. However, in order to draw unambiguous conclusions, it would be necessary to perform several experiments that were not performed due to time constraints.

Next, the signal in line PIN2::AXR3-1-mVenusNESNES was observed not only outside the nucleus, in the cytoplasm and around the nucleus, but a small part of the signal was still observed in the nucleus. At the macroscopic level, T2 generation was dwarf and roots appeared to be agravitropic. Since we observed different signal distributions within the cell, a more detailed analysis is needed, which will be carried out in the near future. PIN2::AXR3-1-mVenusNESNES line could allow us to verify the effect of GR on

AXR3-1 activity, since in both cases the AXR3-1 protein is found in the cytoplasm (not in the nucleus). It is clear from the analysis of T2 generation that if the AXR3-1 protein is being pulled out of the nucleus (PIN2::AXR3-1-mVenusNESNES), plant phenotype is substantially different from plants having the AXR3-1 protein held in the cytoplasm (PIN2::GR-AXR3-1-mVenus). Whereas the signal in PIN2::AXR3-1-mVenusNESNES line is still present also in the nucleus (although to a small extent) the difference could be due to this fact. However, if we found PIN2::AXR3-1-mVenusNESNES lines that have a signal exclusively outside the nucleus and their phenotype will be still the same as in the PIN2::AXR3-1-mVenusNESNES lines observed so far, this would indicate that in the PIN2::GR-AXR3-1-mVenus line, the AXR3-1 protein function is really affected in some way.

The prepared lines will be used for testing the second established hypothesis and analysing whether AXR3-1 changes its subcellular localization after auxin perception.

Does a change in the expression of AXR3-1 protein at the tissue level affect the plant phenotype?

The above-mentioned GAL4>>UAS::ER-GFP lines allowed us to draw some conclusions about the tissue-specific expression of AXR3-1 protein and its importance for gravitropism. However, it was not possible to accurately monitor the expression of the AXR3-1 protein in these lines, therefore several other constructs were generated using different promoters. Microscopic analysis of T1 lines containing tissue-specific promoters showed expression of AXR3-1 protein in the expected regions, but in many cases also in other tissues and in the aboveground part (which is discussed in the next paragraph). Plants expressing AXR3-1 driven by PIN2 and PEP also had very reduced ability to grow. These lines were not further analysed due to lack of time (and Covid-19 pandemic), but later analyses may provide interesting results on tissue-specific AXR3-1 protein production and its role. Next, it would be interesting, for example, to create J2821>>UAS::AXR3-1-mVenusNESNES, J0391>>UAS::AXR3-1-mVenusNESNES and J0951>>UAS::AXR3-1-mVenusNESNES lines to verify whether the results of tissue-specific expression are matching.

Is there intercellular mobility of AXR3-1 protein?

Interestingly, analysis of several lines showed the presence of a AXR3-1 signal also in the vascular cylinder of the root .

When analysing lines containing AXR3-1 driven by PIN2 promoter, I observed the presence of AXR3-1 outside of the PIN2 promoter expression domain - i.e. outside the lateral root cap, root epidermis, and root cortex (Müller et al., 1998) - in the vascular cylinder and (in some cases) in the aboveground part. The presence of the signal in the vascular cylinder was also observed in other lines (PEP::AXR3-1-mScarlet, GL2::AXR3-1-mScarlet, COBL9::AXR3-1-mScarlet).

Presence of the AXR3-1 protein signal in the vascular cylinder indicates that it is transported. Transport of Aux/IAA mRNA has so far been demonstrated (Notaguchi et al., 2012). The movement of proteins or their mRNAs is an important part of plant developmental processes and our results suggests a possible role of root produced AXR3-1 protein in other parts of the plant.

Since the signal was also present in other tissues than expected, we cannot clearly determine what is the reason for the altered phenotype of these plants and further analyses are needed. For example, it is necessary to find plants that have a signal only in the expected tissues and not in the aboveground part. However, if it is true that AXR3-1 protein is transported, such plants are unlikely to be found. In this case, it is necessary to verify the correctness of the transformation, e.g. by isolating and verifying the transformed DNAs. On the other hand, the fact that some lines containing the PIN2 promoter have a signal expressed only in the PIN2 promoter expression domain and have no signal in above ground part and at the same time we still observed the AXR3-1 signal in the vascular cylinder suggests that the possibility of protein movement through the vasculature is more likely than non-specific expression of the PIN2 promoter domain.

Interestingly, observations so far show that if the AXR3-1 protein was held executively in the cytoplasm (PIN2::GR-AXR3-1-mVenus), the signal was not observed in the vascular cylinder. In contrast with that, after DEX application to GR-containing roots, the signal shifted to the nucleus and appeared in the vascular cylinder, indicating that the AXR3-1 protein is transported only when it could be located in the nucleus. Even in this case, further analyses are needed.

How does the *axr3-1* mutant respond to treatments?

As well as the previous lines (HS::AXR3-1 with or without DII-Venus, g1090::XVE>>AXR3-1-mCherry) the T2 generation PIN2::AXR3-1-mVenus was analysed for growth response after auxin application. Compared to the control, PIN2::AXR3-1-mVenus grew more slowly even in mock conditions. Such growth retardation has been observed previously in the *axr3-1* dominant mutant (although after a longer measurement time – several days). Leyser et al. (1996) showed that dominant *axr3-1* mutant has a shortened primary root length. Interestingly, according to our results, compared to the mock conditions, the root growth of PIN2::AXR3-1-mVenus was stimulated after auxin application. In contrast, our results of HS::AXR3-1 or g1090::XVE>>AXR3-1-mCherry lines analysis point to auxin insensitivity in inducible systems. Leyser et al. (1996) studied the effect of auxin on the dominant *axr3-1* mutant, which showed insensitivity to auxin compared to control. However, their results were measured after 3 days of auxin application. Moreover, these experiments still need to be repeated.

The degree of agravitropism was much higher in PIN2::AXR3-1-mVenus lines compared to the control. Agravitropism of the *axr3-1* mutant has been shown in previous studies (Leyser et al., 1996). In addition, the phenotypic similarity of the dominant *axr3-1* mutant with the line we generated - PIN2::AXR3-1-mVenus again confirms the importance of the epidermis, cortex and LRC (PIN2 expression domain) in the gravitropic root response. My results and their comparison with the literature suggest that the root growth response is highly time-dependent and changes within seconds, so more detailed analyses are needed.

Conclusions and future perspectives

My diploma thesis set several goals, which we managed to fulfil to a large extent. I managed to analyse plants containing AXR3-1 inducible systems and tissue specific *axr3-1* expression. I analysed their phenotype, growth rate and response to auxin application. In addition, I prepared several transgenic plant lines allowing further analysis of the dynamics and effects of tissue-specific expression of AXR3-1 protein. However, the acquisition and analysis of the T3 generation remains to be done in the near future.

From the obtained results up to date, we have confirmed the involvement of AXR3-1 protein in the regulation of root growth, gravitropic response, root hair formation and auxin signalling.

In addition, this work has yielded several new results such as the positive effect of AXR3-1 protein on growth in the early phases of its induction, followed by slowing to a halt. It was also interesting to note that upon activation of AXR3-1 protein production, the DII-Venus signal is disrupted, suggesting changes in the auxin signalling pathway. Another interesting observation was the presence of the AXR3-1 protein signal in the vascular cylinder when expressed specifically in the epidermal and cortical layers. However, it is not yet entirely clear whether this is non-specific expression outside the PIN2 expression domain, or whether the signal is present precisely due to the possible transport of the AXR3-1 protein or its mRNA.

Many of these new results need further experiments in order to be explained. Aux/IAAs are known to have many interactors, they are regulated at different levels, but it is not always known what the molecular mechanism of their action is. We have succeeded in creating several transgenes that can serve as a tool for a deeper understanding of the molecular, cellular and tissue mechanisms regulating root growth, especially in relation to the auxin signalling and gravitropism.

Their further analyses will be, among other things, the subject of my graduate study. In the future, it will be interesting to:

- analyse *Arabidopsis* transformants - to analyse their reactions to auxin or gravitational stimulation with focus on:
    - initial rapid responses of roots to auxin,

    - the effect of altering the subcellular or tissue localization of the AXR3-1 protein on the root phenotype,
- prepare and analyse transformants *of Arabidopsis* containing novel versions of the DII-mVenus reporter, which could refine the visualization of auxin responses in the roots,
- process the already obtained RNA seq transcriptomic dataset from the analysis of HS::AXR3-1 and g1090::XVE>>AXR3-1-mCherry, which brings the possibility to select candidate genes important in gravitropic responses,
- prepare and analyse other mutants with altered Aux/IAA (e.g., their affected ability to bind to each other, bind ARF, or be ubiquitinated, with disrupted NLS, …),
- …

References

Abel, S., & Theologis, A. (1996). Early Genes and Auxin Action. *Plant Physiology*, *111*(1), 9–17. https://doi.org/10.1104/pp.111.1.9

Abel, Stephen, Oeller, P. W., & Theologis, A. (1994). Early auxin-induced genes encode short-lived nuclear proteins. *Proceedings of the National Academy of Sciences*, *91*(1), 326–330. https://doi.org/10.1073/pnas.91.1.326

Arase, F., Nishitani, H., Egusa, M., Nishimoto, N., Sakurai, S., Sakamoto, N., & Kaminaka, H. (2012). IAA8 Involved in Lateral Root Formation Interacts with the TIR1 Auxin Receptor and ARF Transcription Factors in Arabidopsis. *PLoS ONE*, *7*(8), e43414. https://doi.org/10.1371/journal.pone.0043414

Audran-Delalande, C., Bassa, C., Mila, I., Regad, F., Zouine, M., & Bouzayen, M. (2012). Genome-Wide Identification, Functional Analysis and Expression Profiling of the Aux/IAA Gene Family in Tomato. *Plant and Cell Physiology*, *53*(4), 659–672. https://doi.org/10.1093/pcp/pcs022

Balleza, E., Kim, J. M., & Cluzel, P. (2018). Systematic characterization of maturation time of fluorescent proteins in living cells. *Nature Methods*, *15*(1), 47–51. https://doi.org/10.1038/nmeth.4509

Bindels, D. S., Haarbosch, L., van Weeren, L., Postma, M., Wiese, K. E., Mastop, M., Aumonier, S., Gotthard, G., Royant, A., Hink, M. A., & Gadella, T. W. J. (2017). mScarlet: a bright monomeric red fluorescent protein for cellular imaging. *Nature Methods*, *14*(1), 53–56. https://doi.org/10.1038/nmeth.4074

Bishopp, A., Help, H., El-Showk, S., Weijers, D., Scheres, B., Friml, J., Benková, E., Mähönen, A. P., & Helariutta, Y. (2011). A Mutually Inhibitory Interaction between Auxin and Cytokinin Specifies Vascular Pattern in Roots. *Current Biology*, *21*(11), 917–926. https://doi.org/10.1016/j.cub.2011.04.017

Brand, A. H., & Perrimon, N. (1993). Targeted gene expression as a means of altering cell fates and generating dominant phenotypes. *Development*, *118*(2), 401–415.

Brunoud, G., Wells, D. M., Oliva, M., Larrieu, A., Mirabet, V., Burrow, A. H., Beeckman, T., Kepinski, S., Traas, J., Bennett, M. J., & Vernoux, T. (2012). A novel sensor to map auxin response and distribution at high spatio-temporal resolution. *Nature*, *482*(7383), 103–106. https://doi.org/10.1038/nature10791

Chen, Y., Yang, Q., Sang, S., Wei, Z., & Wang, P. (2017). Rice Inositol Polyphosphate

Kinase (OsIPK2) Directly Interacts with OsIAA11 to Regulate Lateral Root Formation. *Plant and Cell Physiology*, *58*(11), 1891–1900. https://doi.org/10.1093/pcp/pcx125

Clough, S. J., & Bent, A. F. (1998). Floral dip: a simplified method for*Agrobacterium*-mediated transformation ofArabidopsis thaliana. *The Plant Journal*, *16*(6), 735–743. https://doi.org/10.1046/j.1365-313x.1998.00343.x

Cui, P., Liu, H., Ruan, S., Ali, B., Gill, R. A., Ma, H., Zheng, Z., & Zhou, W. (2017). A zinc finger protein, interacted with cyclophilin, affects root development via IAA pathway in rice. *Journal of Integrative Plant Biology*, *59*(7), 496–505. https://doi.org/10.1111/jipb.12531

Darwin, C. R. (1869). *On the origin of species by means of natural selection, or the preservation of favoured races in the struggle for life.* (L. J. Murray (ed.); 5th ed.). Tenth thousand. http://darwin-online.org.uk/content/frameset?itemID=F387&viewtype=text&pageseq=82

De Rybel, B., Vassileva, V., Parizot, B., Demeulenaere, M., Grunewald, W., Audenaert, D., Van Campenhout, J., Overvoorde, P., Jansen, L., Vanneste, S., Möller, B., Wilson, M., Holman, T., Van Isterdael, G., Brunoud, G., Vuylsteke, M., Vernoux, T., De Veylder, L., Inzé, D., … Beeckman, T. (2010). A Novel Aux/IAA28 Signaling Cascade Activates GATA23-Dependent Specification of Lateral Root Founder Cell Identity. *Current Biology*, *20*(19), 1697–1706. https://doi.org/10.1016/j.cub.2010.09.007

De Smet, I., Tetsumura, T., De Rybel, B., Frey, N. F. d., Laplaze, L., Casimiro, I., Swarup, R., Naudts, M., Vanneste, S., Audenaert, D., Inze, D., Bennett, M. J., & Beeckman, T. (2007). Auxin-dependent regulation of lateral root positioning in the basal meristem of Arabidopsis. *Development*, *134*(4), 681–690. https://doi.org/10.1242/dev.02753

Dindas, J., Scherzer, S., Roelfsema, M. R. G., von Meyer, K., Müller, H. M., Al-Rasheid, K. A. S., Palme, K., Dietrich, P., Becker, D., Bennett, M. J., & Hedrich, R. (2018). AUX1-mediated root hair auxin influx governs SCFTIR1/AFB-type Ca2+ signaling. *Nature Communications*, *9*(1), 1174. https://doi.org/10.1038/s41467-018-03582-5

Fendrych, M., Akhmanova, M., Merrin, J., Glanc, M., Hagihara, S., Takahashi, K., Uchida, N., Torii, K. U., & Friml, J. (2018). Rapid and reversible root growth inhibition by TIR1 auxin signalling. *Nature Plants*, *4*(7), 453–459. https://doi.org/10.1038/s41477-018-0190-1

Feng, L., Li, G., He, Z., Han, W., Sun, J., Huang, F., Di, J., & Chen, Y. (2019). The ARF, GH3, and Aux/IAA gene families in castor bean (Ricinus communis L.): Genome-wide identification and expression profiles in high-stalk and dwarf strains. *Industrial Crops and Products*, *141*(April), 111804. https://doi.org/10.1016/j.indcrop.2019.111804

Grabov, A., Ashley, M. K., Rigas, S., Hatzopoulos, P., Dolan, L., & Vicente-Agullo, F. (2004). Morphometric analysis of root shape. *New Phytologist*, *165*(2), 641–652. https://doi.org/10.1111/j.1469-8137.2004.01258.x

Gray, W. M., Kepinski, S., Rouse, D., Leyser, O., & Estelle, M. (2001). Auxin regulates SCFTIR1-dependent degradation of AUX/IAA proteins. *Nature*, *414*(6861), 271–276. https://doi.org/10.1038/35104500

Guseman, J. M., Hellmuth, A., Lanctot, A., Feldman, T. P., Moss, B. L., Klavins, E., Calderon Villalobos, L. I. A., & Nemhauser, J. L. (2015). Auxin-induced degradation dynamics set the pace for lateral root development. *Development*, *142*(5), 905–909. https://doi.org/10.1242/dev.117234

Hamann, T., Benkova, E., Bäurle, I., Kientz, M., & Jürgens, G. (2002). Gene Encodes an Auxin Response Protein Inhibiting Embryo Patterning. *Genes Development*, *16*(13), 1610–1615. https://doi.org/10.1101/gad.229402.clonal

Han, M., Park, Y., Kim, I., Kim, E. H., Yu, T. K., Rhee, S., & Suh, J. Y. (2015). Correction for Han et al., Structural basis for the auxin-induced transcriptional regulation by Aux/IAA17. *Proceedings of the National Academy of Sciences*, *112*(6), E602–E602. https://doi.org/10.1073/pnas.1500535112

Haseloff, J. (1998). *Chapter 9: GFP Variants for Multispectral Imaging of Living Cells* (pp. 139–151). https://doi.org/10.1016/S0091-679X(08)61953-6

Herud, O., Weijers, D., Lau, S., & Jürgens, G. (2016). Auxin responsiveness of the MONOPTEROS-BODENLOS module in primary root initiation critically depends on the nuclear import kinetics of the Aux/IAA inhibitor BODENLOS. *The Plant Journal*, *85*(2), 269–277. https://doi.org/10.1111/tpj.13108

Kalluri, U. C., DiFazio, S. P., Brunner, A. M., & Tuskan, G. A. (2007). Genome-wide analysis of Aux/IAA and ARF gene families in Populus trichocarpa. *BMC Plant Biology*, *7*(1), 59. https://doi.org/10.1186/1471-2229-7-59

Kang, B., Zhang, Z., Wang, L., Zheng, L., Mao, W., Li, M., Wu, Y., Wu, P., & Mo, X. (2013). OsCYP2, a chaperone involved in degradation of auxin-responsive proteins, plays crucial roles in rice lateral root initiation. *The Plant Journal*, *74*(1), 86–97.

https://doi.org/10.1111/tpj.12106

Kim, H., Park, P.-J., Hwang, H.-J., Lee, S.-Y., Oh, M.-H., & Kim, S.-G. (2006). Brassinosteroid Signals Control Expression of the AXR3/IAA17 Gene in the Cross-Talk Point with Auxin in Root Development. *Bioscience, Biotechnology, and Biochemistry*, *70*(4), 768–773. https://doi.org/10.1271/bbb.70.768

Kitomi, Y., Inahashi, H., Takehisa, H., Sato, Y., & Inukai, Y. (2012). OsIAA13-mediated auxin signaling is involved in lateral root initiation in rice. *Plant Science*, *190*, 116–122. https://doi.org/10.1016/j.plantsci.2012.04.005

Knox, K. (2003). AXR3 and SHY2 interact to regulate root hair development. *Development*, *130*(23), 5769–5777. https://doi.org/10.1242/dev.00659

Kumar, R., Agarwal, P., Pareek, A., Tyagi, A. K., & Sharma, A. K. (2015). Genomic Survey, Gene Expression, and Interaction Analysis Suggest Diverse Roles of ARF and Aux/IAA Proteins in Solanaceae. *Plant Molecular Biology Reporter*, *33*(5), 1552–1572. https://doi.org/10.1007/s11105-015-0856-z

Leyser, O., Pickett, F. B., Dharmasiri, S., & Estelle, M. (1996). Mutations in the AXR3 gene of Arabidopsis result in altered auxin response including ectopic expression from the SAUR-AC1 promoter. *The Plant Journal*, *10*(3), 403–413. https://doi.org/10.1046/j.1365-313x.1996.10030403.x

Leyser, O. (2018). Auxin Signaling. *Plant Physiology*, *176*(1), 465–479. https://doi.org/10.1104/pp.17.00765

Li, H., Cheng, Y., Murphy, A., Hagen, G., & Guilfoyle, T. J. (2009). Constitutive Repression and Activation of Auxin Signaling in Arabidopsis. *Plant Physiology*, *149*(3), 1277–1288. https://doi.org/10.1104/pp.108.129973

Li, S.-B., Xie, Z.-Z., Hu, C.-G., & Zhang, J.-Z. (2016). A Review of Auxin Response Factors (ARFs) in Plants. *Frontiers in Plant Science*, *7*(FEB2016), 1–7. https://doi.org/10.3389/fpls.2016.00047

Liscum, E., & Reed, J. W. (2002). Genetics of Aux/IAA and ARF action in plant growth and development. *Plant Molecular Biology*, *49*(3–4), 387–400. https://doi.org/10.1023/A:1015255030047

Liu, K., Yuan, C., Feng, S., Zhong, S., Li, H., Zhong, J., Shen, C., & Liu, J. (2017). Genome-wide analysis and characterization of Aux/IAA family genes related to fruit ripening in papaya (Carica papaya L.). *BMC Genomics*, *18*(1), 351. https://doi.org/10.1186/s12864-017-3722-6

Lucas, M., Godin, C., Jay-Allemand, C., & Laplaze, L. (2008). Auxin fluxes in the root

apex co-regulate gravitropism and lateral root initiation. *Journal of Experimental Botany*, *59*(1), 55–66. https://doi.org/10.1093/jxb/erm171

Ludwig, Y., Berendzen, K. W., Xu, C., Piepho, H.-P., & Hochholdinger, F. (2014). Diversity of Stability, Localization, Interaction and Control of Downstream Gene Activity in the Maize Aux/IAA Protein Family. *PLoS ONE*, *9*(9), e107346. https://doi.org/10.1371/journal.pone.0107346

Luo, J., Zhou, J.-J., & Zhang, J.-Z. (2018). Aux/IAA Gene Family in Plants: Molecular Structure, Regulation, and Function. *International Journal of Molecular Sciences*, *19*(1), 259. https://doi.org/10.3390/ijms19010259

Mähönen, A. P., Tusscher, K. ten, Siligato, R., Smetana, O., Díaz-Triviño, S., Salojärvi, J., Wachsman, G., Prasad, K., Heidstra, R., & Scheres, B. (2014). PLETHORA gradient formation mechanism separates auxin responses. *Nature*, *515*(7525), 125–129. https://doi.org/10.1038/nature13663

Maraschin, F. dos S., Memelink, J., & Offringa, R. (2009). Auxin-induced, SCF TIR1 -mediated poly-ubiquitination marks AUX/IAA proteins for degradation. *The Plant Journal*, *59*(1), 100–109. https://doi.org/10.1111/j.1365-313X.2009.03854.x

Monshausen, G. B., Miller, N. D., Murphy, A. S., & Gilroy, S. (2011). Dynamics of auxin-dependent Ca2+ and pH signaling in root growth revealed by integrating high-resolution imaging with automated computer vision-based analysis. *The Plant Journal*, *65*(2), 309–318. https://doi.org/10.1111/j.1365-313X.2010.04423.x

Müller, A., Guan, C., Gälweiler, L., Tänzler, P., Huijser, P., Marchant, A., Parry, G., Bennett, M., Wisman, E., & Palme, K. (1998). AtPIN2 defines a locus of Arabidopsis for root gravitropism control. *The EMBO Journal*, *17*(23), 6903–6911. https://doi.org/10.1093/emboj/17.23.6903

Němec. (1900). Ueber die Art der Wahrnehmung des Schwek- raftreizes bei den Pflanzen. *Berichte Der Deutschen Botanischen Gesellschaft*, *18*, 241–245.

Notaguchi, M., Wolf, S., & Lucas, W. J. (2012). Phloem-Mobile Aux / IAA Transcripts Target to the Root Tip and Modify Root Architecture F. *Journal of Integrative Plant Biology*, *54*(10), 760–772. https://doi.org/10.1111/j.1744-7909.2012.01155.x

Oono, Y., Ooura, C., Rahman, A., Aspuria, E. T., Hayashi, K., Tanaka, A., & Uchimiya, H. (2003). p -Chlorophenoxyisobutyric Acid Impairs Auxin Response in Arabidopsis Root. *Plant Physiology*, *133*(3), 1135–1147. https://doi.org/10.1104/pp.103.027847

Ouellet, F., Overvoorde, P. J., & Theologis, A. (2001). IAA17/AXR3: Biochemical

Insight into an Auxin Mutant Phenotype. *The Plant Cell*, *13*(4), 829–841. https://doi.org/10.1105/tpc.13.4.829

Overvoorde, P., Fukaki, H., & Beeckman, T. (2010). Auxin Control of Root Development. *Cold Spring Harbor Perspectives in Biology*, *2*(6), a001537–a001537. https://doi.org/10.1101/cshperspect.a001537

Padmanabhan, M. S., Goregaoker, S. P., Golem, S., Shiferaw, H., & Culver, J. N. (2005). Interaction of the Tobacco Mosaic Virus Replicase Protein with the Aux/IAA Protein PAP1/IAA26 Is Associated with Disease Development. *Journal of Virology*, *79*(4), 2549–2558. https://doi.org/10.1128/JVI.79.4.2549-2558.2005

Prát, T., Hajný, J., Grunewald, W., Vasileva, M., Molnár, G., Tejos, R., Schmid, M., Sauer, M., & Friml, J. (2018). WRKY23 is a component of the transcriptional network mediating auxin feedback on PIN polarity. *PLOS Genetics*, *14*(1), e1007177. https://doi.org/10.1371/journal.pgen.1007177

Prigge, M. J., Platre, M., Kadakia, N., Zhang, Y., Greenham, K., Szutu, W., Pandey, B. K., Bhosale, R. A., Bennett, M. J., Busch, W., & Estelle, M. (2020). Genetic analysis of the Arabidopsis TIR1/AFB auxin receptors reveals both overlapping and specialized functions. *ELife*, *9*, 1–28. https://doi.org/10.7554/eLife.54740

Procko, C., Burko, Y., Jaillais, Y., Ljung, K., Long, J. A., & Chory, J. (2016). The epidermis coordinates auxin-induced stem growth in response to shade. *Genes & Development*, *30*(13), 1529–1541. https://doi.org/10.1101/gad.283234.116

Rouse, D. (1998). Changes in Auxin Response from Mutations in an AUX/IAA Gene. *Science*, *279*(5355), 1371–1373. https://doi.org/10.1126/science.279.5355.1371

Sarrion-Perdigones, A., Falconi, E. E., Zandalinas, S. I., Juárez, P., Fernández-del-Carmen, A., Granell, A., & Orzaez, D. (2011). GoldenBraid: An Iterative Cloning System for Standardized Assembly of Reusable Genetic Modules. *PLoS ONE*, *6*(7), e21622. https://doi.org/10.1371/journal.pone.0021622

Sato, A., & Yamamoto, K. T. (2008). Overexpression of the non-canonical Aux/IAA genes causes auxin-related aberrant phenotypes in Arabidopsis. *Physiologia Plantarum*, *133*(2), 397–405. https://doi.org/10.1111/j.1399-3054.2008.01055.x

Sato, E. M., Hijazi, H., Bennett, M. J., Vissenberg, K., & Swarup, R. (2015). New insights into root gravitropic signalling. *Journal of Experimental Botany*, *66*(8), 2155–2165. https://doi.org/10.1093/jxb/eru515

Schindelin, J., Arganda-Carreras, I., Frise, E., Kaynig, V., Longair, M., Pietzsch, T., Preibisch, S., Rueden, C., Saalfeld, S., Schmid, B., Tinevez, J.-Y., White, D. J.,

Hartenstein, V., Eliceiri, K., Tomancak, P., & Cardona, A. (2012). Fiji: an open-source platform for biological-image analysis. *Nature Methods*, *9*(7), 676–682. https://doi.org/10.1038/nmeth.2019

Schmitt, J., & Stunnenberg, H. G. (1993). The glucocorticoid receptor hormone binding domain mediates transcriptional activation in vitro in the absence of ligand. *Nucleic Acids Research*, *21*(11), 2673–2681. https://doi.org/10.1093/nar/21.11.2673

Schwarzerová, K., Bellinvia, E., Martinek, J., Sikorová, L., Dostál, V., Libusová, L., Bokvaj, P., Fischer, L., Schmit, A. C., & Nick, P. (2019). Tubulin is actively exported from the nucleus through the Exportin1/CRM1 pathway. *Scientific Reports*, *9*(1), 5725. https://doi.org/10.1038/s41598-019-42056-6

Shi, H., Liu, W., Wei, Y., & Ye, T. (2017). Integration of auxin/indole-3-acetic acid 17 and RGA-LIKE3 confers salt stress resistance through stabilization by nitric oxide in Arabidopsis. *Journal of Experimental Botany*, *68*(5), 1239–1249. https://doi.org/10.1093/jxb/erw508

Shih, H.-W., DePew, C. L., Miller, N. D., & Monshausen, G. B. (2015). The Cyclic Nucleotide-Gated Channel CNGC14 Regulates Root Gravitropism in Arabidopsis thaliana. *Current Biology*, *25*(23), 3119–3125. https://doi.org/10.1016/j.cub.2015.10.025

Siligato, R., Wang, X., Yadav, S. R., Lehesranta, S., Ma, G., Ursache, R., Sevilem, I., Zhang, J., Gorte, M., Prasad, K., Wrzaczek, M., Heidstra, R., Murphy, A., Scheres, B., & Mähönen, A. P. (2016). MultiSite Gateway-Compatible Cell Type-Specific Gene-Inducible System for Plants. *Plant Physiology*, *170*(2), 627–641. https://doi.org/10.1104/pp.15.01246

Simon, M. L. A., Platre, M. P., Marquès-Bueno, M. M., Armengot, L., Stanislas, T., Bayle, V., Caillaud, M.-C., & Jaillais, Y. (2016). A PtdIns(4)P-driven electrostatic field controls cell membrane identity and signalling in plants. *Nature Plants*, *2*(7), 16089. https://doi.org/10.1038/nplants.2016.89

Swarup, R., Kramer, E. M., Perry, P., Knox, K., Leyser, H. M. O., Haseloff, J., Beemster, G. T. S., Bhalerao, R., & Bennett, M. J. (2005). Root gravitropism requires lateral root cap and epidermal cells for transport and response to a mobile auxin signal. *Nature Cell Biology*, *7*(11), 1057–1065. https://doi.org/10.1038/ncb1316

Tao, L., Cheung, A. Y., Nibau, C., & Wu, H. (2005). RAC GTPases in Tobacco and Arabidopsis Mediate Auxin-Induced Formation of Proteolytically Active Nuclear Protein Bodies That Contain AUX/IAA Proteins. *The Plant Cell*, *17*(8), 2369–2383.

https://doi.org/10.1105/tpc.105.032987

Tatematsu, K., Kumagai, S., Muto, H., Sato, A., Watahiki, M. K., Harper, R. M., Liscum, E., & Yamamoto, K. T. (2004). MASSUGU2 Encodes Aux/IAA19, an Auxin-Regulated Protein That Functions Together with the Transcriptional Activator NPH4/ARF7 to Regulate Differential Growth Responses of Hypocotyl and Formation of Lateral Roots in Arabidopsis thaliana. *The Plant Cell*, *16*(2), 379–393. https://doi.org/10.1105/tpc.018630

Terrile, M. C., París, R., Calderón-Villalobos, L. I. A., Iglesias, M. J., Lamattina, L., Estelle, M., & Casalongué, C. A. (2012). Nitric oxide influences auxin signaling through S-nitrosylation of the Arabidopsis TRANSPORT INHIBITOR RESPONSE 1 auxin receptor. *The Plant Journal*, *70*(3), 492–500. https://doi.org/10.1111/j.1365-313X.2011.04885.x

Tian, H., Niu, T., Yu, Q., Quan, T., & Ding, Z. (2013). Auxin gradient is crucial for the maintenance of root distal stem cell identity in Arabidopsis. *Plant Signaling & Behavior*, *8*(12), e26429. https://doi.org/10.4161/psb.26429

Voinnet, O., Rivas, S., Mestre, P., & Baulcombe, D. (2015). Retraction: 'An enhanced transient expression system in plants based on suppression of gene silencing by the p19 protein of tomato bushy stunt virus.' *The Plant Journal*, *84*(4), 846–846. https://doi.org/10.1111/tpj.13066

Wang, R., & Estelle, M. (2014). Diversity and specificity: auxin perception and signaling through the TIR1/AFB pathway. *Current Opinion in Plant Biology*, *21*, 51–58. https://doi.org/10.1016/j.pbi.2014.06.006

Wang, R., Zhang, Y., Kieffer, M., Yu, H., Kepinski, S., & Estelle, M. (2016). HSP90 regulates temperature-dependent seedling growth in Arabidopsis by stabilizing the auxin co-receptor F-box protein TIR1. *Nature Communications*, *7*(1), 10269. https://doi.org/10.1038/ncomms10269

Weiste, C., Pedrotti, L., Selvanayagam, J., Muralidhara, P., Fröschel, C., Novák, O., Ljung, K., Hanson, J., & Dröge-Laser, W. (2017). The Arabidopsis bZIP11 transcription factor links low-energy signalling to auxin-mediated control of primary root growth. *PLOS Genetics*, *13*(2), e1006607. https://doi.org/10.1371/journal.pgen.1006607

Wen, R., Wang, S., Xiang, D., Venglat, P., Shi, X., Zang, Y., Datla, R., Xiao, W., & Wang, H. (2014). UBC13, an E2 enzyme for Lys63-linked ubiquitination, functions in root development by affecting auxin signaling and Aux/IAA protein stability. *The*

Plant Journal, *80*(3), 424–436. https://doi.org/10.1111/tpj.12644

Woodward, A. W. (2005). Auxin: Regulation, Action, and Interaction. *Annals of Botany*, *95*(5), 707–735. https://doi.org/10.1093/aob/mci083

Wu, W., Liu, Y., Wang, Y., Li, H., Liu, J., Tan, J., He, J., Bai, J., & Ma, H. (2017). Evolution Analysis of the Aux/IAA Gene Family in Plants Shows Dual Origins and Variable Nuclear Localization Signals. *International Journal of Molecular Sciences*, *18*(10), 2107. https://doi.org/10.3390/ijms18102107

Yang, B.-J., Han, X.-X., Yin, L.-L., Xing, M.-Q., Xu, Z.-H., & Xue, H.-W. (2016). Arabidopsis PROTEASOME REGULATOR1 is required for auxin-mediated suppression of proteasome activity and regulates auxin signalling. *Nature Communications*, *7*(1), 11388. https://doi.org/10.1038/ncomms11388

Yang, X., Lee, S., So, J., Dharmasiri, S., Dharmasiri, N., Ge, L., Jensen, C., Hangarter, R., Hobbie, L., & Estelle, M. (2004). The IAA1 protein is encoded by AXR5 and is a substrate of SCFTIR1. *The Plant Journal*, *40*(5), 772–782. https://doi.org/10.1111/j.1365-313X.2004.02254.x

Zhang, H., Linster, E., Gannon, L., Leemhuis, W., Rundle, C. A., Theodoulou, F. L., & Wirtz, M. (2019). Tandem Fluorescent Protein Timers for Noninvasive Relative Protein Lifetime Measurement in Plants. *Plant Physiology*, *180*(2), 718–731. https://doi.org/10.1104/pp.19.00051

Zhang, Y., He, P., Ma, X., Yang, Z., Pang, C., Yu, J., Wang, G., Friml, J., & Xiao, G. (2019). Auxin-mediated statolith production for root gravitropism. *New Phytologist*, *224*(2), 761–774. https://doi.org/10.1111/nph.15932

Zuo, J., Niu, Q.-W., & Chua, N.-H. (2000). An estrogen receptor-based transactivator XVE mediates highly inducible gene expression in transgenic plants. *The Plant Journal*, *24*(2), 265–273. https://doi.org/10.1046/j.1365-313x.2000.00868.x